Modeling of active consumers and their impact on the Smart Grid: A cyber physical social and economic perspective

by

Kumarsinh Jhala

B.E., Gujarat Technological University, 2014

M.S., Kansas State University, 2015

AN ABSTRACT OF A DISSERTATION

submitted in partial fulfillment of the
requirements for the degree

DOCTOR OF PHILOSOPHY

Department Electrical and Computer Engineering
College of Engineering

KANSAS STATE UNIVERSITY
Manhattan, Kansas

2018

Abstract

Active consumers who engage in energy consumption, production, storage and provide ancillary services in a dynamic and interactive manner will be an integral part of the future grid. Firstly, this dissertation models and analyzes the interaction between active consumers and aggregators with a specific focus on consumer actions in response to real-time electricity pricing and the resulting impact on grid voltage. A unique prospect theory based consumer behavior model is introduced. This model captures wide range of consumers each with their individual preferences by modeling the interaction between the active consumers and the aggregator as a Stackelberg game. However, unlike existing game theoretic efforts that assume rational behavior of consumers, the prospect theory based models systematically incorporate realistic consumer behavior including irrationality.

Secondly, this dissertation develops probabilistic voltage sensitivity analysis. In contrast to prior approaches that limit themselves to economic aspects, the proposed techno-economic perspective provides an understanding of the impact of large scale penetration of active consumers on the physical grid. Most current studies are scenario-based, and derived results are scenario specific. Determining the impact of spatially distributed active consumers with temporally variable behavior requires investigation of a large number of scenarios, which is computationally intractable using current iterative power flow algorithms. This work provides a new analytical method of voltage sensitivity analysis that allows for stochastic analysis of change in grid voltage due to change in consumer behavior (load and generation choices). This work first derives an upper bound for change in voltage at a particular bus due to change in power consumption at other buses in a radial distribution network. Next, this bound is used to derive the probability distribution of change voltage at a bus due to randomly changing power consumption/injection of random spatial distribution of the active

consumers. This upper bound is also used to develop an algorithmic approach to identify the dominant influencer of voltage fluctuations in the power distribution system.

Thirdly, security and stability aspects of transactive energy market based power distribution system is investigated. Specifically, the impact of attacks on pricing/load signals on the physical grid is quantified. This work models the interaction between real-time electricity price and total energy demand in the form of a discrete time non-linear autonomous dynamical system. Equilibrium electricity price and energy demand associated with this coupled dynamical system is derived and conditions for bounded input bounded output (BIBO) stability are identified. Then, a BIBO stable algorithm to design real-time electricity pricing scheme from a techno-economic perspective is developed. Finally, the impact of various level of false data injection (FDI) attack on price of electricity, demand and distribution system voltage is investigated. This dissertation shows that impact of FDI attack on electricity prices is more severe than an attack on electricity demand.

Modeling of active consumers and their impact on the Smart Grid: A cyber physical social and economic perspective

by

Kumarsinh Jhala

B.E., Gujarat Technological University, 2014

M.S., Kansas State University, 2015

A DISSERTATION

submitted in partial fulfillment of the
requirements for the degree

DOCTOR OF PHILOSOPHY

Department Electrical and Computer Engineering
College of Engineering

KANSAS STATE UNIVERSITY
Manhattan, Kansas

2018

Approved by:

Major Professor
Dr. Balasubramaniam Natarajan

Copyright

Abstract

Active consumers who engage in energy consumption, production, storage and provide ancillary services in a dynamic and interactive manner will be an integral part of the future grid. Firstly, this dissertation models and analyzes the interaction between active consumers and aggregators with a specific focus on consumer actions in response to real-time electricity pricing and the resulting impact on grid voltage. A unique prospect theory based consumer behavior model is introduced. This model captures wide range of consumers each with their individual preferences by modeling the interaction between the active consumers and the aggregator as a Stackelberg game. However, unlike existing game theoretic efforts that assume rational behavior of consumers, the prospect theory based models systematically incorporate realistic consumer behavior including irrationality.

Secondly, this dissertation develops probabilistic voltage sensitivity analysis. In contrast to prior approaches that limit themselves to economic aspects, the proposed techno-economic perspective provides an understanding of the impact of large scale penetration of active consumers on the physical grid. Most current studies are scenario-based, and derived results are scenario specific. Determining the impact of spatially distributed active consumers with temporally variable behavior requires investigation of a large number of scenarios, which is computationally intractable using current iterative power flow algorithms. This work provides a new analytical method of voltage sensitivity analysis that allows for stochastic analysis of change in grid voltage due to change in consumer behavior (load and generation choices). This work first derives an upper bound for change in voltage at a particular bus due to change in power consumption at other buses in a radial distribution network. Next, this bound is used to derive the probability distribution of change voltage at a bus due to randomly changing power consumption/injection of random spatial distribution of the active

consumers. This upper bound is also used to develop an algorithmic approach to identify the dominant influencer of voltage fluctuations in the power distribution system.

Thirdly, security and stability aspects of transactive energy market based power distribution system is investigated. Specifically, the impact of attacks on pricing/load signals on the physical grid is quantified. This work models the interaction between real-time electricity price and total energy demand in the form of a discrete time non-linear autonomous dynamical system. Equilibrium electricity price and energy demand associated with this coupled dynamical system is derived and conditions for bounded input bounded output (BIBO) stability are identified. Then, a BIBO stable algorithm to design real-time electricity pricing scheme from a techno-economic perspective is developed. Finally, the impact of various level of false data injection (FDI) attack on price of electricity, demand and distribution system voltage is investigated. This dissertation shows that impact of FDI attack on electricity prices is more severe than an attack on electricity demand.

Table of Contents

List of Figures

List of Tables

Acknowledgments

I would like to express my heartfelt gratitude to my supervisor *Dr. Bala Natarajan* whose guidance, support and encouragement has been the driving force behind my work. I am very thankful to him for being always available in spite of his busy schedules and for his interest in my research work. His ability to instruct, guide, and inspire is truly remarkable and is only surpassed by his knowledge and passion for work. I have also had the fortune to interact with him and his family on a personal level and cherish every one of these moments. He has always been a caring and understanding mentor and has always made an effort to make me feel comfortable so far away from home. As I set out towards a career in research, his valuable comments will always help me on my way. My sincere gratitude to my doctoral committee members *Dr. Anil Pahwa*, *Dr. Hongyu Wu*, *Dr. Scott DeLoach*, and *Dr. Lance Bachmeier* for their feedback and advice on to improve quality of my research.

I would like to thank my colleges *Dr. Mohammad Nazif Faqiry*, and *Dr. Pavel Janovsky* for working alongside and providing me motivation. Special thanks to members of the WICOM group *Wenji Zhang*, *Dr. S M Shafiul Alam*, and *Hazhar Sufi Karimi* for thorough discussions and feedback on several key topics presented in this dissertation. I especially owe much gratitude to *Alaleh Alivar*, *Solmaz Niknam* and *Reza Barazieh* for their support, encouragement, and guidance.

This thesis is dedicated to my parents Rajkumari Jhala and Mahendrasinh Jhala, and my brother Hardeep, and sister-in-law Vijeta for their patience, encouragement, and unquestioned support during my education. This work is supported by National Science Foundation through award No. CNS-1544705.

Chapter 1

Introduction

The power and energy field has changed significantly over the last decade. Specifically, renewable generation has increased multi-fold, new technologies for smart grid are being implemented, and electric vehicles are gaining popularity. A smart power grid leverages advances in sensing, communication, computing, and control to increase grid reliability, resiliency, efficiency, and flexibility [1]. Integration of these technologies also allows higher deployment of large and small-scale renewable energy resources. With incorporation of renewable generation and "active consumers", there will be continuing need for improvements in the grid analysis, operation and planning tools in addition to changes in the operation of electricity market in power distribution system. The most significant impact of these changes is being felt at the consumer level. Understanding consumer behavior and developing useful models will be one of the primary challenges in future smart grid. New generation of appliances within the home are becoming smarter with load management and communication capabilities. As a result of these advances, future consumers will be very different from those today. It is expected that active consumers who engage in managing energy use, production, storage and providing other ancillary services in a dynamic and interactive manner will be an integral part of the future grid. There will be a continuing need to integrate cyber-physical system (CPS) advances into the operation, control, and design of these systems. Therefore, understanding, modeling and quantifying the impact of the active consumers under the

umbrella of cyber physical social and economic systems is an important and much needed research thrust.

Historically, residential consumers have paid a fixed price for electricity regardless of the time at which the consumption takes place. Some utilities have implemented time-of-use and critical peak pricing on a limited basis [2, 3, 4, 5]. Real-time pricing of electricity for the residential consumers has been tested for demand response, but wide scale implementation will require overcoming various technical and logistical challenges [6, 7] However, with advances in communications and cyber technologies, these challenges can be addressed and real-time pricing for consumers can become a reality. Hence, the biggest change the consumers will see in the future is more engagement and ability to actively participate in the Transactive Energy market [8, 9] Transactive Energy as defined by GridWise Alliance in a December 2014 report is *"The ability for consumers and end devices to buy and sell energy and related services in a dynamic and interactive manner."* For an individual customer, it will be impossible to keep track of various decisions that will be required in real-time as well in the immediate future in a highly dynamic transactive energy market. Therefore, each home is expected to be equipped with a home energy management system [10, 11, 12, 13, 14] or a complex computer, which will use real-time price, real-time data on loads, generation, energy storage, weather, and customer preferences to schedule different devices in homes.

Second major challenge is to understand the impact of multiple active consumer and renewable energy sources on the power distribution system. At the utility level, new dynamics may emerge due to participation of new active customers in the market place that could create conditions detrimental to reliability and resiliency of the power distribution system. Analyzing impact of multiple active consumers changing their energy consumption in accordance with renewable generational and forces of transactive energy market on distribution grid voltage in a computationally efficient manner is a crucial aspect of this dissertation. Currently, Monte-Carlo simulation based scenario analysis is primary tool to understand impact of random fluctuations of renewable generation on the distribution grid voltage. Major drawbacks of theses scenario based analysis are higher computational complexity and lack of analytical insight. Higher computationally complexity of such scenario based analysis is a

major hurdle in implementation of true techno-economic analysis of the distribution system and makes it simulation of a transactive energy system challenging. For example, one might be interested in understanding impact of $X\%$ penetration of rooftop PVs in a distribution system with N consumers or identifying most dominant influencer of voltage fluctuations for a node experiencing low voltage problems in the power distribution system. In this example, to answer question like "For given PV penetration is it possible to maintain the distribution system voltage within permissible limits without any control actions?" using traditional scenario based analysis, one will have to follow two steps.

1. Create a system model with fixed location of PVs and run Newton-Raphson based Monte-Carlo simulation to capture temporal variation on PV generation.

2. Repeat step-1 for all possible spatial distribution of PV generation.

Computational complexity of such scenario based analysis increases exponentially with the size of the network.

Finally, analyzing impact of cyber attack on reliability and stability of power distribution system is crucial. Future power distribution system with smart meters and advanced metering infrastructure (AMI) will have bidirectional communication between active consumer and aggregators. In the transactive energy framework, the price of electricity for the active consumers decided by the aggregator and the energy consumption of the active consumers is communicated over AMI. This information exchange between the aggregator and the active consumers is prone of cyber attack. There is plethora of work done to design strategies to prevent and detect such cyber attacks; however, no attack detection/prevention mechanism is perfect. Therefore, it is crucial to understand impact of cyber attacks in presence of such detection and prevention mechanism.

Based on these perspectives, we seek to address a few fundamental research questions in this dissertation. These questions and the contributions of this dissertation to address them are discussed in the following sections.

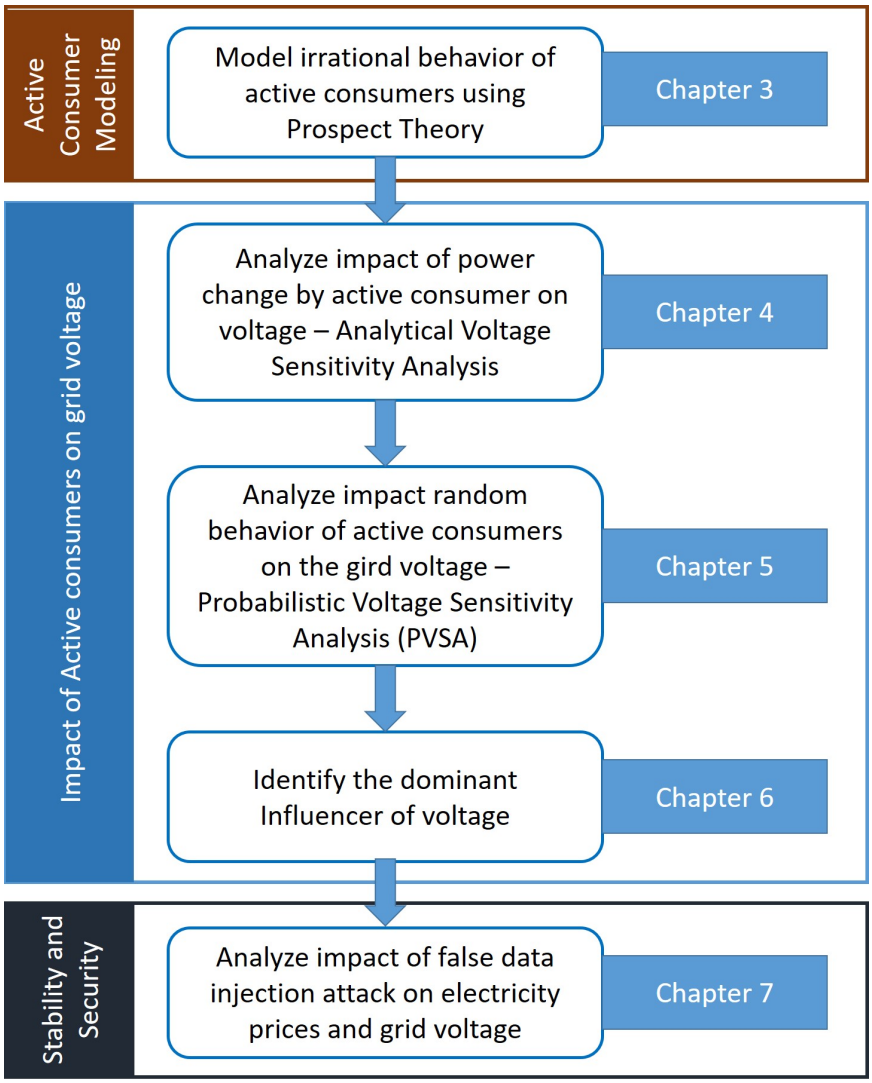

Figure 1.1: *Outline of the Dissertation*

1.1 Research Questions

Question 1: *How can we model different consumer types, capturing their preferences and reactions to changes in electricity price? What modeling approaches can support power distribution systems (PDS) operation and can also aid in representing consumers in other CPS domains?*

Question 2: *For a given penetration of active consumers, how can we approximate the impact of their actions on the distribution system voltage in a computationally efficient manner?*

Question 3: *How can we calculate impact of random power change caused by multiple re-*

newable energy sources located at random spatial locations in the power distribution system?

Question 4: *In the power distribution system where actions of multiple active consumers cause random voltage fluctuations, how can we identify the dominant influencer of voltage fluctuations?*

Question 5: *What are the cyber-security concerns in a power distribution system with active consumers interacting with aggregators? For example, what is the impact of false data injection attack on this system? What are some design guidelines for this transactive energy market based power distribution system that ensures stability of a real-time pricing scheme?*

1.2 Contributions of the Dissertation

To address research question 1, Chapter 3 of this dissertation proposes a Prospect Theory based model of active consumers making subjective actions under uncertain price of electricity and analyzes the impact of their actions on the distribution grid voltage. Major contributions of this chapter are listed below.

- This work models interaction between an aggregator and multiple active consumers connected to a power distribution system as a Stackelberg leader-follower game, where the aggregator acts as a leader and the active consumers are followers.
- A general model that efficiently captures consumers with varying preferences for electricity consumption is considered. For the first time, the subjective behavior of consumers in response to variations in the price of electricity is modeled using the Prospect Theory.
- Behavior of the aggregator is modeled by considering both technical and economic aspects of grid operation. The economic goal of maximizing profit is integrated with the technical goal of maintaining the grid voltage within permissible limits in the game formulation.

- Actions of active consumers at the Nash equilibrium and its impact on the distribution grid voltage is analyzed using simulations on the modified IEEE 69 bus test system.

- The difference between expected utility theory to the Prospect Theory formulations are highlighted. Specifically the impact of lack of rationality on the physical grid voltage and monetary payoffs for both the consumer and the aggregator is quantified.

More details related to this approach is in Chapter 3 and published in the following article: [15]: K. Jhala, B. Natarajan, and A. Pahwa,"Prospect Theory based Active Consumer Behavior Under Variable Electricity Pricing," *IEEE Transactions on Smart Grid,* 2018. doi: 10.1109/TSG.2018.2810819.

A new probabilistic voltage sensitivity analysis (PVSA) approach is proposed to address research questions 2 and 3. Chapter 4 and 5 of this dissertation proposes a stochastic method of grid analysis that provides a probabilistic view of the system and presents the likelihood of system voltage exceeding operational bounds. Major contributions of this work are listed below.

- This work develops an analytical expression (Theorem 1) to compute the upper bound of change in bus voltage due to change in power consumption at another bus in a radial distribution network. The derived analytical expression is proven to abide by the law of superposition, which enables us to study the effect of multiple active consumers on distribution grid voltage. This upper-bound is verified using simulation results on IEEE 69 bus test system. (chapter 4)

- A method to compute an upper bound on sensitivity matrix is demonstrated. The proposed approach is computationally efficient.

- This work introduces a novel concept of probabilistic voltage sensitivity analysis (PVSA). PVSA allows the calculation of probability distribution of voltage change due to random change in real and reactive power consumption across different buses of distribution grid.

- PVSA for known/fixed and random spatial distribution of active consumers is developed in chapter 5.

- The proposed method is used to the analyze the aggregate effect of spatially distributed active consumers on feeder voltage and determine that the probability of bus voltage exceeding allowable values. Analytical results are validated using simulation results on IEEE 69 bus test system.

More details on probabilistic voltage sensitivity analysis can be found in Chapters 4 and 5 and in the following articles:
[16]: K. Jhala, B. Natarajan and A. Pahwa, "Probabilistic Voltage Sensitivity Analysis (PVSA)A Novel Approach to Quantify Impact of Active Consumers," in *IEEE Transactions on Power Systems*, vol. 33, no. 3, pp. 2518-2527, May 2018. doi: 10.1109/TPWRS.2017.2745411
[17]: K. Jhala, B. Natarajan and A. Pahwa, "Probabilistic Voltage Sensitivity Analysis (PVSA) for Random Spatial Distribution of Active Consumers," in *2018 IEEE Power Energy Society Innovative Smart Grid Technologies Conference (ISGT)*, Feb 2018, pp. 1-5.

To address research question 4, chapter 6 of this dissertation introduces an analytical method to identify the dominant influencer of the voltage fluctuations using various information theoretic metrics.

- This work introduces the concept of the dominant influencer of the voltage fluctuations in a radial power distribution system. The dominant influencer of the voltage fluctuations at is the largest contributor of source of voltage change at the observation node.

- A Monte-Carlo simulation based numerical method to identify the dominant influencer of the voltage fluctuations is proposed, which is shown to be computationally cumbersome.

- Various information theoretic indicators to identify the dominant influencer of the voltage fluctuations are proposed.
- All the proposed indicators of the dominant influencer of the voltage fluctuations are analytically derived and their effectiveness is tested using the IEEE 69 bus balanced test system.
- It is shown that differential entropy, Kullback-Leibler distance, and Frechet distance are excellent and computationally efficient indicators of the dominant influencer of the voltage fluctuations.

More detail of this work are discussed in chapter 6 and under review in the following article: [18]: K. Jhala, B. Natarajan, and A. Pahwa,"Algorithmic Approach to Identify Dominant Influencer of Voltage Fluctuations," *IEEE Transactions on Smart Grid (Under Review)*, 2018.

Finally, a novel control theoretic perspective is used to address search question 5. Chapter 7 of this dissertation discusses the impact of cyber attacks on stability and security of transactive energy based power distribution system.

- This work models interaction between real-time electricity pricing and demand as a discrete time non-linear autonomous dynamical system, where the aggregator decides electricity price based on total demand and multiple active consumers decide their consumption based on electricity prices. Based on this coupled dynamical system model, equilibrium electricity price and demand is derived (Theorem 5 and 6) and conditions for BIBO stability of the proposed system model are identified (Lemma 2 and 3)
- This work develops an algorithm to design a BIBO stable TE market based real-time electricity price scheme that considers financial interests of the aggregator in addition to system resiliency.

- The impact of FDI attack on price of electricity and demand is quantified. This paper shows that impact of FDI attack on electricity prices is more severe than an attack on electricity demand. The impact of FDI attack on real-time electricity prices, demand and distribution system voltage is illustrated using simulation of an IEEE 69 bus test system.

More details on this approach can be found in the following article:
[19]: K. Jhala, B. Natarajan, A. Pahwa, and H. Wu, "Security and Stability of Transactive Energy Marked-based Power Distribution System," *IEEE Transactions on Smart Grid (Under Review)*, 2018.

1.3 Organization of the Dissertation

Rest of this dissertation is organized as following. Chapter 2, discuses related work in the area of demand response, consumer modeling, traditional methods of sensitivity analysis and cyber security of power distribution system. A prospect theory based model of irrational active consumers is developed in chapter 3, which captures the behavior of the active consumers with different socio-economic background and varying preferences for electricity consumption. Chapter 4 develops an analytical method of voltage sensitivity analysis, which is computationally efficient. Chapter 5 develops probabilistic voltage sensitivity analysis for known and random spatial distribution of active consumers to analyze impact of multiple active consumers on distribution grid voltage. Chapter 6 develops an algorithmic approach to identify dominant influencer of voltage fluctuation. Chapter 7 analyzes stability and security of transactive energy market based power distribution system and develops criteria for designing a bounded input bounded output (BIBO) stable real-time electricity pricing scheme. Concluding remarks and future work is discussed in chapter 8. e

Chapter 2

Literature Review

This chapter discusses the related work in area of Demand response(DR), distributed generation(DG) management, consumer modeling, voltage sensitivity analysis, and security of power distribution system.

2.1 Related Work on Demand Response

Over the past decade, there have been numerous efforts that have attempted to model, manage and optimize participation of consumers in the power distribution system. These efforts can be broadly classified into two classes: (1) demand response (DR) programs focusing only on load management; (2) demand response and distributed generation (DG) management. The first dimension of the work relates to residential demand response, which typically leverages price and generation forecasts to either shift or reduce load consumption in order to maximize some utility function (e.g., energy costs [20]) under some constraints (levels of comfort/convenience [21]). One approach is to implement direct load control where a utility or an aggregator can remotely control certain loads in a household based on an a priori agreement [22]. User privacy is the primary barrier for large scale implementation of such direct load control methods. Alternately, smart pricing (e.g., critical peak pricing (CPP), TOU pricing and real time pricing (RTP)) can be used to encourage consumers to

individually manage their loads [2]. A plethora of deterministic centralized and distributed optimization [23], model predictive control [24], reinforcement learning [25] as well as game theoretic methods [26] have been proposed to attack these problems. Recently, there have been some efforts to systematically model uncertainties in this framework and implement stochastic versions of optimization [27], and dynamic programming [28] methods.

2.2 Related Work on Consumer Modeling

There is a plethora of research in the area of smart buildings energy management systems. Authors in [29] define a building management system that controls energy flow inside a smart building with renewable energy sources and energy storage using a heuristic optimization process. [30] reviews some of the technical opportunities provided by internet of things in smart building management area. Authors in [31] build a building energy management system including a grid-connected PV system and a storage system using the mixed-integer linear programming framework for the purpose of optimizing scheduling of building elements in order to achieve a pre-specified objective. In [32], an intelligent residential energy management system to reduce electricity bills for prosumers of smart residential buildings is proposed, and its benefits are demonstrated through a case study.

Many of the prior efforts in the area of DR and DG management tend to take a user/home centric approach. That is, the goal is to minimize energy costs for a home owner by scheduling and reducing load and managing generation and storage [33, 34, 35, 36]. While this is an essential step in understanding optimal actions for a consumer, it is important to note that the consumer is not acting in isolation and the operational cost and stability of the grid is dependent on the cumulative actions of multiple consumers. This aspect was brought out in [26], where a demand side management scheme based on collaborative game theoretic approach is proposed. The efforts within the control theory community that focuses on modeling consumer behavior also rely on deterministic frameworks [37]. A data driven approach to model consumers demand response behavior was presented in [38], where authors hypothesize a long term steady behavior and short term dynamic response behavior. Since,

the analysis was data based, the generality of this model is unclear. There have been many game theoretic efforts to address some of the challenges in smart grid. All these efforts use classical EUT assuming rational behavior of players [39, 40], which is not pragmatic. There are few efforts that use the Prospect Theory to address some of the challenges in power systems. Most of these efforts are limited to investigating the energy interactions between micro-grids [41, 42].

2.3 Related Work on Voltage Sensitivity Analysis

There have been numerous efforts to solve issue of voltage control in distribution system with distributed generation (DG) using sensitivity analysis based methods. These efforts mainly use traditional methods of sensitivity analysis to address the issue of voltage control [43, 44, 45, 46, 47]. Traditional methods of sensitivity analysis and drawbacks of such methods are discussed in section 4.1. These traditional methods of sensitivity analysis do not provide analytical insight into the underlying physics of the system and are computationally complex. There is a limit body of work focused on developing analytical approximation of voltage sensitivity [48, 49, 50, 51]. Unfortunately, most of these efforts are over simplistic and their accuracy is not verified through numerical simulation of test systems. The problem of voltage regulation in smart grid using reactive power control using sensitivity analysis based approach is addressed in [48]. Similarly, authors in [49, 50, 51] proposes a sensitivity analysis based algorithm to keep voltage within permitted limits by modifying active and reactive power of DGs. A direct sensitivity analysis method is proposed in these papers that gives voltage variation at given bus with respect to voltage at slack bus. However, this method assumes voltage angle to be negligible and does not consider complex value of voltage change. These papers do not provide any simulation result to verify the validity of method. Therefore, an analytical framework for understanding and quantify the effect of random active and reactive power perturbation on bus voltages is needed. Authors in [52] present a probabilistic method that uses sensitivity analysis and smart meter measurements for setting boundary values for distribution system operation indices. [52] assumes that

real and reactive power consumption of homes is independent, which is not the case usually. Secondarily, one of the key drawbacks of this work lies in its dependance on extensive Monte-carlo (MC) simulation and data from smart meters to quantify the distribution of voltage variation. This approach is not scalable for large distribution networks. Our proposed analytical approximation aid in performing voltage sensitivity analysis in a scalable, low complexity means.

2.4 Related Work on Security and Stability

There are some efforts to investigate impact of cyber attack on smart grid. The possible impacts of the FDI attack on power system have been reported in [53, 54]. A coordinated attack by forcing system to an insecure or uneconomic state of operation can further lead to a collapse if not detected in time as presented in [55]. Many methods have been reported in the literature to alleviate FDI attacks in the smart grid. The defense techniques can be broadly classified into two categories: (1) Protection-based defense, and (2) Detection-based defense. As power grid covers a vast geographical area with hundreds and thousands of smart meters/sensors, the cost of protecting all smart meters can be very high. A lightweight watermarking technique is proposed to defend against the FDI attacks [56]. Authors in [57] presented a strategy for detection of FDI attacks by reconfiguring the micro-grids dynamically and makes it impossible to organize a synchronized injection. [58] consider the distributed load sharing problem of the microgrids operating in autonomous mode under FDI. The impact of real time pricing attacks on the demand dynamics is quantified in [59]. [60] propose joint-transformation-based scheme to detect FDI attacks in real time using Kullback-Leibler distance to find the difference between probability distributions obtained from measurement variations. The smart meters can be protected by continuously monitoring the measured data or by encrypting the measured data. Shortcomings of the protection based defense are twofold; firstly, securing the critical set of measurements leads to decrease in redundant trustworthy measurements; secondly, the assumption of making a completely hack-proof smart sensor is unrealistic. Therefore, understanding dynamics and stability of

electricity price and demand in addition to impact of a successful FDI attack in the TE based distribution system is critical to answer questions like "What is the level of attack the system can tolerate?" and "When does the system swing into instability or experience voltage violations?"

Chapter 3

Prospect Theory based Active Consumer Behavior Under Variable Electricity Pricing

Future power distribution with distributed renewable generation, electric vehicles and implementation of new smart grid technologies will be very different from today. The most significant impact of these changes is being felt at the consumer level. The biggest change the consumers will see in the future is more engagement and ability to actively participate in the Transactive Energy Market (TEM) [9]. As envisioned, large commercial, industrial customers, and individual homeowners will be able to participate directly in markets set up by the utility or by third party aggregators. For an individual customer, it will be impossible to keep track of various decisions that will be required in real-time as well as in the immediate future in a highly dynamic transactive energy market. Therefore, each home is expected to be equipped with a home energy management system [10, 12, 13, 14] or a complex computer, which will use real-time electricity price, real-time data on loads/generation, and customer preferences to schedule different devices in homes. These efforts primarily focus on cost saving for the consumer as discussed thoroughly in the next subsection. However, it is important to note that at the utility level, new dynamics may emerge due to participation of

new active customers in the market place that could create conditions detrimental to reliability and resiliency of the system. Utilities will have to implement appropriate controls to keep the system stable and within bounds. High penetration of solar PV can also cause technical issues as recently reported for Hawaii [61], where the utilities are refusing interconnection of additional rooftop PV systems due to operating issues. To address some of these challenges it is important to integrate physical grid constraints and economic aspects resulting in techno-economic analysis of the underlying grid.

With the anticipated growth in active consumers, modeling consumer behavior to changing price of electricity is a crucial aspect of this work. Although the most common reaction for any consumer is to take actions which will save money, there are consumers who give more importance to other factors such as environment and comfort. Frugal consumers are typically more concerned about saving money at the cost of comfort and environment. Green consumers give higher importance to the environment relative to money and comfort. On the other hand, comfort maybe the most important aspect for affluent consumers. Additionally, there may be consumers who do not care and thus they will not make any adjustments to their power usage pattern based on pricing. Many prior efforts attempt to model consumer actions in response to pricing within the framework of game theory.

Traditional game theory assumes that players in the game are rational and uninfluenced by real-life perceptions. Most of game theoretic work in smart grid are based on assumption that consumers make decisions according to their expected utility. However, real-life decision making of consumers is influenced by their perceived subjectivity which cannot be explained by expected utility theory (EUT). A Nobel Prize winning theory, Prospect Theory [62] explains the fact that people usually over-weigh low probability bad outcomes and under-weigh high probability favorite outcomes. This work uses the Prospect Theory to capture subjective behavior of active consumers for uncertain price of electricity. A unique aspect of this work is the modeling of a wide range of consumers and their behavior/response to pricing using the Prospect Theory.

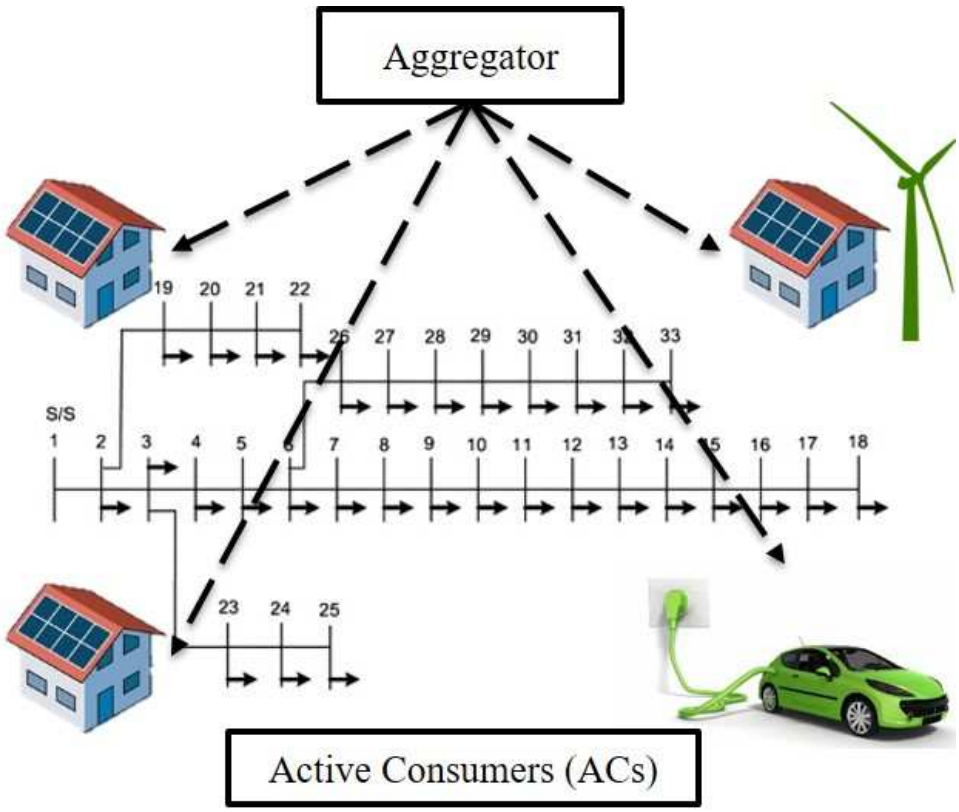

Figure 3.1: *System Model*

3.1 System Model

The future power distribution systems will involve multiple active consumers interacting with a third party aggregator as shown in Fig. 3.1. This work considers a scenario where multiple active consumers that are part of the power distribution network have a contractual agreement with a third party aggregator. The aggregator buys electricity in a day-ahead wholesale market from the independent system operator (ISO) and sells it to consumers. Any additional energy required is purchased in the real-time market. Based on the day-ahead agreement that the aggregator makes with ISO, the aggregator decides the electricity pricing to influence electricity consumption of active consumers. In addition to all financial transactions, the aggregator is also responsible for maintaining the grid voltage within allowable limits. In case of a voltage violation, the aggregator pays a penalty to the electric utility company that owns the physical grid infrastructure. Therefore, the aggregator decides the price of electricity that maximizes the profit while keeping voltages of distribution system

within limits.

In a Transactive Energy Market, each active consumer can interact with the grid by changing its energy consumption or by providing real power support from the local renewable generation. In essence, each consumer chooses an action a_i, which is power drawn from the grid or power supplied back to the grid. The consumer's choice of action a_i is based on its perceived payoff that is determined by the price of electricity. It should be noted that the payoff could depend on more than a single metric. For example, the payoff for an active consumer could depend on (1) cost of electricity; (2) comfort achieved by consuming energy, and (3) impact of their action on the distribution grid voltage. Aggregation of payoff metrics in the payoff vector to decide the optimal action would depend on the class to which the consumer belongs. Goal of a comfort seeking consumer is to maximize the comfort achieved by consuming energy. Some consumers may want to minimize the cost of electricity consumption. Active consumers who consider the physical grid voltage while making their decision want to keep the distribution grid voltage at the node of connection close to the rated value. While at this point of time, a grid-conscious consumers may seem utopian, it is interesting to model and consider the impact of such customers. One may expect such consumer types in community owned microgrids where the social aspect of maintaining grid constraints play an important role. In this work, it is assumed that a consumer connected to node i of the distribution system knows i^{th} diagonal element of the sensitivity matrix, which is used to compute change in voltage at node i due to change in action of i^{th} consumer. Additionally, electricity prices would be communicated to consumers by the aggregator over the cyber infrastructure. Price of electricity, which is decided by the aggregator, can take values from a set ρ, where $\rho = \{\rho_1, \rho_2, \cdots, \rho_n\}$. However exact price of electricity is unknown to consumers. The aggregator decides the probability distribution of electricity prices. Let $\mathbb{P}$ be vector of probabilities given by:

$$\mathbb{P} = \left[\mathbb{P}(\rho = \rho_1), \mathbb{P}(\rho = \rho_2), \cdots, \mathbb{P}(\rho = \rho_n)\right]^T. \tag{3.1}$$

Active consumers decide their energy consumption based on their perceived probability dis-

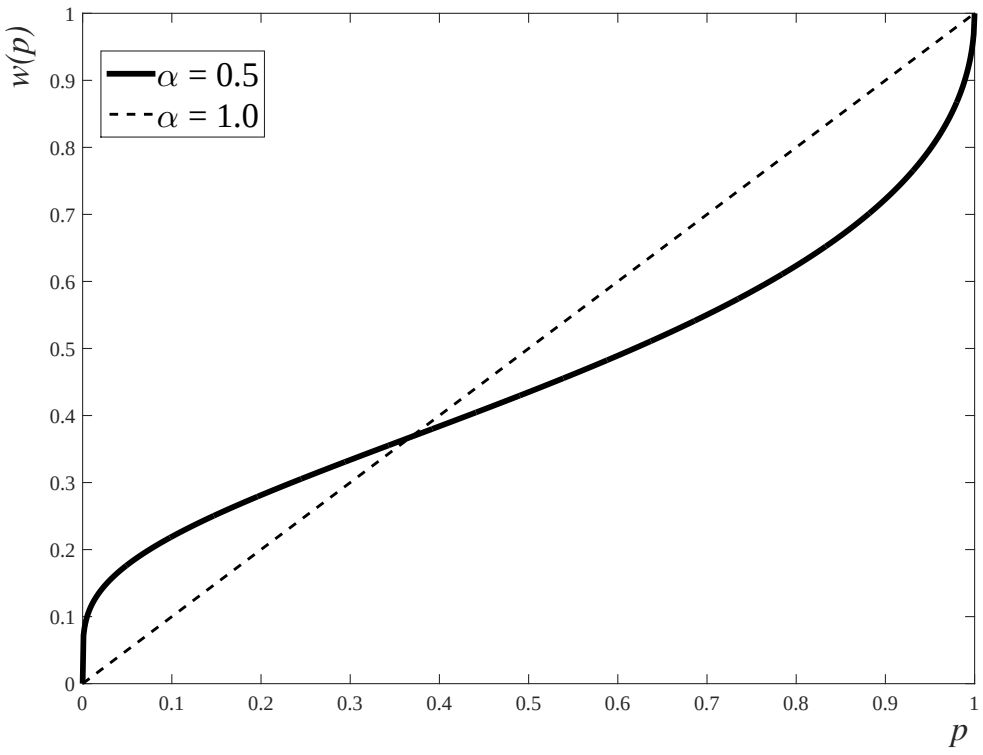

Figure 3.2: *Probability weighting function* $\omega(p)$

tribution of electricity prices. The Prospect Theory is used to understand decision making of a subjective consumer under uncertainty.

3.2 Background: Expected Utility Theory vs Prospect Theory

Traditional game theory assumes that players behave rationally while making decisions under risk. Most game theoretic studies in the field of power system assume that player makes decisions according to their expected utility. However, it is well known that people do not behave rationally under uncertainty and their decisions are influenced by their real-life perception. Traditional Expected Utility Theory (EUT) cannot explain deviations in player's actions due to end user subjectivity as illustrated by Allaiss paradox [62].

The Prospect Theory (PT) provides a user-centric view to address this issue by applying probability weighting effect to transform objective probabilities of players into subjective probabilities [62, 63]. The Nobel Prize winning theory explains the fact that people usually over-weigh low probability outcomes and under-weigh outcomes with moderate to high probabilities, which the EUT fails to explain [62]. According to the PT, people use their subjective probabilities ($\omega(p)$) rather than objective probabilities (p) to weight the values of possible outcomes. This phenomenon is observed in many social science studies. Authors in [63] propose an original form of probability weighting function based on experiments. Although, there have been numerous efforts to mathematically model the subjectivity in human behavior, most of these models are mathematically complex, which makes them difficult to use in real-life. Authors in [64] developed a new version of the Prospect Theory using cumulative representation of uncertainty that captures risk aversion for gains and risk seeking behavior for losses of high probability with in a low complexity analytical form. Therefore, in this work the one proposed by Prelec in [64] is used and corresponds to

$$\omega(p) = exp(-(-\log p)^{\alpha}), 0 \leq \alpha \leq 1, \tag{3.2}$$

where p is the objective probability and $\omega(p)$ is the subjective probability. Here α is the coefficient of rationality that reveals how a person's subjective evaluation distorts the objective probabilities ($\mathbb{P}$). Active consumers who are more rational have higher value for coefficient of rationality (α), whereas customers that are more subjective have lower α. Fig. 3.2 shows probability weighting function for $\alpha = 0.5$ and $\alpha = 1.0$, where $\alpha = 1$ implies that player is completely rational and behaves according to the EUT. Using the Prospect Theory, this work develops a model of a general active consumer that may not behave rationally and makes subjective decisions. In the proposed system model, the home energy management system makes real-time decisions on behalf of active consumers. Such devices must be programmed according to consumer's preferences. Different consumers can have different preferences for energy consumption and their preference can be possibly irrational, especially in the presence of uncertainty. For example, some consumers may be more risk

taking while some may be more risk averse and this variability is captured in the Prospect Theory based model. In either case, consumer preferences and their inherent irrationality can be programmed into such smart home energy management system. Since devices merely reflect consumer choices, they will not override any irrational choice made by a risk aware consumer even if it contradicts an objective option. Interaction between the consumers and the aggregator is modeled as a Stackelberg leader-follower game as discussed next.

3.2.1 Background: Stackelberg Leader-Follower Game

In game theory, Stackelberg leadership model is a strategic game in which the leader moves first and then the followers move sequentially. In the power distribution system model this corresponds to the following: the aggregator plays a mixed strategy first. The active consumers observe mixed strategy of the aggregator and decide energy consumption that maximizes their payoff function. Existence of the Stackelberg equilibrium is dependent on the following assumptions: (1) the leader chooses the optimal strategy first and it is irreversible, (2) the leader knows ex ante that the followers observe the strategy, and (3) the followers have no means of committing to a non-Stackelberg follower action and the leader knows this. In this scenario, it is assumed that the aggregator will play the optimal mixed strategy estimating the best response action of the active consumers. The active consumers will observe the mixed strategy played by the aggregator and play their best response action under uncertain price of electricity. In this Stackelberg leader-follower game between the consumers and the aggregator, the aggregator act as a leader that plays mixed strategy by deciding probability distribution for electricity prices and the consumers are followers that play pure strategy by deciding the power drawn or injected into the grid.

The proposed Prospect Theory based framework is general enough to be used for real-time or day-ahead applications. The proposed game theoretic framework models behavior of irrational active consumer for only one time instant, which can be used to model elasticity of loads. However, it does not capture time dependent model of an active consumer's behavior. A time dependent model of active consumer behavior along with correlated load scheduling

will be pursued as part of the future work which will capture shift in demands due to price of electricity.

3.3 Active Consumer Modeling

Modeling different consumer types, capturing their preferences and reactions to changes in electricity price and renewable generation is challenging. Consumers may belong to different socioeconomic classes with different value or preference for electricity consumption. In the Transactive Energy Market, the active consumers decide their energy consumption based on price of electricity that they receive from the aggregator. Actions of consumers are based on their perceived payoff. The payoff function could be composed of more than a single objective. For example, in this work, the payoff function of an active consumer incorporates three metrics corresponding to economics, comfort and environmental costs. The payoff function for i^{th} active consumer can be written as:

$$u_i(a_i, \rho) = \beta_i \log(a_i + R_i + 1) - \rho a_i - \gamma_i(\mathbf{v}(i) + \mathbf{S}(i,i)(\hat{a}_i - a_i) - 1)^2 \tag{3.3}$$

where, a_i is action of ith active consumer that represents energy purchased from the grid or sold to the grid. R_i is the amount of renewable generation available to the i^{th} consumer, which is known to the aggregator, and β_i is the comfort coefficient to represent comfort seeking level of a particular active consumer. Each active consumer gains some utility for consuming electricity as per the energy gain function, which can be written as $\beta_i \log(a_i + R_i + 1)$ [65]. The energy gain function of a consumer is an increasing function of a_i with diminishing returns. For instance, an active consumer consuming less energy benefits much more from receiving additional unit of energy than the active consumer consuming higher energy. ρ is the price of electricity that a consumer pays to the aggregator. The active consumer have to pay ρa_i amount of money to the aggregator. $v(i)$ is the distribution grid voltage at node i, and $\hat{a}_i$ indicates previous action of the i^{th} active consumer when voltage at node i of the distribution grid was $v(i)$. $\mathbf{S}(i,i)$ is i^{th} diagonal element of the voltage sensitivity matrix, and

γ_i is coefficient of grid awareness that indicates level of the i^{th} consumer's concerns for the grid voltage while taking action. Positive values of a_i indicates that the active consumer is buying energy from the grid and negative values of a_i indicate that the active consumer is selling energy back to the grid. $a_i > -R_i$, which implies that the active consumer cannot sell more energy than produced by the renewable generation. Different consumers may give different weightage to different metrics. Aggregation of these metrics into a single payoff function to decide the optimal action would depend on the class to which the active consumer belongs. For example, a highly comfort seeking consumer may have higher values of β_i compared to a low comfort seeking consumer.

This work assumes that consumers can measure the distribution grid voltage at their node of connection. However, information about voltage at nodes other than node i is not available to an active consumer not connected at node i of the distribution grid. An active consumer connected to the i^{th} node in the distribution system is also assumed to know i^{th} diagonal element of the sensitivity matrix, which can be used to compute change in voltage at node i due to change in power at node i. An analytical method to compute sensitivity matrix is proposed in [16, 17], using which an active consumer can compute i^{th} diagonal element of the sensitivity matrix ($\mathbf{S}(i,i)$). Goal of grid aware active consumers is to keep the voltage at point of connection close to the rated value by adjusting electricity consumption by minimizing $\gamma_i(\mathbf{v}(i) + \mathbf{S}(i,i)(\hat{a}_i - a_i) - 1)^2$.

In this work, type of consumers are differentiated based on their comfort requirement, price responsiveness and awareness towards grid voltage. The proposed framework is general enough to accommodate size and elasticity of different types of consumers. So, other categories/types of consumers (i.e. residential, commercial and industrial) can be seamlessly integrated into the model. Since actions of such consumers will be primarily dictated by their priorities/preferences, we use the comfort, price, and grid awareness categories to highlight the efficiency of the proposed approach. For example, among residential consumers we may have some who prefer to keep cost low while some may choose to pay higher cost to maintain their comfort levels. Similarly among industrial consumers, grid stability might be more important.

Theorem 1. *The payoff function of active consumer $u_i(a_i, \rho)$ given by equation (3.3) is a concave function of a_i.*

Proof. The payoff function for an active consumer is sum of following three terms: 1) $\beta_i \log(a_i+R_i+1)$, 2) $-\rho a_i$, and 3) $-\gamma_i(\mathbf{v}(i)+\mathbf{S}(i,i)(\hat{a}_i-a_i)-1)^2$. First term $\beta_i \log(a_i+R_i+1)$ is concave function of a_i for $\beta_i > 0$ and $a_i > -R_i$. Second term is an affine function of a_i, and third term $-\gamma_i(\mathbf{v}(i) + \mathbf{S}(i,i)(\hat{a}_i - a_i) - 1)^2$ is also concave function of a_i. As sum of concave functions is concave, payoff function for an active consumer shown in equation (3.3) is concave function of a_i. □

The electricity price, which is decided by the aggregator is unknown to the active consumers. The active consumers observe the probability distribution of uncertain electricity price and decide their action. The active consumers decides the optimal strategy based on the perceived payoff. Equation (3.4) represent expected payoff of an active consumer according to the EUT, whereas equation (3.5) shows perceived payoff of an active consumer according to the Prospect Theory.

$$\Pi_i^{EUT} = \sum_j u_i(a_i, \rho_j)\mathbb{P}(\rho = \rho_j) \tag{3.4}$$

$$\Pi_i^{PT} = \sum_j u_i(a_i, \rho_j)\omega(\mathbb{P}(\rho = \rho_j)) \tag{3.5}$$

Goal of the active consumers is to maximize their perceived payoff based on their subjective probabilities, which is given by equation (3.5). Theorem 2 shows the best response action of an active consumer.

Theorem 2. *The best response action of an active consumer that maximizes its perceived payoff is given by equation (3.6).*

$$a_i^* = arg\max_{a_i} \Pi_i^{PT} = \frac{-2z}{y - \sqrt{y^2 - 4xz}}, \tag{3.6}$$

where,

$$x = -2\gamma_i \mathbf{S}(i,i)^2, \tag{3.7}$$

$$y = 2\gamma_i \mathbf{S}(i,i)(\mathbf{v}(i) + \mathbf{S}(i,i)\hat{a}_i - 1) - \hat{P} - 2\gamma_i \mathbf{S}(i,i)^2(R_i + 1) \tag{3.8}$$

$$z = \beta_i - \hat{P}(R_i + 1) + 2\gamma_i \mathbf{S}(i,i)(\mathbf{v}(i) + \mathbf{S}(i,i)\hat{a}_i - 1)(R_i + 1) \tag{3.9}$$

Proof. The perceived payoff of an active consumer for taking action a_i for given mixed strategy of the aggregator can be written by substituting equation (3.3) in (3.5):

$$\begin{aligned} \Pi_i^{PT} = \sum_j [&\beta_i \log(a_i + R_i + 1) - \rho_j a_i \\ &-\gamma_i(\mathbf{v}(i) + \mathbf{S}(i,i)(\hat{a}_i - a_i) - 1)^2] \, \omega(\mathbb{P}(\rho = \rho_j)) \end{aligned} \tag{3.10}$$

The active consumers take an action that maximizes their perceived payoff Π_i^{PT}. Let a_i^* be an optimal action of the active consumer given by:

$$a_i^* = \arg\max_{a_i} \Pi_i^{PT}, \tag{3.11}$$

where a_i^* is the optimal action of an active consumer that maximizes the perceived payoff. The optimal action of an active consumer can be found by differentiating the perceived payoff by action of the active consumer and equating it to zero.

$$\begin{aligned} &\frac{\partial \Pi_i^{PT}}{\partial a_i} = 0 \\ &\sum_j \left[\frac{\beta_i}{a_i + R_i + 1} - \rho_j - 2\gamma_i \mathbf{S}(i,i)(\mathbf{v}(i) \right. \\ &\left. + \mathbf{S}(i,i)(\hat{a}_i - a_i) - 1) \right] \omega(\mathbb{P}(\rho = \rho_j)) = 0, \end{aligned} \tag{3.12}$$

Dividing with $\omega(\mathbb{P}(\rho = \rho_j))$ we wet

$$\begin{aligned} &\frac{\beta_i}{a_i + R_i + 1} - \frac{\sum_j \rho_j \omega(\mathbb{P}(\rho = \rho_j))}{\sum_j \omega(\mathbb{P}(\rho = \rho_j))} \\ &- 2\gamma_i \mathbf{S}(i,i)(\mathbf{v}(i) + \mathbf{S}(i,i)(\hat{a}_i - a_i) - 1) = 0. \end{aligned} \tag{3.13}$$

Let $\hat{P}$ be the perceived price of electricity defined as:

$$\hat{P} = \frac{\sum_j \rho_j \omega(\mathbb{P}(\rho = \rho_j))}{\sum_j \omega(\mathbb{P}(\rho = \rho_j))}. \tag{3.14}$$

Substituting equation (3.14) into equation (3.13):

$$\frac{\beta_i}{a_i + R_i + 1} - \hat{P} - 2\gamma_i \mathbf{S}(i,i)(\mathbf{v}(i) + \mathbf{S}(i,i)(\hat{a}_i - a_i) - 1) = 0. \tag{3.15}$$

Multiplying equation (3.15) with $a_i + R_i + 1$ and simplifying to standard quartic form, we get

$$\begin{aligned} &- 2\gamma_i \mathbf{S}(i,i)^2 a_i^2 + \Big[2\gamma_i \mathbf{S}(i,i)(\mathbf{v}(i) + \mathbf{S}(i,i)\hat{a}_i - 1) - \hat{P} \\ &-2\gamma_i \mathbf{S}(i,i)^2 (R_i + 1)\Big] a_i + \Big[\beta_i - \hat{P}(R_i + 1) \\ &+2\gamma_i \mathbf{S}(i,i)(\mathbf{v}(i) + \mathbf{S}(i,i)\hat{a}_i - 1)(R_i + 1)\Big] = 0 \end{aligned} \tag{3.16}$$

Solution of above quadratic equation corresponds to:

$$a_i^* = \frac{-2z}{y - \sqrt{y^2 - 4xz}} \tag{3.17}$$

where x, y and z are given by equation (3.7)(3.8) and (3.9). □

Although an individual active residential consumers may not cause or solve voltage violation in the distribution system due to relatively low value of energy consumption or generation, commutative actions of multiple active consumers with distributed energy sources could cause voltage changes in the power distribution system, which would be detrimental to all consumers. In the envisioned transactive energy system with consumer owned distributed generation, voltage violations can be avoided by raising consumer awareness about

grid voltage and programming grid awareness into smart home energy management systems. Additionally, large industrial consumers with large load/generation can make a significant impact on voltage profile and may have to pay penalties for voltage violations. In such scenarios, the active consumers may care about the grid voltage profile. This is especially applicable for microgrid environment, where the distribution system is more prone to voltage fluctuations. However, in this work, violations in the distribution system voltages are not modeled as a hard constraint, which may results in infeasible solution. Although idea of grid aware consumers may be futuristic at this point, this work demonstrates that one way to solve voltage violation in the future smart grid is by the active consumer participation. Further, this work assumes that the aggregator and the active consumers can calculate the line voltage at the point of grid connection using smart meter data. This will allow the active consumer to know the grid voltage. Based on the voltage information and location of the household in the grid, an active consumer can compute value of $\mathbf{S}(i,i)$ using an analytical method of voltage sensitivity analysis proposed in [16, 17]. Further, this work assumes that the aggregator has some method of estimating coefficient of rationality of the active consumers. In practice, the aggregator can observe past responses of active consumers to change in price of electricity and the distribution system voltages to estimate coefficient of rationality α_i and other behavioral parameters such as β_i and γ_i. This can be done using regression and curve fitting algorithms. There is a plethora of techniques available in the area of machine learning to estimates the best response strategy of the active consumers. Exact method of estimating such parameters is outside the scope of this research. We believe that the advances in data analytic in the smart grid domain will make this feasible in the near future. Based on estimated best response actions of all the active consumers, the aggregator decides the optimal probability distribution of electricity prices that maximizes the payoff.

3.4 Behavior of the Aggregator

Goal of the aggregator is to maximize the monetary profit while improving voltage profile of the power distribution grid. The aggregator purchases A kWh of energy from day-ahead

market at cost ρ_{da} unit/kWh. Any additional energy is purchased in the real-time market at ρ_{rt} unit/kWh. It is assumed that the aggregator knows best response action of all active consumers. In other words, the aggregator is assumed to know $\beta_i, \gamma_i, R_i, \mathbf{v}, \mathbf{S}, \hat{a}_i$ and the coefficient of rationality for all the active consumers. The impact of lack of knowledge or incorrect information about consumer behavior is analyzed in the results section. Let $\mathbf{a}$ be a vector of the best response action of all the active consumers, $\hat{\mathbf{a}}$ be a vector of previous action of all the active consumers, $\mathbf{v}$ be a vector of the distribution grid voltage and $\mathbf{S}$ be the sensitivity matrix. Payoff function of the aggregator can be written as:

$$u_a = \mathbb{P}^T \rho \mathbf{a^T 1} - \rho_{da} A - \theta \|\mathbf{v} + \mathbf{S}(\hat{\mathbf{a}} - \mathbf{a}) - \mathbf{1}\| - \rho_{rt}(\mathbf{a^T 1} - A), \tag{3.18}$$

where $\mathbf{1}$ is vector of all 1's and θ is the coefficient of grid awareness for the aggregator that indicates how much the aggregator is committed to maintaining the physical grid voltage. Here, $\mathbb{P}^T \rho \mathbf{a^T 1}$ indicates the total income of the aggregator from money charged to the active consumers. Second term in equation (3.18), $\rho_{da} A$, is the amount that the aggregator pays to the independent system operator (ISO) for buying bulk electricity in the day-ahead market. Last term in equation (3.18), $\rho_{rt}(\mathbf{a^T 1} - A)$, indicates the cost of additional energy purchased from the real-time market. Finally, $\|\mathbf{v} + \mathbf{S}(\hat{\mathbf{a}} - \mathbf{a}) - \mathbf{1}\|$ is the metric that indicates deviation of the distribution grid voltage from the rated voltage. The aggregator decides the probability distribution of electricity prices that maximizes (3.18).

Theorem 3. *For* $0.1\mathbf{1} \leq \mathbb{P} \leq 0.9\mathbf{1}$*, payoff function of an aggregator is a concave function of* $\mathbb{P}$ *.*

Proof. Payoff function of the aggregator is given by equation (3.18). From lemma 1, it can be proven that the optimal action of an active consumer a_i is a convex decreasing function of $\mathbb{P}$. As sum of convex functions is convex, $\mathbf{a_i^T 1}$ is also a convex function of $\mathbb{P}$ for $0.1\mathbf{1} \leq \mathbb{P} \leq 0.9\mathbf{1}$.

The first term of equation (3.18), $\mathbb{P}^T \rho \mathbf{a^T 1}$ is a concave function of $\mathbb{P}$ as it is product of a linearly increasing function of $\mathbb{P}$ ($\mathbb{P}^T \rho$) and a convex decreasing function of $\mathbb{P}$ ($\mathbf{a^T 1}$). The second term of equation (3.18), $-\rho_{da} A$ is a constant. As convex function of a convex function

is convex, $-\theta\|\mathbf{v}+\mathbf{S}(\hat{\mathbf{a}}-\mathbf{a})-\mathbf{1}\|$ is a concave function of $\mathbb{P}$. From lemma 1, it can be shown that $-\rho_{rt}(\mathbf{a^T 1}-A)$ is a concave function of $\mathbb{P}$ as ρ_{rt} and A are constant. Summation of concave functions is concave leading to Theorem 3.

□

The optimal mixed strategy of the aggregator corresponds to (3.19)

$$\mathbb{P}^* = \arg\max_{\mathbb{P}} u_a, \tag{3.19}$$

which can be found numerically. Based on estimated best response of the active consumers, the aggregator decides the optimal probability distribution of electricity prices that maximize the aggregator's objective function, which is the Stackelberg equilibrium strategy of the aggregator. In a highly dynamic transactive energy market, electricity prices changes in real-time. In the proposed system model, the aggregator can determine the distribution for price of electricity (based on estimated response) and announce mixed strategy to the active consumers. This probability distribution for electricity price can be treated as the preliminary handshake process that establishes equilibrium electricity prices. The aggregator will decide and announce the actual price of electricity based on the equilibrium probability distribution. The active consumers observe the aggregator's mixed strategy and decide their optimal response based on their perceived probability distribution. This leader follower game results in a Stackelberg equilibrium where all the active consumers and the aggregator are playing their optimal strategy. Change in the Stackelberg equilibrium with change in consumer type and rationality and their impact on physical grid voltage is investigated in the next section.

3.5 Simulation and Results

To investigate the Stackelberg equilibrium of the proposed system, we use a modified IEEE 69 bus system as shown in Fig. 3.3. A scenario is considered where four type of active consumers exist in the distribution grid. Type-A active consumers are highly comfort-seeking

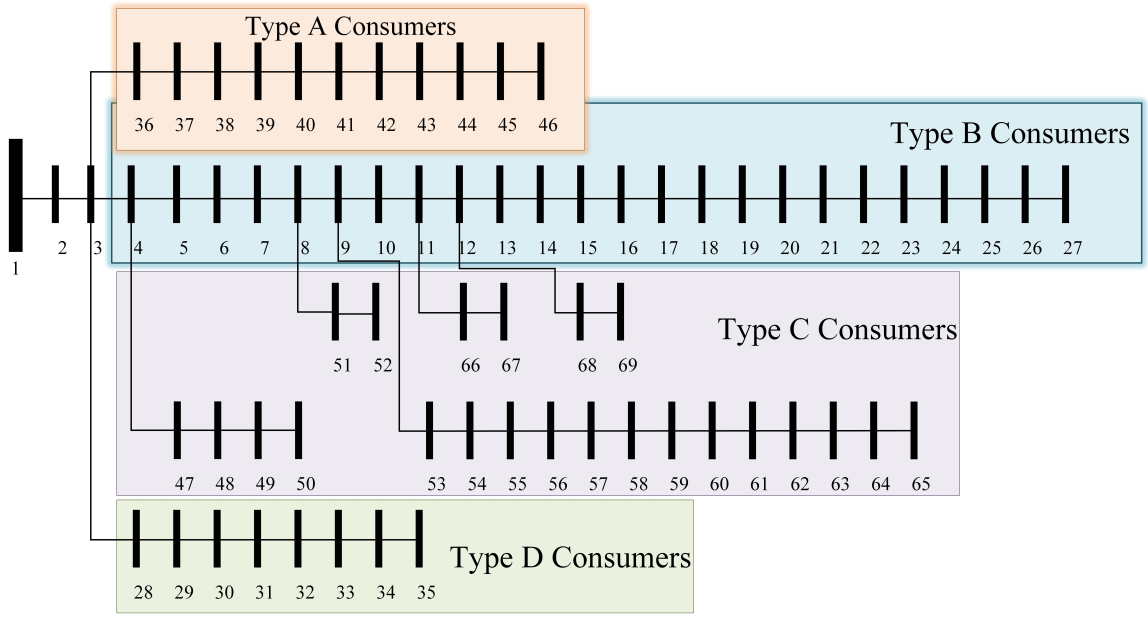

Figure 3.3: *Consumer Types and location on IEEE 69 bus test system*

Table 3.1: *Consumer Types*

Consumer Type	β	γ
A - Highly comfort-seeking and grid aware	0.85	1
B - Comfort-seeking and grid aware	0.75	1
C - Comfort-seeking and grid unaware	0.75	0
D - Low comfort-seeking and grid aware	0.40	1

and consider grid voltage while making decisions. Type-B active consumers are relatively low comfort-seeking and are also grid aware. Type-C active consumers have the same level of comfort requirement as type-B active consumers but they do not consider physical grid voltage while making decisions, and type-D active consumers are the least comfort-seeking with the lowest value of β. Table 3.1 summarizes the type of active consumers and their value of β and γ. In order to maintain fairness of weights, values of β and γ are normalized using weight fairness model proposed in [66]. Fig. 3.3 shows location of different kind of active consumers in the distribution grid. There are no active consumers connected to bus 1 to 3. Note that the modeling and analysis approach is general and is applicable to other scenarios as well. For simplicity in interpretation, renewable generation for each active consumer (R_i) is set at 10 kWh. The price of electricity can take one of the following values: (1) 0.1

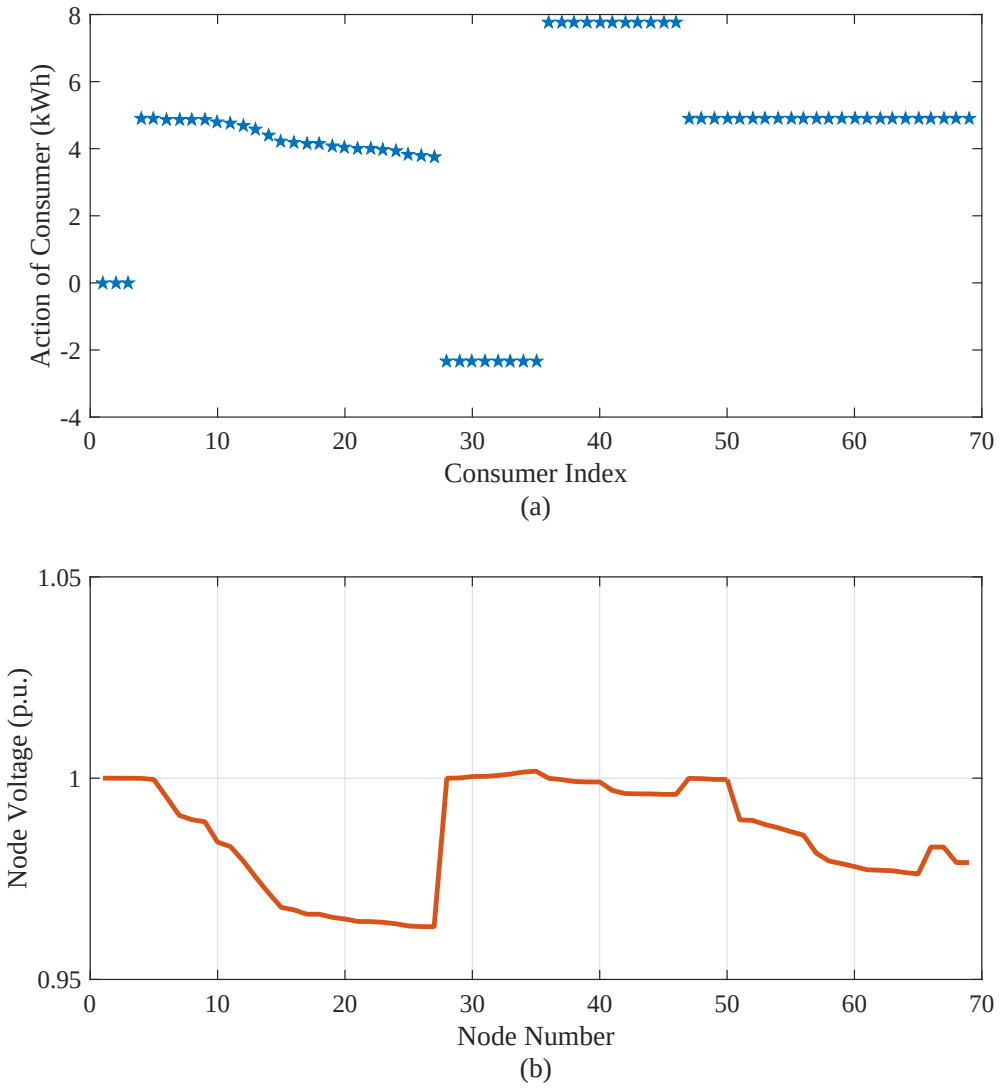

Figure 3.4: *Stackelberg equilibrium and corresponding voltage level*

unit/kWh; (2) 0.5 unit/kWh, and (3)1.0 unit/kWh ($\rho = \{0.1, 0.5, 1.0\}$). For this case, the optimal mixed strategy of the aggregator at the Stackelberg equilibrium is shown in Table 3.2. Actions of a consumer in response to the optimal mixed strategy of the aggregator are shown in Fig. 3.4(a) and corresponding distribution grid voltage levels are shown in Fig. 3.4(b). From Fig. 3.4(a) it can be seen that energy consumptions of type-A active consumers are much higher compare to the other active consumers because of higher value of β_i. On the contrary, type-D active consumers which are low comfort-seeking prefer to sell

Table 3.2: *Stackelberg equilibrium strategy of the aggregator*

Price of electricity (ρ)	0.1	0.5	1.0
Probability $\mathbb{P}(\rho)$	0.16	0.18	0.66

some of the renewable generation back to the grid in order to make more money resulting it negative values of a_i. Voltages at bus 28 to 35 are higher than 1 p.u. because of the active consumers injecting power into the grid. Although all type-B active consumers have same value of β and γ, their actions are different because they adjust their energy consumption in accordance with physical grid voltage as shown in Fig. 3.4(a). On the other side, actions of all type-C consumers are the same as they do not consider physical grid voltage while making their decisions. The best response action of an active consumers can be computed using analytical expression provided by Theorem 2, which can be computed quickly. For the aggregator, computation of the optimal mixed strategy requires estimation of the best response strategy of all the active consumers. Although the exact computational complexity of such estimation can vary based on the exact method used, this step has to be performed only once and does not have to be done in real-time. Once the best response action of all the active consumers is estimated, the optimal mixed strategy of the aggregator $\mathbb{P}^*$ can be computed numerically as unconstrained convex optimization problem. Computation time to calculate the Stackelberg equilibrium for the IEEE 69 bus distribution system is 1.81 second. The IEEE 69 bus distribution system is used in this work, which is adequate to demonstrate the methodology presented in this work.

Fig. 3.5 shows change in consumer action with rationality level of the active consumer. An active consumer is considered with $\beta = 0.65$, $\gamma = 1, R_i = 10kWh$ located at node 16 of the IEEE 69 bus test system. In this scenario price of electricity can take only two values $0.1(unit/kWh)$ and $0.5(unit/kWh)$ ($\rho = \{0.1, 0.5\}$). The curve with triangle markers represents a case where $\mathbb{P}(\rho = 0.1) = 0.8$ and $\mathbb{P}(\rho = 0.5) = 0.2$, and the expected value of price of electricity is 0.18 unit. It can be observed that the active consumers with lower rationality are more risk averse when expected price of electricity is low. Curve with diamond marker represent a case where $\mathbb{P}(\rho = 0.1) = 0.2$ and $\mathbb{P}(\rho = 0.5) = 0.8$, with the expected

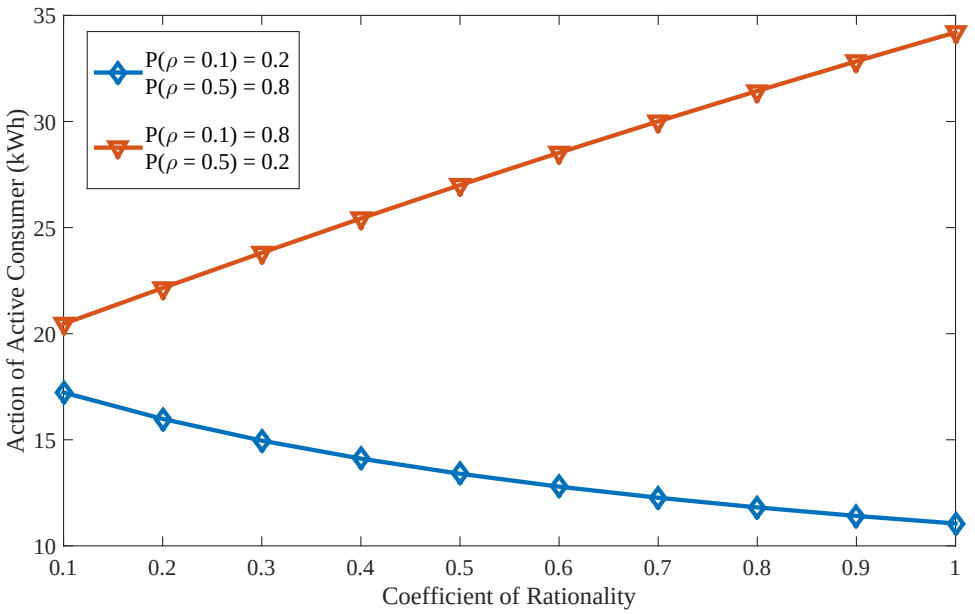

Figure 3.5: *Change in active consumer action with coefficient of rationality*

value of price of electricity of 0.42 unit. The active consumers with lower rationality are more risk taking when expected price of electricity is high for lower values of α.

Fig. 3.6 shows change in the aggregator profit and number of voltage violations at the Stackelberg equilibrium for different coefficient of rationality of the active consumers. Here, it is assumed that all the active consumers have same coefficient of rationality and the aggregator is assumed to know it. From Fig. 3.6(a) it can be seen that the aggregator's monetary profit decreases as the active consumers become more rational. This implies that the aggregator can exploit irrational behavior of the active consumers. Grid aware the active consumers modify their power based on voltage at the point of connection. However, the profit of the aggregator depends on how the active consumers respond to changes in electricity prices. Therefore, the profit of the aggregator does not change significantly based on grid awareness of consumers. Fig. 3.6(b) shows number of voltage violations at the Stackelberg equilibrium for different coefficient of rationality, when the active consumers have high coefficient of grid awareness ($\gamma = 1$) and when the active consumers are grid unaware ($\gamma = 0$). It can be seen from Fig. 3.6(b) that number of voltage violations are less when the active consumers are grid aware. Fig. 3.6(b) also shows that number of voltage

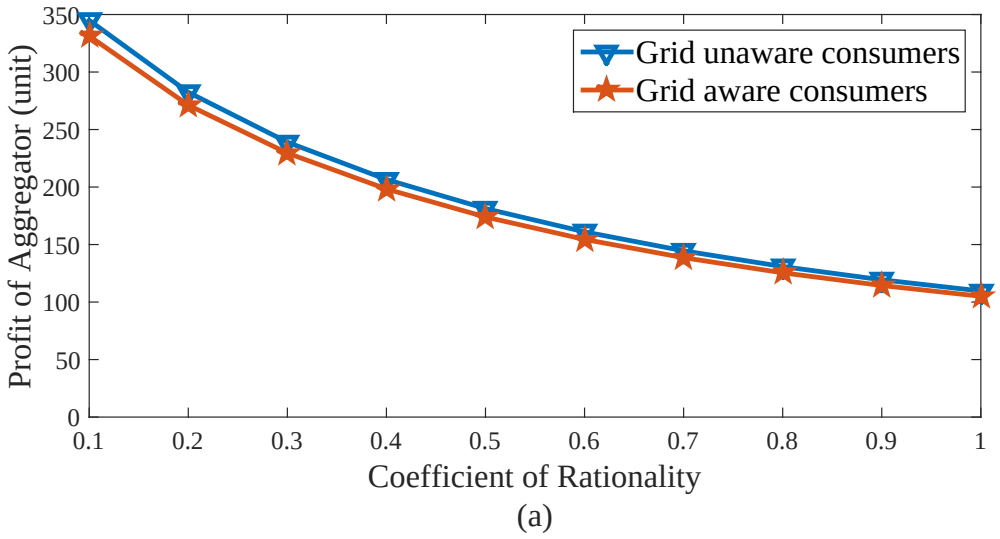

(a)

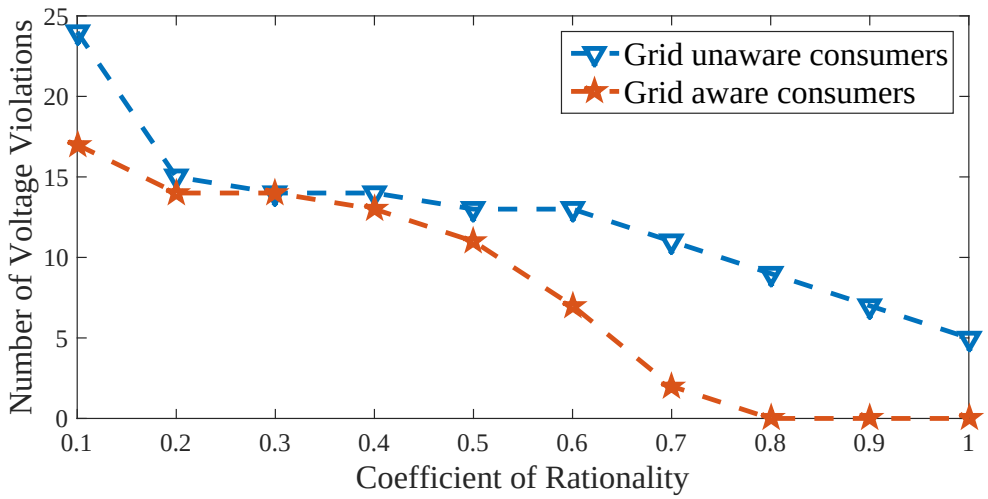

(b)

Figure 3.6: *(a) Change in the aggregator profit at equilibrium with coefficient of rationality (b) Corresponding number of voltage violations*

violations decrease as consumers behave more rationally.

To highlight difference between the EUT and the Prospect Theory models, we consider two different scenarios and observe action of the active consumers for each case. In case one, the support set for price of electricity is $\rho = \{0.1, 0.5, 1.0\}$ and for the second case support set for price of electricity is $\rho = \{0.5, 0.7, 1.0\}$. In both the scenarios expected price of electricity is kept the same to 0.9 unit/kWh. All other parameters are kept the same in both cases.

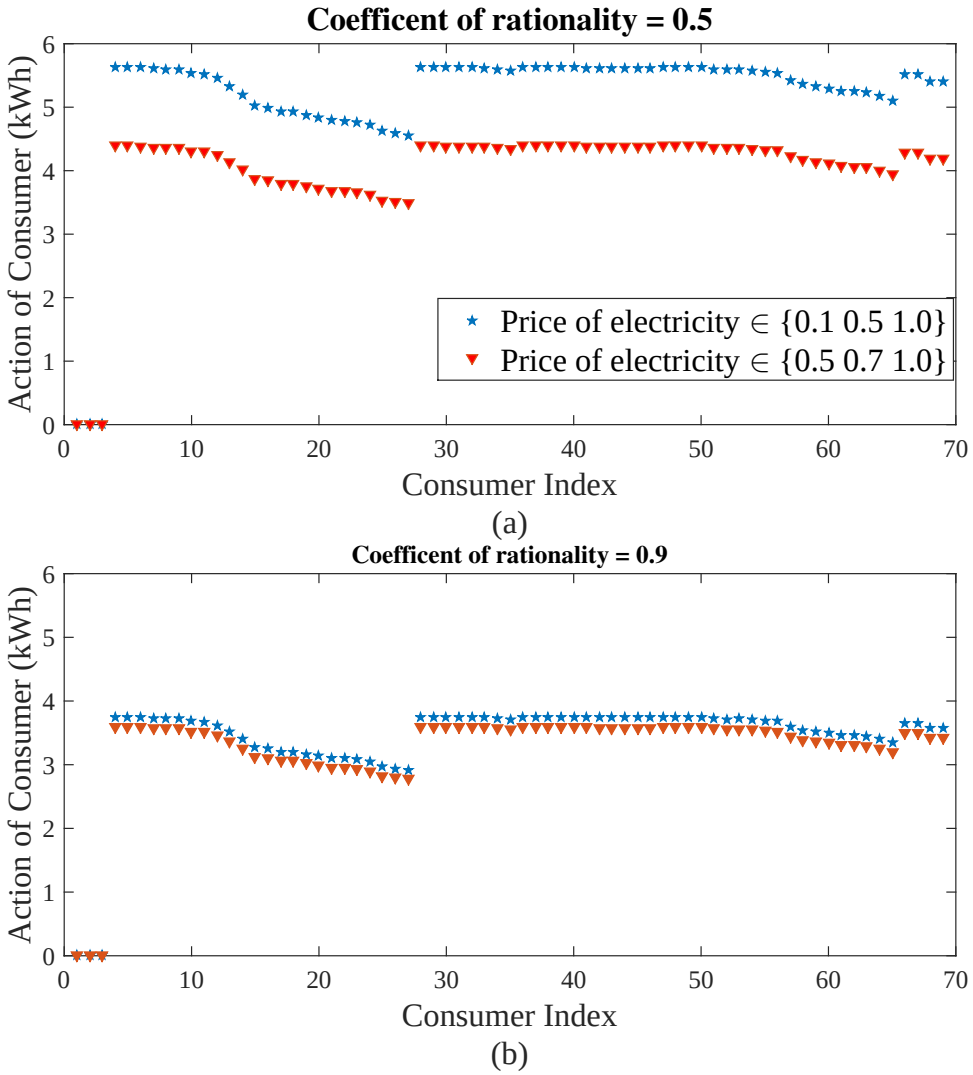

Figure 3.7: *Change in consumer behavior with change in reference price level*

According to the EUT, the action of the active consumers should be the same in both cases, which is not the case in reality. When the active consumers are not completely rational, their actions differ in both cases as shown in Fig. 3.7. Fig. 3.7(a) and 3.7(b) show actions of all the active consumers when coefficient of rationality for all the active consumers are set to 0.5 and 0.9 respectively. From Fig. 3.7(a), it can be observed that actions of the active consumers are very different for these scenarios when the active consumers are relatively less rational ($\alpha = 0.5$); however, actions of the active consumers are almost the same for both scenarios as they are highly rational ($\alpha = 0.9$) as shown in Fig. 3.7(b).

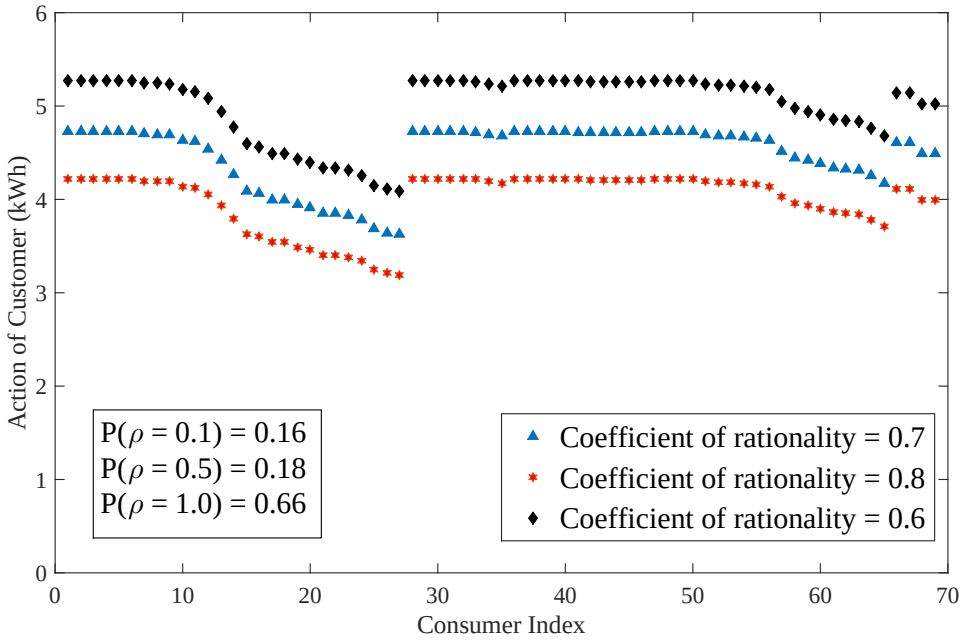

Figure 3.8: *Active consumer actions for different coefficient of rationality*

The active consumers with different levels of rationality take different actions under the same probability distribution of electricity price. A scenario is considered when there is an error in the aggregator's estimate of coefficient of rationality (α). The aggregator decides the optimal mixed strategy assuming $\alpha_i = 0.7$ for all the active consumers. However, actual coefficient of rationality for the active consumers is different. In this scenario, values of $\beta = 0.85$ and $\gamma = 1$ are assumed to be known to the aggregator. Sample space for the price of electricity is $\{0.1, 0.5, 1.0\}$ and the optimal mixed strategy of the aggregator is $\{0.16, 0.18, 0.66\}$ assuming $\alpha = 0.7$. Fig. 3.8 shows response of the active consumers for a given mixed strategy of the aggregator. Expected response of the active consumers by the aggregator is represented by curve with triangle markers, which corresponds to the case where $\alpha = 0.7$ for all the active consumers. If coefficient of rationality for all the active consumers is 0.6 or 0.8, actual response of the active consumers is represented by curve with diamond and hexagram markers respectively. This shows that incorrect estimation of coefficient of rationality can result in actions different from actions expected from the consumers.

Number of physical voltage violations can be reduced when the active consumers do

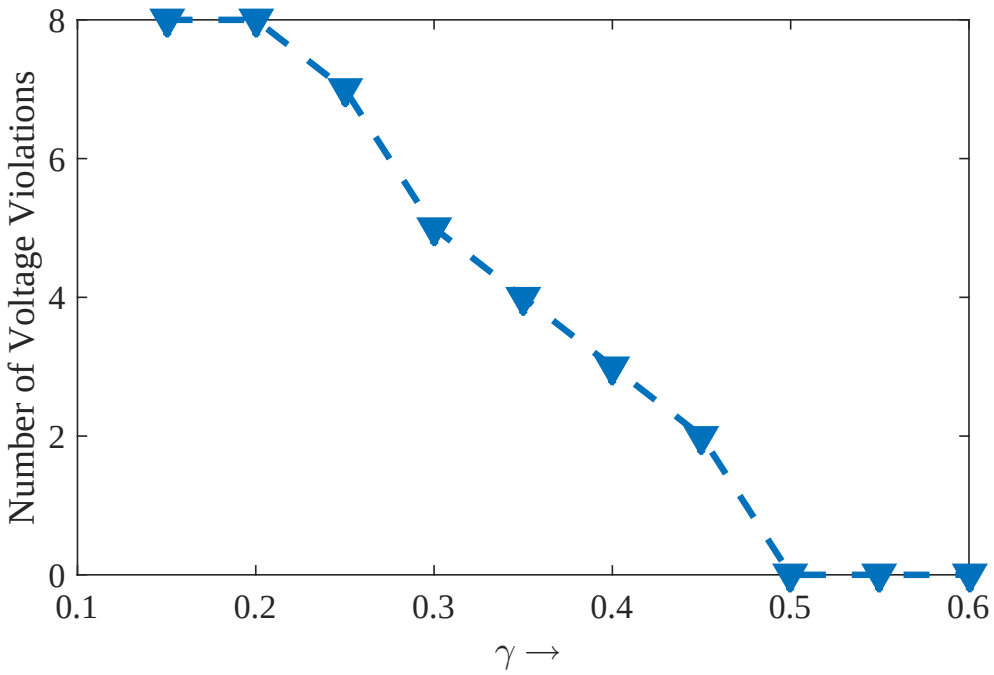

Figure 3.9: *Change in number of voltage violation at equilibrium with* γ

consider physical voltage while taking actions. To observe change in number of voltage violations with γ, a scenario is considered where $\alpha = 0.8$ and $\beta = 0.85$ for all the consumers. Fig. 3.9 shows change in number of voltage violation for different values of γ. As value of γ increases number of voltage violations decrease.

3.6 Summary

This chapter develops a Prospect Theory based realistic model of the active consumers with varied preferences for electricity consumption and different levels of rationality. The interaction between the active consumers and the aggregator is modeled as a Stackelberg leader-follower game from a techno-economic perspective by including physical grid constraints in terms of voltage violation within the analysis. The interaction between the active consumers and the aggregator is analyzed using simulations on the IEEE 69 bus test system. Impact of consumer actions and irrationality on physical grid voltage and the aggregator payoff is quantified using simulation.

Chapter 4

Analytical Method of Voltage Sensitivity Analysis

After developing model of active consumer in last chapter, in the next two chapters we will develop probabilistic voltage sensitivity analysis - an analytical tool to investigate impact of large scale penetration of active consumers on distribution system voltage. The power grid will no longer be only a delivery mechanism for electricity after the introduction of active consumers and increasing penetration of renewable generation. These installations will inject current back into the grid, thereby affecting the voltage profile of the distribution network. Analyzing the impact of large-scale penetration of active consumers on the voltage profile will be critical for distribution grid operational planning.

Sensitivity analysis studies change in voltage at a given bus in a distribution system as a function of change in active and reactive power at another bus in the network. Current methods of sensitivity analysis uses numerical methods to compute sensitivity matrix. For example, the sensitivity matrix is usually calculated by perturb and observe method or from inverse of Jacobian matrix used in power flow calculations[67]. Such traditional methods do not provide analytical insight on the impact of change in power consumption at one bus on voltage at other nodes. Most of these studies are simulation based [68, 69, 70]. Random behavior of spatially distributed multiple active consumers can cause random fluctuations in

voltage of distribution network. Traditional method of sensitivity analysis cannot be used to derive the probability distribution of voltage change at any given node in the network. This work aims to help grid operators prepare for the future modernized grid by introducing an analytical method for voltage sensitivity analysis, leading to new insights on the impact of active consumers on grid operations.

4.1 Background: Traditional Methods of Voltage Sensitivity Analysis

Consider a power distribution network with N buses. Let P_i and Q_i be real and reactive power consumption at bus i. Change in real or reactive power consumption at any bus in the network results in change in voltage magnitude $|\Delta V_j|$ and change in angle of voltage $\Delta\theta_j$ at bus j. Sensitivity matrix is a $2N \times 2N$ matrix indicating bus voltage sensitivity in power distribution network due to variations of active and reactive power. Two traditional methods of sensitivity analysis are the Newton-Raphson load flow method and the perturb-and-observe method. The Newton-Raphson load flow algorithm is an iterative approach to calculate network bus voltages. Conventionally, the sensitivity matrix is readily obtained from the inverse of the standard Jacobian matrix $\mathbf{J}$ used in the Newton-Raphson load-flow technique [71]. The updated equation for the algorithm is:

$$\begin{bmatrix} \Delta\theta_2 \\ \vdots \\ \Delta\theta_n \\ \hline \\ \frac{\Delta|V_2|}{|V_2|} \\ \vdots \\ \frac{\Delta|V_n|}{|V_n|} \end{bmatrix} = \mathbf{J^{-1}} \begin{bmatrix} \Delta P_2 \\ \vdots \\ \Delta P_n \\ \hline \\ \Delta Q_2 \\ \vdots \\ \Delta Q_n \end{bmatrix}, \tag{4.1}$$

where $\Delta\theta_n$ is change in phase and $\frac{\Delta|V_n|}{|V_n|}$ is fractional change in voltage at bus n. It must be noted that bus one is not included in calculation as bus one is typically considered to be the substation set at stable voltage of $1\angle 0$ per unit. ΔP_m and ΔQ_m are the real and reactive power injected at bus m. Once the load flow solution converges, the Jacobian matrix specifies the sensitivities of P_m and Q_m with respect to $|V_n|$ and θ_n for the current state of the system. That is, the Jacobian matrix $\mathbf{J}$ corresponds to:

$$\mathbf{J} = \left[\begin{array}{ccc|ccc} \frac{\partial P_2}{\partial \theta_2} & \cdots & \frac{\partial P_2}{\partial \theta_n} & |V_2|\frac{\partial P_2}{\partial |V_2|} & \cdots & |V_n|\frac{\partial P_2}{\partial |V_n|} \\ \vdots & \mathbf{J_{11}} & \vdots & \vdots & \mathbf{J_{12}} & \vdots \\ \frac{\partial P_n}{\partial \theta_2} & \cdots & \frac{\partial P_n}{\partial \theta_n} & |V_2|\frac{\partial P_n}{\partial |V_2|} & \cdots & |V_n|\frac{\partial P_n}{\partial |V_n|} \\ \hline \frac{\partial Q_2}{\partial \theta_2} & \cdots & \frac{\partial Q_2}{\partial \theta_n} & |V_2|\frac{\partial Q_2}{\partial |V_2|} & \cdots & |V_n|\frac{\partial Q_2}{\partial |V_n|} \\ \vdots & \mathbf{J_{21}} & \vdots & \vdots & \mathbf{J_{22}} & \vdots \\ \frac{\partial Q_n}{\partial \theta_2} & \cdots & \frac{\partial Q_n}{\partial \theta_n} & |V_2|\frac{\partial Q_n}{\partial |V_2|} & \cdots & |V_n|\frac{\partial Q_n}{\partial |V_n|}. \end{array}\right] \tag{4.2}$$

The Newton-Raphson method is convenient when the Jacobian of the Newton-Raphson load-flow algorithm is accessible, which is not the case always. Many software packages do not allow users to access Jacobian matrix. An alternative method to perform sensitivity analysis is the *"perturb-and-observe"* approach. This method relies on making small perturbation in complex bus power consumption and measuring the impact on bus voltages of the system [67]. This approach is less efficient because it recomputes the entire network state for any minor changes within the network, making the method slow and computationally complex.

To summarize, existing methods of sensitivity analysis are based on iterative algorithms with significant computational complexity. The Jacobian matrix obtained from the Newton-Raphson method is valid only for a specific state of the system and must be recomputed for major changes in the network state. None of the described methods allow straightforward analytical computation of voltage change at a particular bus as function of complex power injection at another bus in the network. This hampers the investigation of scenarios where one might encounter stochastic behavior of active consumers, power generated etc. Current methods of sensitivity analysis uses numerical methods to compute the sensitivity

matrix. Value of sensitivity matrix computed using such method is valid for given state of the system, and it do not provide any analytical insight into effect of grid state on values of sensitivity matrix. For example, sensitivity matrix computed using such method do not provide information about effect of grid voltage on values of sensitivity matrix. Any probabilistic analysis done using such method is valid for given state of the system only. In a case where state of the distribution system is random, i.e. voltages at actor nodes is random, we need analytical method of sensitivity analysis to derive probability distribution of voltage change. Section 4.2 provides a computationally efficient analytical method of computing an element-wise upper bound on the sensitivity matrix.

4.2 Analytical Method for Sensitivity Analysis

Change in power consumption at any node causes change in voltage at all nodes in a distribution system. In this dissertation, terms node and bus are used interchangeably. Nodes that change their power consumption are referred to as actor nodes, and node where change in voltage is examined is referred to as an observation node. This section develops an analytical upper bound for voltage change at an observation node (ΔV_o) due to change in complex power at an actor node (ΔS_a) in a radial distribution network. It is assumed that the source bus acts like a slack bus. In other words, voltage at the substation is assumed to be constant at all times irrespective of changes in network power consumption. This work assumes a constant power model for loads in the power flow. When an actor node (a) changes its complex power consumption from S_a to $S_a + \Delta S_a$, voltage at observation node changes from V_o to $V_o + \Delta V_{oa}$. Here ΔV_{oa} is change in complex voltage at observation node o due to change in complex power at actor node a. For now, let's assume that power consumption at all other nodes is unchanged.

Theorem 4. *For a radial power distribution network, change in voltage at an observation*

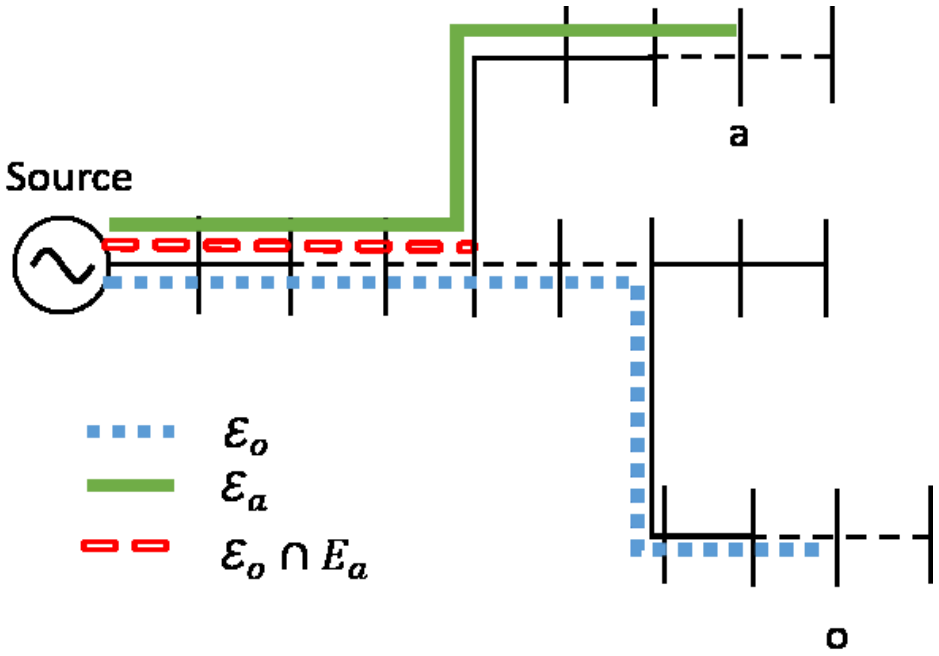

Figure 4.1: *Illustration of shared conductor between two nodes*

node due to change in power consumption of an actor node is upper bounded by

$$\Delta V_{oa} \leq -\frac{\Delta S_a Z_{oa}}{V_a^*}, \tag{4.3}$$

where V_a^* is complex conjugate of voltage at the actor node; and Z_{oa} is impedance of shared line between observation node o and actor node a from the source node, as illustrated in Fig. (4.1) with the red line.

Proof. Voltage at an observation node can be expressed in terms of difference between voltage at source node and sum of voltage drop across all edges between observation node and source node. Let $\mathcal{E}_o$ be a set of edges between source node and observation node. Using Kirchhoff's voltage law (KVL), voltage at node o can be written as:

$$V_o = V_s - \sum_{e \in \mathcal{E}_o} V_e^d, \tag{4.4}$$

where V_e^d is voltage drop across edge e. Let I_e be current flowing though edge e and Z_e be

impedance of edge e. In LV distribution networks, value of shunt impedance in very small and is usually ignored as standard practice [48]. According to KCL voltage at node o can be written in terms of line current and line impedance as follows:

$$V_o = V_s - \sum_{e \in \mathcal{E}_o} I_e Z_e \tag{4.5}$$

Let S_n be complex power consumption/injection at node n, and V_n^* be complex conjugate of voltage at node n. Total current flowing through edge e can be written as $\sum_{n \in \mathcal{N}_e} \frac{S_n}{V_n^*}$, where $\mathcal{N}_e$ is the set of all nodes n for which edge e is between node n and source node. Power from source node to all nodes in the set $\mathcal{N}_e$ flows though edge e. Therefore, change in power consumption at nodes $n \in \mathcal{N}_e$ results in change in current flowing through edge e. Now voltage at observation node can be written as

$$V_o = V_s - \sum_{e \in \mathcal{E}_o} \left(\sum_{n \in \mathcal{N}_e} \frac{S_n}{V_n^*} \right) Z_e. \tag{4.6}$$

$\mathcal{N}_e$ is the set of all nodes n for which e is between node n and source node. Now if power consumption of all nodes change from S_n to S'_n, then voltage at all nodes will change from V_n to V'_n and so voltage at observation node will change to V'_o. Changed voltage (V'_o) at the observation node due to changed power consumption of multiple nodes can be written as:

$$V'_o = V_s - \sum_{e \in \mathcal{E}_o} \left(\sum_{n \in \mathcal{N}_e} \frac{S'_n}{V'^*_n} \right) Z_e, \tag{4.7}$$

where $S'_n = S_n + \Delta S_n$ and $V'_n = V_n + \Delta V_n$ are changed power consumption and changed voltage of node n, respectively. The effective voltage change at observation node can be written as: $\Delta V_o = V'_o - V_o$. From equation (4.6) and (4.7), change in observation node

voltage can be expressed as:

$$\begin{aligned}\Delta V_o &= \sum_{e\in\mathcal{E}_o}\left(\sum_{n\in\mathcal{N}_e}\frac{S_n}{V_n^*}\right)Z_e - \sum_{e\in\mathcal{E}_o}\left(\sum_{n\in\mathcal{N}_e}\frac{S_n'}{V_n'^*}\right)Z_e \\ &= \sum_{e\in\mathcal{E}_o}\left(\sum_{n\in\mathcal{N}_e}\frac{S_n}{V_n^*} - \frac{S_n+\Delta S_n}{V_n^*+\Delta V_n^*}\right)Z_e \\ &= \sum_{e\in\mathcal{E}_o}\left(\sum_{n\in\mathcal{N}_e}\frac{S_n\Delta V_n^* - \Delta S_n V_n^*}{(V_n^*)(V_n^*+\Delta V_n^*)}\right)Z_e\end{aligned} \tag{4.8}$$

For practical purpose it is reasonable to assume that change in voltage is small compared to the actual node voltage. Therefore, it is reasonable to assume that $\Delta V_n^*/V_n^*(V_n^*+\Delta V_n^*) \to 0$ as $\Delta V_n^* << V_n^*(V_n^*+\Delta V_n^*)$. Voltage change at observation node represented by equation (4.8) can be approximated as;

$$\Delta V_{oa} \approx \sum_{e\in\mathcal{E}_o}\left(\sum_{n\in\mathcal{N}_e}\frac{-\Delta S_n}{V_n^*+\Delta V_n^*}\right)Z_e. \tag{4.9}$$

Equation (4.9) holds for cases with more than one actors nodes. Here only one actor node is changing its power consumption; therefore, ΔS_n is zero for all nodes except one particular actor node a. Let $\mathcal{E}_a$ be a set of all edges between actor node and source node. When actor node a changes power consumption, current flowing though edges changes for all edges that belongs to set $\mathcal{E}_a$, and voltage drop across edges changes only for edges that belongs to subset $\mathcal{E}_o \cap \mathcal{E}_a$.

$$\begin{aligned}\Delta V_{oa} &= \sum_{e\in\mathcal{E}_o\cap\mathcal{E}_a}\left(\sum_{n\in\mathcal{N}_e}\frac{-\Delta S_n}{V_n^*+\Delta V_n^*}\right)Z_e \\ &= \sum_{e\in\mathcal{E}_o\cap\mathcal{E}_a}\frac{-\Delta S_a}{V_a^*+\Delta V_{aa}^*}Z_e = \frac{-\Delta S_a}{V_a^*+\Delta V_{aa}^*}Z_{oa},\end{aligned} \tag{4.10}$$

where $Z_{oa} = \sum_{e\in\mathcal{E}_o\cap\mathcal{E}_a} Z_e$ is impedance of the shared line between node o and a from the source node. Equation (4.10) can be written in term of real and imaginary values as follows.

$$\Delta V_{oa}^r = -\left[\frac{(\Delta P_a R_{oa} - \Delta Q_a X_{oa})(V_a^r+\Delta V_{aa}^r)}{(V_a^r+\Delta V_{aa}^r)^2+(V_a^i+\Delta V_{aa}^i)^2} + \frac{(\Delta P_a X_{oa} + \Delta Q_a R_{oa})(V_a^i+\Delta V_{aa}^i)}{(V_a^r+\Delta V_{aa}^r)^2+(V_a^i+\Delta V_{aa}^i)^2}\right], \tag{4.11}$$

where V_a^r and V_a^i are real and imaginary values of voltage at actor node respectively. For positive values of ΔP_a (increase in power consumption or decrease in power injection), ΔV_{aa}^r is negative. For negative values of ΔP_a (decrease in power consumption or increase in power injection), ΔV_{aa}^r is positive. In a power distribution network, voltage angle relative to source node is usually very small making V_a^i and ΔV_a^i very small. Under this assumption, real part of voltage change can be upper bounded by following equation.

$$\Delta V_{oa}^r \leq -\left[\frac{(\Delta P_a R_{oa} - \Delta Q_a X_{oa})V_a^r}{(V_a^r)^2 + (V_a^i)^2} + \frac{(\Delta P_a X_{oa} + \Delta Q_a R_{oa})V_a^i}{(V_a^r)^2 + (V_a^i)^2}\right], \tag{4.12}$$

Similarly, imaginary part of voltage change can be written as:

$$\Delta V_{oa}^i = -\left[\frac{(\Delta P_a X_{oa} + \Delta Q_a R_{oa})(V_a^r + \Delta V_{aa}^r)}{(V_a^r + \Delta V_a^r)^2 + (V_a^i + \Delta V_a^i)^2} - \frac{(\Delta P_a R_{oa} + \Delta Q_a X_{oa})(V_a^i + \Delta V_a^i)}{(V_a^r + \Delta V_a^r)^2 + (V_a^i + \Delta V_a^i)^2}\right], \tag{4.13}$$

For positive values of ΔQ_a and ΔP_a (increase in power consumption or decrease in power injection), ΔV_{aa}^i is negative as value of V_a^i and ΔV_a^i is very small. For negative values of ΔP_a and ΔQ_a (decrease in power consumption or increase in power injection), ΔV_{aa}^i is positive; therefore,

$$\Delta V_{oa}^i \leq -\left[\frac{(\Delta P_a X_{oa} + \Delta Q_a R_{oa})V_{oa}^r}{(V_a^r)^2 + (V_a^i)^2} - \frac{(\Delta P_a R_{oa} + \Delta Q_a X_{oa})V_a^i}{(V_a^r)^2 + (V_a^i)^2}\right], \tag{4.14}$$

Therefore upper bound on complex voltage change can be written as follows.

$$-\frac{\Delta S_a}{V_a^* + \Delta V_{aa}^*} Z_{oa} \leq -\frac{\Delta S_a}{V_a^*} Z_{oa}. \tag{4.15}$$

Hence

$$\Delta V_{oa} \leq -\frac{\Delta S_a}{V_a^*} Z_{oa} \tag{4.16}$$

□

Here, inequality sign for complex number indicates upper bound on real and imaginary values. This notation is used throughout in the dissertation. From equation (4.16), it is

observed that change in voltage at an observation node o due to change in complex power at an actor node a depends on the change in power consumption or injection, value of complex voltage at actor node and location of both nodes that eventually decides Z_{oa}. After calculating the upper bound on voltage change due to one actor node, effect of multiple actor nodes on observation node voltage is given by the following lemma.

Lemma 1. ***Superposition Law:*** *If $\mathcal{A}$ is a set of actor nodes in the network, effective change in complex voltage at the observation node o due to the cumulative effect of all actor nodes is bounded by equation (4.17).*

$$\Delta V_o \leq \sum_{a \in \mathcal{A}} -\frac{\Delta S_a Z_{oa}}{V_a^*}, \tag{4.17}$$

where $\mathcal{A}$ is set of all actor nodes.

Proof. Consider a generic network with multiple actor nodes $a_1, a_2, \cdots, a_L, a_{L+1}, \cdots, a_{L+M} \in \mathcal{A}$ and a generic observation node o as shown in Fig. 4.2. In this network, all actor nodes are ordered in a way that set $\mathcal{E}_{a1} \cap \mathcal{E}_o$ has the least number of elements (edges) and sets $\mathcal{E}_o = \mathcal{E}_{a_{L+1}} \cap \mathcal{E}_o$ to $\mathcal{E}_{a_{L+M}} \cap \mathcal{E}_o$ all have the same and highest number of elements (edges), as represented mathematically in equation (4.18) and graphically in Fig. 4.2. In other words, in a distribution network, length of shared line between actor node a_1 and observation node o from source node is smallest and length of shared line between actor nodes a_{L+1} to a_{L+M} and observation node o from source node is highest.

$$\begin{aligned} &|\mathcal{E}_{a_1} \cap \mathcal{E}_o| \leq |\mathcal{E}_{a_2} \cap \mathcal{E}_o| \leq \cdots \leq |\mathcal{E}_{a_L} \cap \mathcal{E}_o| \\ &\leq |\mathcal{E}_{a_{L+1}} \cap \mathcal{E}_o| = |\mathcal{E}_{a_{L+2}} \cap \mathcal{E}_o| = \cdots = |\mathcal{E}_{a_{L+M}} \cap \mathcal{E}_o|, \end{aligned} \tag{4.18}$$

since $|\mathcal{E}_{a_1} \cap \mathcal{E}_o|$ is the cardinality of set $\mathcal{E}_{a_1} \cap \mathcal{E}_o$. Let's divide the set $\mathcal{E}_o$ into $L+1$ smaller subsets as follows:

$$\begin{aligned} \mathcal{E}_o =& (\mathcal{E}_o \cap \mathcal{E}_{a_1}) \cup (\mathcal{E}_o \cap (\mathcal{E}_{a_2} - \mathcal{E}_{a_1})) \cup \cdots \cup (\mathcal{E}_o \cap (\mathcal{E}_{a_{L+1}} - \mathcal{E}_{a_L})) \\ =& \bigcup_{l=1}^{a_{L+1}} \mathcal{E}_o \cap (\mathcal{E}_{a_l} - \mathcal{E}_{a_{l-1}}) \end{aligned} \tag{4.19}$$

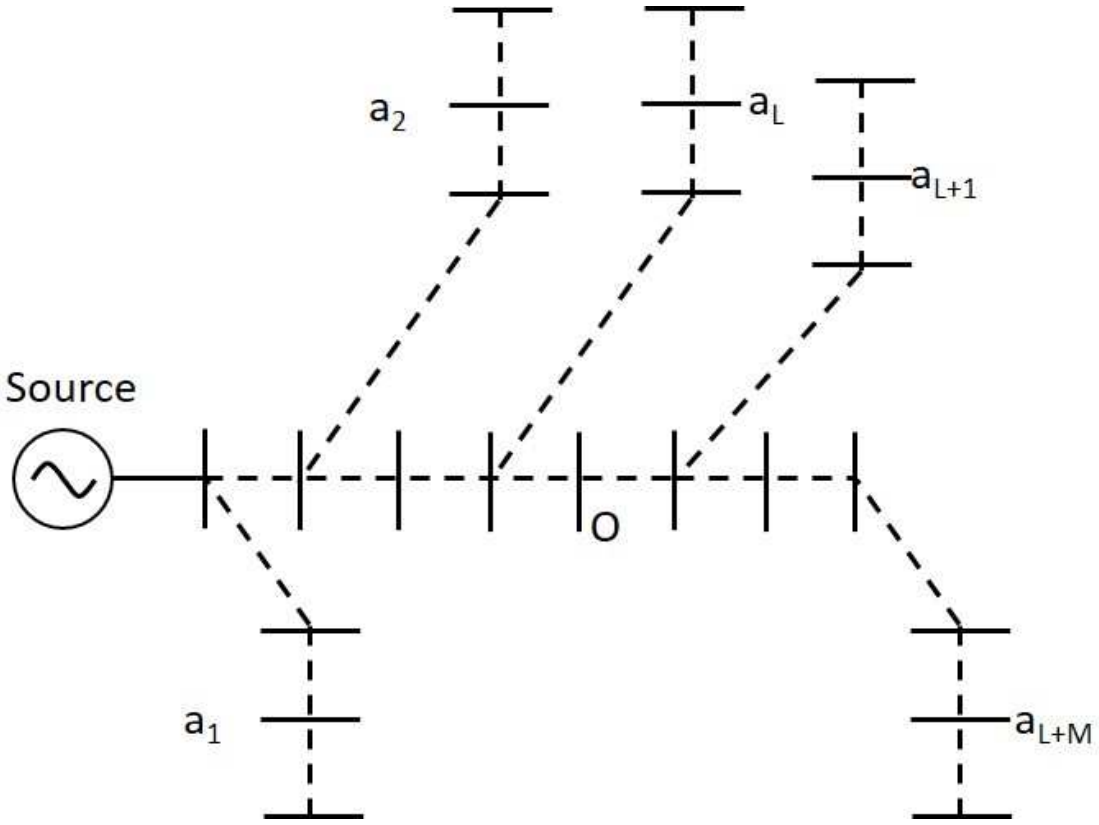

Figure 4.2: *Example of a network with multiple actor nodes*

since $\mathcal{E}_o \cap (\mathcal{E}_{a_l} - \mathcal{E}_{a_{l-1}}) = \phi$ for $a_l = a_{L+2}$ or greater as $\mathcal{E}_o \cap \mathcal{E}_{a_l} = \mathcal{E}_o \cap \mathcal{E}_{a_{l-1}}$. Using this we can rewrite equation (4.9) as:

$$\Delta V_o = \sum_{l=1}^{L+1} \sum_{\substack{e \in \mathcal{E}_o \cap \mathcal{E}_{al} \\ -\mathcal{E}_o \cap \mathcal{E}_{al-1}}} \left(\sum_{n \in \mathcal{N}_e} \frac{-\Delta S_n}{V_n^* + \Delta V_n^*} \right) Z_e \tag{4.20}$$

We can reorder equation (4.20) as

$$\begin{aligned} \Delta V_o &= \sum_{n=a_1}^{a_{L+M}} \sum_{e \in \mathcal{E}_o \cap \mathcal{E}_n} \left(\frac{-\Delta S_n}{V_n^* + \Delta V_n^*} \right) Z_e \\ &= \sum_{n=a_1}^{a_{L+M}} \left(\frac{-\Delta S_n}{V_n^* + \Delta V_n^*} \right) Z_{on} \\ &= \sum_{a \in \mathcal{A}} \left(\frac{-\Delta S_a}{V_a^* + \Delta V_a^*} \right) Z_{oa} \end{aligned} \tag{4.21}$$

Using same argument presented in theorem 1, we can write

$$\begin{aligned} \Delta V_o &\leq \sum_{a \in \mathcal{A}} \left(\frac{-\Delta S_a}{V_a^*} \right) Z_{oa} \\ &= \sum_{a \in \mathcal{A}} \Delta V_{oa} \end{aligned} \tag{4.22}$$

□

Inequality sign shown in equation (4.22) shows upper bound on real and imaginary values of voltage change. This lemma proves that the proposed analytical method represented by equation (4.17) holds the law of superposition.

4.3 Simulation and Results

This section verifies the derived analytical bound via simulation of the IEEE 69 bus test system. The nominal voltage of test system is 12.66 kV. As a benchmark, results from the proposed approach are compared to results of an existing sensitivity analysis method that uses the Newton-Raphson iterative method to compute the sensitivity matrix. IEEE 69 bus radial distribution test system shown in Fig. 4.3 is used as a test network. Fig. 4.4 shows change in voltage at bus 27 as function of change in real power consumption at node 27. Values of ΔP_{27} is varied from -250 kW to $+250$ kW, where negative values of ΔP_{27} represents decrease in power consumption or increase in injection of power into the grid and similarly positive values of ΔP_{27} represents increase in power consumption or reduction in power injection. The solid line in Fig. 4.4 shows values of ΔV_{27} computed using proposed analytical method and dashed line shows values computed using existing Newton-Raphson based iterative sensitivity analysis method. Proposed analytical method of sensitivity analysis provides a good approximation of change in voltage near point of operation, which can be seen in Fig. 4.4. Fig. 4.4 shows that change in voltage calculated from proposed method is approximately equal to actual ΔV for $|\Delta P| \leq 125$ kW, which is very large value of change in power consumption for distribution system. Fig. 4.5 shows an

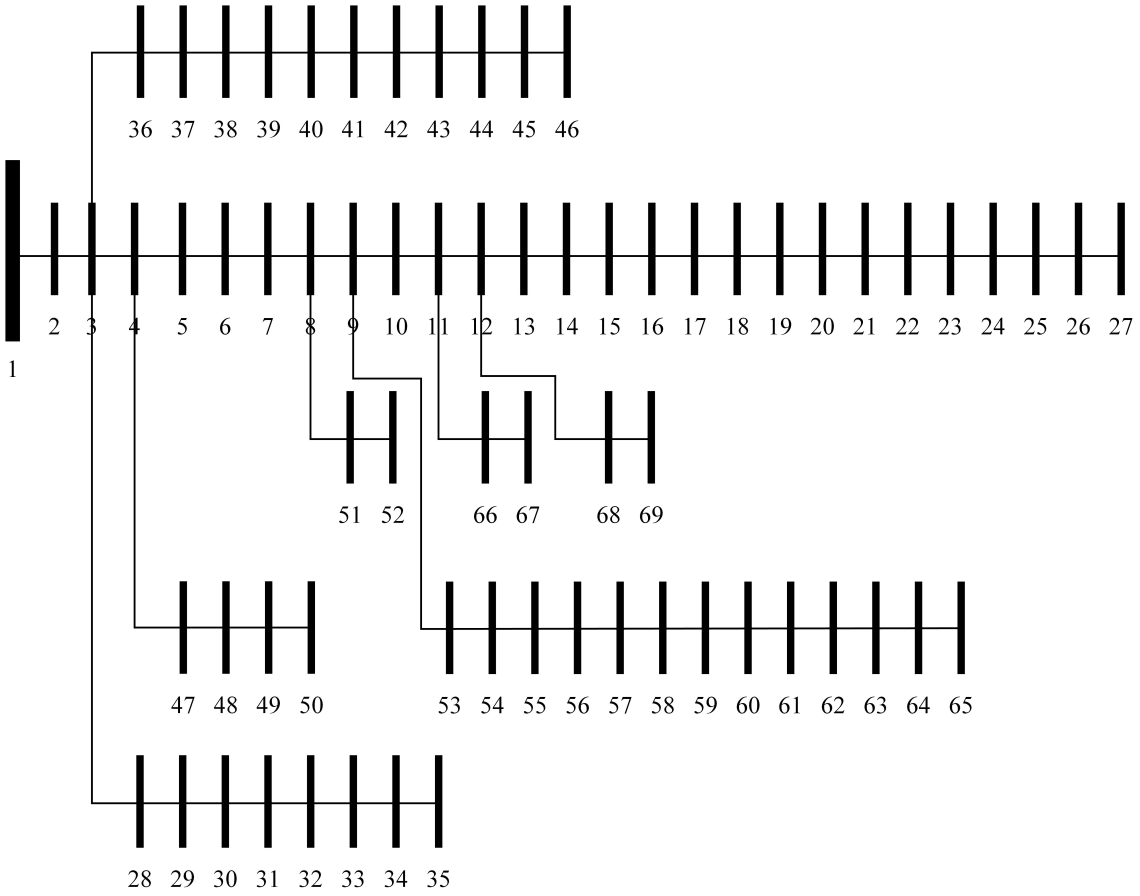

Figure 4.3: *IEEE 69 bus test system*

example when power injection of node 25 is increased by 1 kW and voltage change at all nodes are computed using the proposed approach and the newton-raphson based sensitivity analysis. Here x-axis indicates the node number and y-axis shows magnitude of voltage change at that node. Fig. 4.5 shows that voltage change computed via proposed method is always higher in magnitude compared to results obtained using the existing sensitivity analysis method, which is also supported by equation (4.3). Similarly, Fig. 4.6 shows another example of change in network voltage when power injection of node 15 is increased by 1 kW. These results also illustrates the tightness of the bound in (4.3). From Fig. 4.4 it can be seen that proposed upper bound is tight for smaller value of ΔV_o, especially for $|\Delta V_o| < 0.05$ per unit. For operational planing, the quick calculation can provide upper bound on voltage change in distribution system.

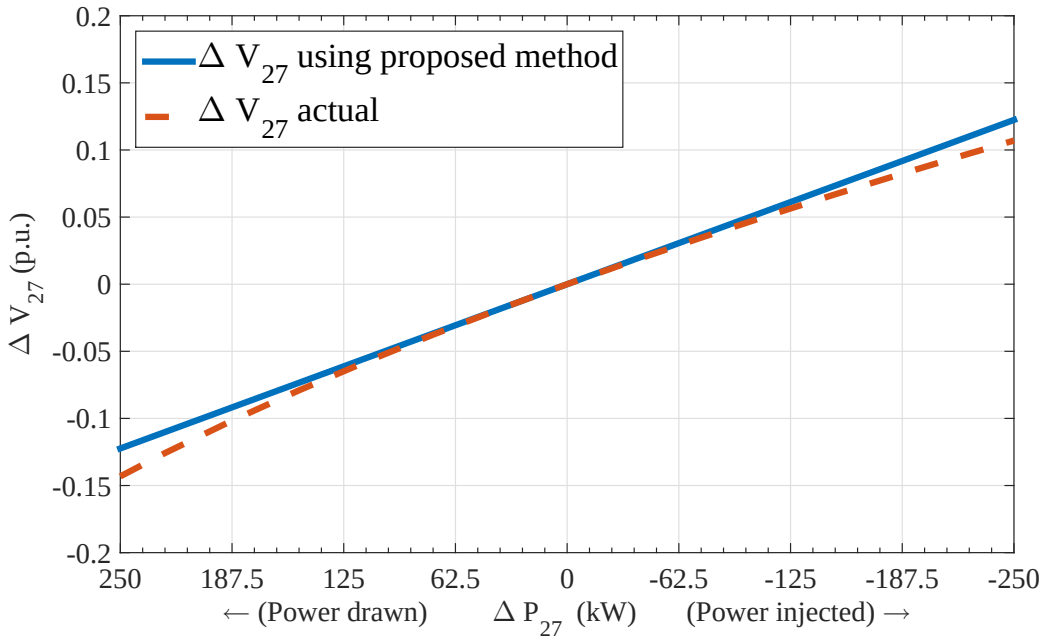

Figure 4.4: *Change in node voltage Vs. Change in power consumption*

4.4 Computation of Sensitivity Matrix

The analytical equation derived in theorem 1 can be used to compute the element-wise upper bound on a sensitivity matrix. Change in voltage magnitude and angle at a particular bus due to change in power consumption at any bus can be expressed as

$$\begin{bmatrix} \Delta\theta \\ \Delta V \end{bmatrix} = \begin{bmatrix} \frac{\partial\theta}{\partial P} & \frac{\partial\theta}{\partial Q} \\ \frac{\partial V}{\partial P} & \frac{\partial\theta}{\partial Q} \end{bmatrix} \begin{bmatrix} \Delta P \\ \Delta Q \end{bmatrix}, \tag{4.23}$$

where the upper bound on values of the sensitivity matrix can be calculated using following analytical relationships,

$$\frac{\partial\theta_o}{\partial P_a} = \angle \left[\frac{\Delta S_a Z_{oa}}{V_a *} \right]_{\Delta S_a = 1} = \angle \left[\frac{Z_{oa}}{V_a *} \right],$$

$$\frac{\partial\theta_o}{\partial Q_a} = \angle \left[\frac{\Delta S_a Z_{oa}}{V_a *} \right]_{\Delta S_a = i} = \angle \left[\frac{i Z_{oa}}{V_a *} \right],$$

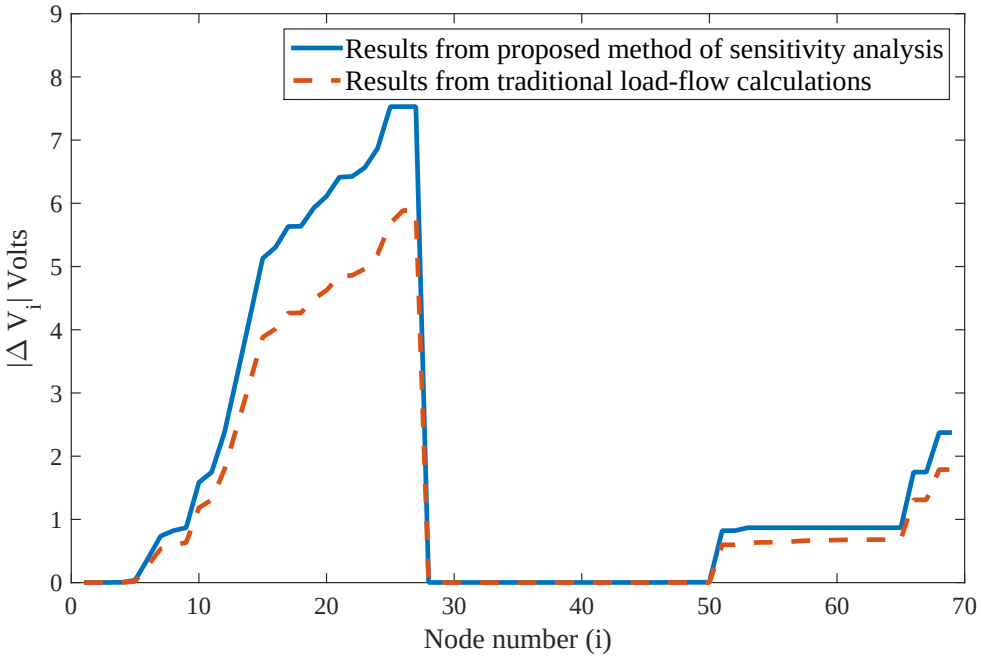

Figure 4.5: *Voltage change at all nodes due to* 1 *kW power injection at node 25*

$$\frac{\partial V_o}{\partial P_a} = \left| \frac{\Delta S_a Z_{oa}}{V_a *} \right|_{\Delta S_a = 1} = \left| \frac{Z_{oa}}{V_a *} \right|,$$

$$\frac{\partial V_o}{\partial Q_a} = \left| \frac{\Delta S_a Z_{oa}}{V_a *} \right|_{\Delta S_a = i} = \left| \frac{i Z_{oa}}{V_a *} \right|,$$

Sensitivity matrices calculated using traditional methods are valid only for small perturbations in state of the system. If system state changes significantly, a sensitivity matrix must be recomputed, which is computationally complex. Proposed analytical method of sensitivity analysis provides an approximation of the sensitivity matrix for a given state of the system. However, the proposed upper-bound is still valid when state of the system changes significantly. Furthermore, proposed method is computationally efficient than classical load-flow method. Computation time to calculate sensitivity matrix for IEEE 69 bus distribution system using classical load-flow method is 4.52 second. However, computing sensitivity matrix using proposed analytical method takes only 0.58 seconds.

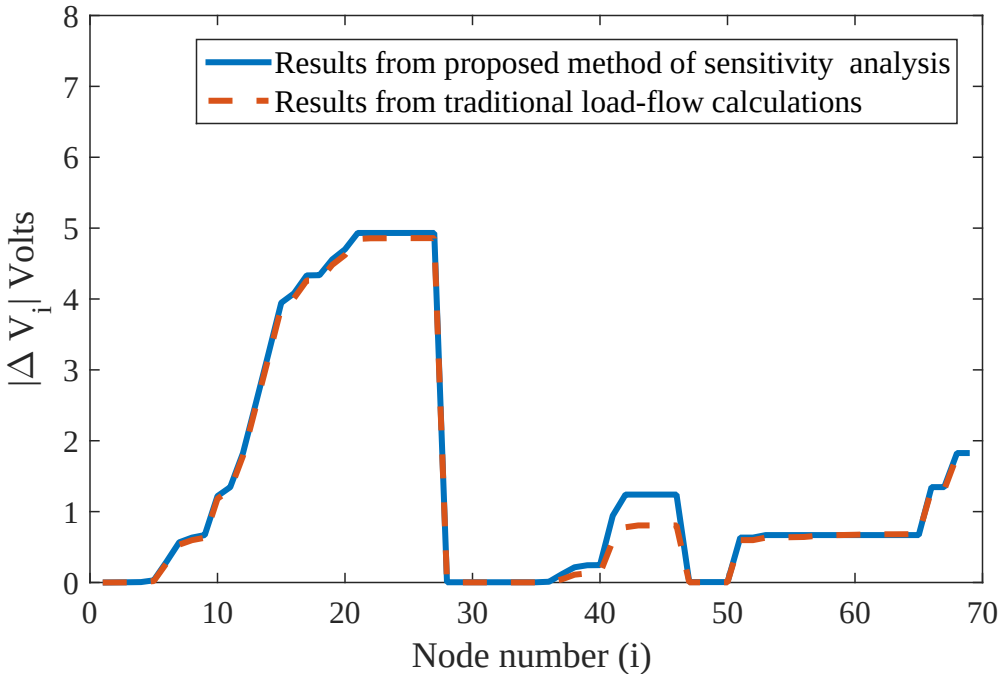

Figure 4.6: *Voltage change at all nodes due to* 1 *kW power injection at node 21 and 42*

4.5 Summary

This chapter proposes an analytical method to compute an upper bound on change in network voltage at a given node as a function of change in complex power consumption at another node and proves that the proposed analytical result follows the law of superposition. This method is then used to compute an upper bound for the sensitivity matrix elements in a computationally efficient manner. Effect of multiple active consumers on voltage at an observation node is studied using this analytical method.

Chapter 5

Stochastic Voltage Sensitivity Analysis

The analytical approach to voltage sensitivity analysis developed in chapter 4 can be used to investigate impact of random change in power drawn/injected due to multiple spatially distributed active consumers on distribution grid voltage. Current scenario-based analysis to examine the effect of random spatial penetration of active consumers and spatiotemporal variation of generation across the network is not scalable due to computational intractability. For example, investigating the effect of a rooftop photovoltaic (PV) located at a random location in the network on voltage of a distribution system with N buses typically involves two steps. First, a system model is developed assuming a fixed PV location, and an iterative power flow algorithm for all random solar generation values is executed. This step that tries to capture the temporal variation of PV generations is computationally expensive. Secondly, the first stage simulation is repeated for all spatial distributions of PV locations to determine worst case or average effect on voltage. Together, the computational cost of such scenario based analysis is large and grows with the size of the distribution system. The impact of the actions of a single active consumer on voltage at other nodes of the network can be perceived in the context of sensitivity analysis.

The main interest of this work is in understanding the impact of higher levels of PV

penetration. Historical data available today do not give us enough information regarding change in voltage due to higher levels of PV penetrations. A purely data driven approach at this stage is therefore not feasible. The proposed method of probabilistic voltage sensitivity analysis (PVSA) can be used for planning purposes to evaluate effect of future PV penetration in distribution systems. This method can be further refined in the future as and when relevant data becomes available.

5.1 Probabilistic Voltage Sensitivity Analysis

One application of the analytical method voltage sensitivity analysis developed in chapter 4 is to analyze the effect of multiple active consumers on the feeder voltage. Economically inspired actions of active consumers have an impact on the physical system. Consumer behavior is random which makes impact of these behavioral changes on feeder voltage also random. For example, the grid operator may want to know probability of voltage change being greater than allowable limit, $P(|\Delta V_o| > 0.05 p.u.)$, when there are arbitrary number of active consumers with PVs at arbitrary known/random locations in distribution grid. Therefore, it is important to derive the probability distribution of magnitude of voltage change at any node in the given distribution system. This section investigates the effect of spatially distributed active consumers on distribution system voltage. Here every active consumer acts like an actor node. The change in complex voltage at an observation node due to change in energy consumption of an actor node (equation 4.3) can be written in term of real and imaginary components:

$$\Delta V_{oa} = \Delta V_{oa}^{r} + i\Delta V_{oa}^{i}, \tag{5.1}$$

where,

$$\Delta V_{oa}^{r} = -\frac{1}{|V_a|}\left(\Delta P_a(R_{oa}\cos\theta_a - X_{oa}\sin\theta_a) - \Delta Q_a(R_{oa}\sin\theta_a + X_{oa}\cos\theta_a)\right), \tag{5.2}$$

and

$$\Delta V_{oa}^{i} = -\frac{1}{|V_a|}\left(\Delta Q_a(R_{oa}\cos\theta_a - X_{oa}\sin\theta_a) + \Delta P_a(R_{oa}\sin\theta_a + X_{oa}\cos\theta_a)\right). \tag{5.3}$$

From superposition law (Lemma 1), change in voltage at an observation node due to cumulative effect of multiple spatially distributed actor nodes can be written as sum of change in voltage at the observation node due to every actor node.

$$\Delta V_o = \sum_a \Delta V_{oa} = \sum_a \Delta V_{oa}^{r} + i\sum_a \Delta V_{oa}^{i}, \tag{5.4}$$

Behavior of an active consumer can be modeled as random variable. In this work, change in real and reactive power consumption of an active consumer is modeled as zero mean Gaussian random variable. Now let us define $\Delta S = [\Delta P_1, \cdots, \Delta P_n, \Delta Q_1, \cdots, \Delta Q_n]^T$ as Gaussian random vector with mean $\mu = \mathbf{0}$ and covariance matrix $\mathbf{\Sigma}$. Value of covariance matrix $\mathbf{\Sigma}$ can be estimated in practice based on a number of factors. Variance of change in real and reactive power can be estimated based on size of home, size of connected renewable generation and type of generation. Renewable energy sources such as PV and wind generation are random and spatially correlated. Effect of geographical proximity of such renewable generation is captured by the off-diagonal elements of the covariance matrix. Exact method to calculate covariance matrix is out of the scope of this research. The goal of this work is to derive the probability distribution of magnitude of change in observation node voltage.

5.2 Probability Distribution of Voltage Change due to Known Active Consumer Location

In this section, we will look at a case where location of all the active consumers is known. Method to compute distribution of $|\Delta V_o|^2$ is shown below using following steps:

1. Define Σ, and compute vectors $\mathbf{C_r}$ and $\mathbf{C_i}$

$$\mathbf{\Sigma} = \begin{bmatrix} \sigma_{p1}^2 & \cdots & \text{cov}(pn, p1) & \text{cov}(q1, p1) & \cdots & \text{cov}(qn, p1) \\ \vdots & \ddots & \vdots & \vdots & \ddots & \vdots \\ \text{cov}_(p1, pn) & \cdots & \sigma_{pn}^2 & \text{cov}(q1, pn) & \cdots & \text{cov}(qn, pn) \\ \text{cov}_(p1, q1) & \cdots & \text{cov}(pn, q1) & \sigma_{q1}^2 & \cdots & \text{cov}(qn, p1) \\ \vdots & \ddots & \vdots & \vdots & \ddots & \vdots \\ \text{cov}_(p1, qn) & \cdots & \text{cov}(pn, qn) & \text{cov}(q1, qn) & \cdots & \sigma_{qn}^2 \end{bmatrix} \tag{5.5}$$

Values of variance and covariance depends on size of network and size of house connected to a bus. For homes that do not have PVs, values of variance can be set to zero. In this work, we assume that network topology is known. Therefore, value of complex bus voltage and line impedance are assumed to be known. Let us define two vectors C_r and C_i as follows. Values of C_r and C_i can be computed using following equation.

$$\mathbf{C_r} = \begin{bmatrix} \_\frac{R_{o1}\cos\theta_1 - X_{o1}\sin\theta_1}{|V_1|} \\ \vdots \\ \_\frac{R_{on}\cos\theta_n - X_{on}\sin\theta_n}{|V_n|} \\ \frac{R_{o1}\sin\theta_1 + X_{o1}\cos\theta_1}{|V_1|} \\ \vdots \\ \frac{R_{on}\sin\theta_n + X_{on}\cos\theta_n}{|V_n|} \end{bmatrix}, \tag{5.6}$$

and

$$\mathbf{C_i} = \begin{bmatrix} \_\frac{R_{o1}\sin\theta_1 + X_{o1}\cos\theta_1}{|V_1|} \\ \vdots \\ \_\frac{R_{on}\sin\theta_n + X_{on}\cos\theta_n}{|V_n|} \\ \_\frac{R_{o1}\cos\theta_1 - X_{o1}\sin\theta_1}{|V_1|} \\ \vdots \\ \_\frac{R_{on}\cos\theta_n - X_{on}\sin\theta_n}{|V_n|} \end{bmatrix}. \tag{5.7}$$

2. Compute distribution of ΔV_o^r and ΔV_o^i

Real and Imaginary part of change in voltage at an observation node can be written as weighted sum of elements of vector ΔS as depicted by equation (5.8) and (5.9). Weighted sum of Gaussian random variables are normally distributed. Therefore, probability distribution of ΔV_o^r and ΔV_o^i can be derived as follows.

$$\Delta V_o^r = \sum_a \Delta V_{oa}^r = \mathbf{C_r^T \Delta S} \sim \mathcal{N}(0, \mathbf{C_r^T \Sigma C_r}) \tag{5.8}$$

$$\Delta V_o^i = \sum_a \Delta V_{oa}^i = \mathbf{C_i^T \Delta S} \sim \mathcal{N}(0, \mathbf{C_i^T \Sigma C_i}) \tag{5.9}$$

3. Define bi-variate normal vector $\mathbf{\Delta \hat{V}_o}$

Covariance between ΔV_o^r and ΔV_o^i can be written $\text{cov}\left(\Delta V_o^r, \Delta V_o^i\right) = \mathbf{C_r^T \Sigma C_i}$. Therefore, the change in real and imaginary part of voltage change will be a bi-variate normal vector, i.e.

$$\mathbf{\Delta \hat{V}_o} \triangleq \begin{bmatrix} \Delta V_o^r \\ \Delta V_o^i \end{bmatrix} \sim \mathcal{N}\left(\mathbf{0}, \mathbf{\Sigma_1}\right) \tag{5.10}$$

where,

$$\mathbf{\Sigma_1} = \begin{bmatrix} \mathbf{C_r^T \Sigma C_r} & \mathbf{C_r^T \Sigma C_i} \\ \mathbf{C_r^T \Sigma C_i} & \mathbf{C_i^T \Sigma C_i} \end{bmatrix} \tag{5.11}$$

The relationship between $\mathbf{\Delta \hat{V}_o}$ and $|\Delta V_o|^2$ corresponds to,

$$|\Delta V_o|^2 = \left|\sum_a \Delta V_{oa}^r\right|^2 + \left|\sum_a \Delta V_{oa}^i\right|^2 = \|\mathbf{\Delta \hat{V}_o}\|^2,$$

where $\|\mathbf{\Delta \hat{V}_o}\|$ is 2-norm of $\mathbf{\Delta \hat{V}_o}$.

4. Perform decorrelation operation

Covariance matrix of $\mathbf{\Delta \hat{V}_o}$ ($\mathbf{\Sigma_1}$) is not diagonal and can be diagonalized by eigenvalue decomposition as:

$$\mathbf{\Sigma_1 = Q \Lambda Q^T} \Rightarrow \mathbf{\Lambda = diag}\{\lambda_1, \lambda_2\} = \mathbf{Q^T \Sigma_1 Q},$$

where, $\mathbf{\Lambda}$ is diagonal matrix whose diagonal elements are eigenvalues of Σ_1 and i^{th} column of $\mathbf{Q}$ is the corresponding eigenvector, such that $\mathbf{Q^T Q = Q Q^T = I}$. This decorrelation operation involves the transformation of $\mathbf{\Delta \hat{V}_o}$ using $\mathbf{Q^T}$, i.e., $\mathbf{Y = Q^T \Delta \hat{V}_o}$. Therefore, the norm of $\mathbf{Y}$ can be written as:

$$\|\mathbf{Y}\| = \mathbf{Y^T Y} = \mathbf{\Delta \hat{V}_o}^{\mathbf{T}} \mathbf{Q^T Q \Delta \hat{V}_o} = \mathbf{\Delta \hat{V}_o}^{\mathbf{T}} \mathbf{\Delta \hat{V}_o} = \|\mathbf{\Delta \hat{V}_o}\|$$

5. Find distribution of $\|\mathbf{Y}\|^2$

As $\Delta \hat{V}_o$ is Gaussian random vector, $\mathbf{Y}$ is also Gaussian random vector with co-variance matrix Λ. $\|\mathbf{Y}\|^2$ is sum of square of Gaussian random variables and have following values of mean and variance.

$$\text{mean}(\|\mathbf{Y}\|^2) = \lambda_1 + \lambda_2, \text{ and } \text{var}(\|\mathbf{Y}\|^2) = 2(\lambda_1^2 + \lambda_2^2)$$

Weighted sum of chi-square random variables can be approximated by gamma distribution [72]. Shape (k) and scale (θ) parameters of such Gamma approximation can be calculated to match first two moments of $\|Y\|^2$ such that $k\theta = E[\|Y\|^2]$ and $k\theta^2 = \text{var}(\|Y\|^2)$. Once distribution of $\|Y\|^2$ is known, which is same as distribution of $|\Delta V_o|^2$, one can find probability of $|\Delta V_o| > \alpha$.

$$\mathbb{P}(|\Delta V_o| > \alpha) = \mathbb{P}(|\Delta V_o|^2 > \alpha^2) = \int_{\alpha^2}^{\infty} f(\|Y\|^2, k, \theta) d\|Y\|^2, \tag{5.12}$$

where $f(\cdot)$ is probability density function of gamma random variable. Algorithm 1 summarizes procedure to compute probability density function of $|\Delta V_o|^2$.

Algorithm 1 Derivation of probability distribution for $|\Delta V_o|^2$

1: Define Σ, and compute vectors $\mathbf{C_r}$ and $\mathbf{C_i}$
2: Compute distribution of ΔV_o^r and ΔV_o^i
3: Define bi-variate normal vector $\mathbf{\Delta \hat{V}_o}$
4: Perform decorrelation operation
5: Find distribution of $\|\mathbf{Y}\|^\mathbf{2}$

The result in equation (5.12) is quite useful in practice. For example, information about probability distributions of voltage change at all nodes can be used to identify most vulnerable node in the distribution system for a given penetration of active consumers. This result will have grid operators to plan the system better and find most vulnerable point from voltage violation perspective. Proposed method of PVSA can be applied for distribution system with voltage regulators and tap changing substation transformers with little modification. Voltage regulators and substation transformers with on load tap changing can been seen as corrective control action. Proposed approach of PVSA is a precursor to any control actions. The step type voltage regulator takes an incoming voltage that will vary with load conditions and maintain a constant output voltage. In this case, we can consider down-stream distribution system connected to voltage regulator as an independent network and perform PVSA for the smaller network. To analyze up-stream distribution system, we can consider voltage regulator as a single node representing cumulative load of down-stream network. Proposed analytical method of sensitivity analysis does not change due to on load tap changing transformer. Sensitivity matrix has to be recomputed using proposed method every time transformer changes its tap setting because change in substation voltage changes the voltage at all the nodes in the network.

5.2.1 Verification using Simulation

In order to test the proposed probability distribution of $|\Delta V_o|^2$, we use the IEEE 69 bus single phase system shown in Fig. 4.3. The nominal voltage of test system in 12.66 kV. In this simulation, actual distribution of $|\Delta V_o|^2$ is obtained using Newton-Raphson based sensitivity analysis method, and theoretical distribution is obtained using method proposed

in section 5.1. A scenario is considered where all even number of nodes have an active consumer. All active consumers change their power consumption randomly. Change in power consumptions of active consumers can be correlated. This correlation exist because change in power consumption depends on change in price of electricity or change in solar generation in area. The covariance matrix Σ is user defined and the Σ used in this simulation is given below. Values of variance may depend on size of home, and correlation coefficient may depend on geographical proximity. For simulation setup, a banded structure of covariance matrix is used to capture correlation between change in renewable generation between neighboring nodes. However, the actual structure of covariance matrix depends on topology of the network. It is important to note that proposed approach is quite general and can be applied to other covariance structures as well. In this simulation change in real and reactive power consumption is modeled as a Gaussian random variable. For nodes with active consumers, variance of change in real power (ΔP) is set to 10 kW and variance of change in reactive power ΔQ is set to 2 kvar. For nodes that does not represent an active consumer, variance of ΔP and ΔQ is set to zero. In covariance matrix, off diagonal elements represents covariance between random variables, which is given by following expression. $Cov(x, y) = \rho_{xy}\sqrt{var(x)var(y)}$, where ρ_{xy} is correlation coefficient. Correlation co-efficient between ΔP's for different actor nodes ($\rho(P_i, P_j)$, where i, j are only even numbers) is set to 0.2. Correlation coefficient between ΔP and ΔQ is set as -0.1. For example, covariance between ΔP_2 and ΔP_4 $cov(p2, p4) = 0.2\sqrt{10 * 10}$. For simplicity of demonstration, all PVs are set to have same variance; however, depending upon size and location of PVs, values of variance and correlation coefficient can be different for different nodes.

$$\mathbf{\Sigma} = \begin{bmatrix} 0 & 0 & 0 & 0 & \cdots & 0 & 0 & 0 & 0 & \cdots \\ 0 & 10 & 0 & 2 & \cdots & 0 & -0.45 & 0 & 0 & \cdots \\ 0 & 0 & 0 & 0 & \cdots & 0 & 0 & 0 & 0 & \cdots \\ 0 & 2 & 0 & 10 & \cdots & 0 & 0 & 0 & -0.45 & \cdots \\ \vdots & \vdots & \vdots & \vdots & \ddots & \vdots & \vdots & \vdots & \vdots & \ddots \\ 0 & 0 & 0 & 0 & \cdots & 0 & 0 & 0 & 0 & \cdots \\ 0 & -0.45 & 0 & 0 & \cdots & 0 & 2 & 0 & 0 & \cdots \\ 0 & 0 & 0 & 0 & \cdots & 0 & 0 & 0 & 0 & \cdots \\ 0 & 0 & 0 & -0.45 & \cdots & 0 & 0 & 0 & 2 & \cdots \\ \vdots & \vdots & \vdots & \vdots & \ddots & \vdots & \vdots & \vdots & \vdots & \ddots \end{bmatrix} \tag{5.13}$$

To obtain actual distribution of $|\Delta V_o|^2$, power consumptions of all nodes with active consumers are changed randomly and change in voltage at a particular node is calculated using Newton-Raphson based sensitivity analysis method. This is repeated $100,000$ times. Scaled histogram of $|\Delta V_o|^2$ is plotted as solid line in Fig. 5.3. To compute the theoretical distribution, value of vectors $\mathbf{C_r}$ and $\mathbf{C_i}$ is calculated from actual values from network. Σ_1 can be calculated based on $\Sigma, \mathbf{C_r}$ and $\mathbf{C_i}$ using equation (5.11), which is eventually used to find Q and Λ, which are as follows.

$$\mathbf{\Sigma} = \begin{bmatrix} 7.4030 & 2.6427 \\ 2.6427 & 1.5647 \end{bmatrix}, \tag{5.14}$$

$$\mathbf{Q} = \begin{bmatrix} 0.3536 & -0.9331 \\ -0.9331 & -0.3596 \end{bmatrix}, \mathbf{\Lambda} = \begin{bmatrix} 0.5462 & 0 \\ 0 & 8.4216 \end{bmatrix} \tag{5.15}$$

We can calculate mean and variance of $\|Y\|^2$ as: $E[\|Y\|^2] = 8.93$, and $\text{var}(\|Y\|^2) = 140.09$. This information is used to find shape and scale parameter of gamma distribution. $\|Y\|^2 \sim \Gamma(k, \theta)$, where $k = 0.57$ and $\theta = 15.69$. Fig. 5.3, shows actual probability distribution of $|\Delta V_{27}|^2$ and theoretical PDF of Gamma random variable with shape and scale parameters approximated using shown method. It can be seen that proposed approximated distribution

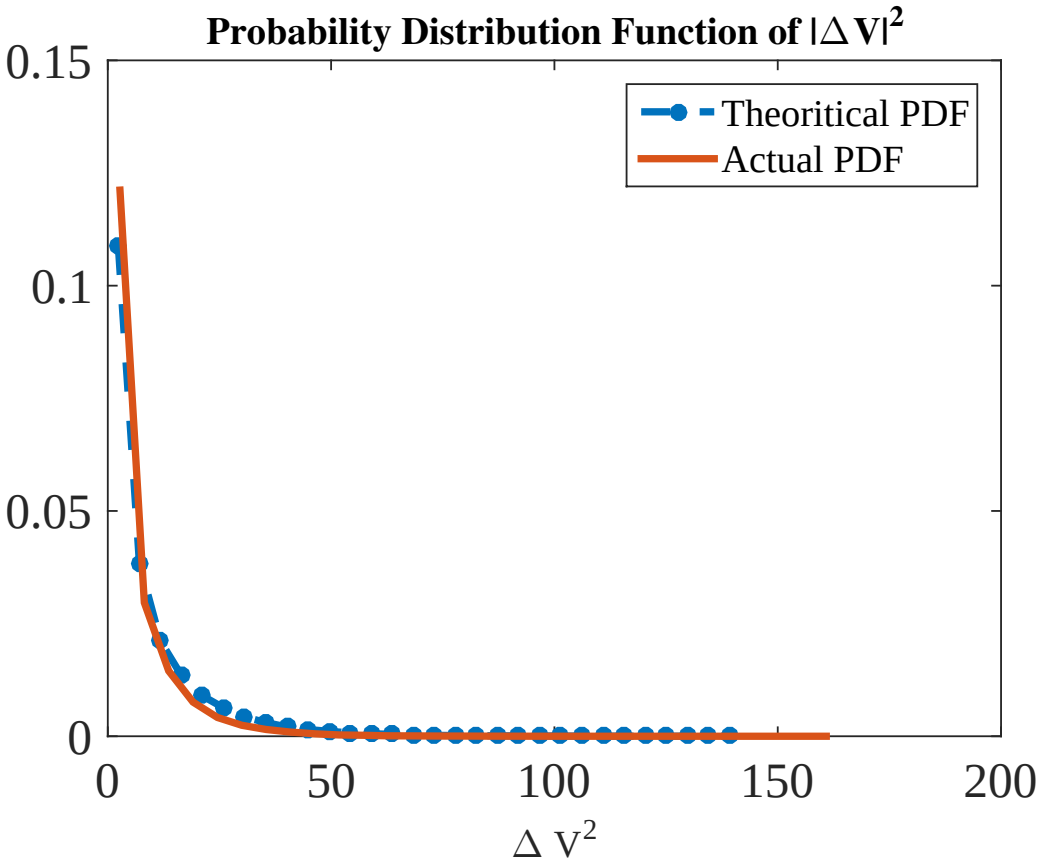

Figure 5.1: *Probability Distribution of* $|\Delta V_{27}|^2$

is very close to the actual distribution demonstrating the effectiveness of the proposed PVSA.

To test robustness of the proposed PVSA, a scenario is considered where physical parameters of the network are uncertain. For example, line impedance of distribution system changes with temperature. To test the impact of this temperature dependent uncertainty of line impedance on grid voltage, a scenario is considered where the line impedances are modeled as correlated Gaussian random variables with mean value provided by IEEE 69-bus test system and variance equal to 20% of average line impedance. The correlation coefficient which captures temperature dependent correlation of line impedance is set to 0.5. Fig 5.2 shows probability distribution of $|\Delta V|^2$ for this scenario. From this figure, it can be seen that proposed PVSA is robust to temperature induced uncertainty in line impedances as PDF for this case is very close to the theoretical PDF obtained by proposed method.

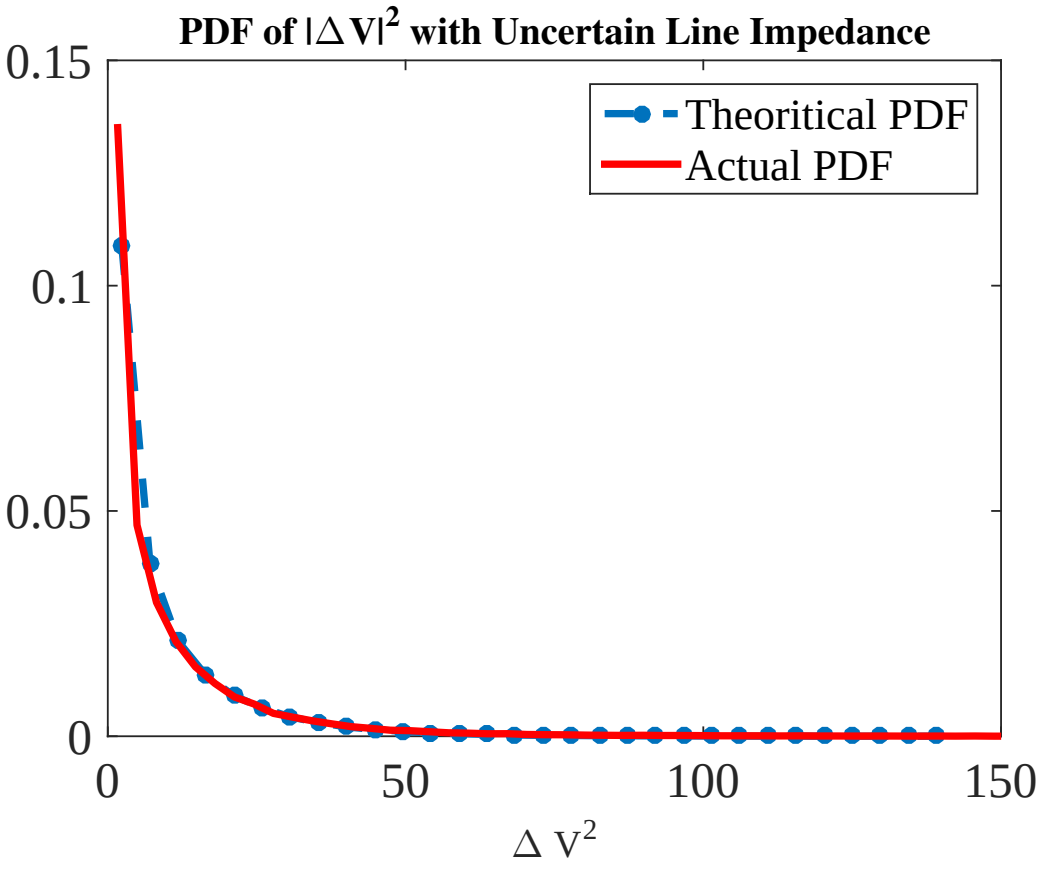

Figure 5.2: *PDF of* $|\Delta V_{27}|^2$ *with uncertainty in line impedance*

5.3 Probability Distribution of Voltage Change due to Random Spatial Distribution of Active Consumers

Another application of the proposed analytical method of sensitivity analysis is to analyze the effect of random spatial distribution of multiple active consumers on the feeder voltages. Line voltage of network is always kept within permissible limits; therefore, it is reasonable to assume $V_a \approx 1\angle 0°$. Based on this assumption equation (5.2) and (5.3) can be rewritten as:

$$\Delta V_{oa}^{r} = -\left(\Delta P_a R_{oa} - \Delta Q_a X_{oa}\right), \tag{5.16}$$

$$\Delta V_{oa}^{i} = -\left(\Delta Q_a R_{oa} + \Delta P_a X_{oa}\right). \tag{5.17}$$

To represent random behavior of an active consumer change in real and reactive power of an active consumer is modeled as zero mean Gaussian random variable. Therefore, vector $[\Delta P, \Delta Q]^T$ is defined as zero mean Gaussian random vector with covariance matrix shown below:

$$\begin{bmatrix} \Delta P_a \\ \Delta Q_a \end{bmatrix} \sim \mathcal{N}\left(\begin{bmatrix} 0 \\ 0 \end{bmatrix}, \begin{bmatrix} \sigma_p^2 & \rho_{pq}\sigma_p\sigma_q \\ \rho_{pq}\sigma_p\sigma_q & \sigma_q^2 \end{bmatrix} \right). \tag{5.18}$$

Here, off diagonal elements of the covariance matrix represent correlation between real and reactive power of an active consumer; and ρ_{pq} is correlation coefficient between ΔP_a and ΔQ_a. Impedance of a shared line between a given observation node (o) and a random actor node can be modeled as correlated random variable. For a given observation node, mean, variance and covariance of R_{oa} and X_{oa} can be estimated based on actual line impedance data. Let μ_{Ro} and μ_{Xo} indicate sample mean of R_{oa} and X_{oa}. Similarly, σ_{Ro}^2 and σ_{Xo}^2 denote sample variance of R_{oa} and X_{oa}; and ρ_{RX} indicate the correlation coefficient between R_{oa} and X_{oa}. The goal of this work is to derive probability distribution of the complex voltage change at an observation node due to random power change of active consumers located at random nodes. Probability distribution for real and imaginary components of the voltage change (ΔV_{oa}^r and ΔV_{oa}^i) due to random spatial distribution of multiple active consumers can be derived using following algorithm:

Algorithm 2 Derivation of probability distribution for real and imaginary components of the voltage change due to random spatial distribution of multiple active consumers

1: Calculate mean and variance of ΔV_{oa}^r and ΔV_{oa}^i
2: Calculate covariance between ΔV_{oa}^r and ΔV_{oa}^i
3: Calculate covariance between $\Delta V_{oa1}^{(r,i)}$ and $\Delta V_{oa2}^{(r,i)}$
4: Calculate mean and variance between ΔV_o^r and ΔV_o^i

1. Calculate mean and variance of ΔV_{oa}^r and ΔV_{oa}^i

Change in complex power at node a (ΔS_a) and impedance of shared line between node o and a (Z_{oa}) are mutually independent. Therefore, real and imaginary components of the voltage

change are zero mean random variable as shown in (5.19) and (5.20)

$$\text{mean}(\Delta V_{oa}^{r}) = -E[\Delta P_{oa} R_{oa}] + E[\Delta Q_{oa} X_{oa}] = 0, \tag{5.19}$$

$$\text{mean}(\Delta V_{oa}^{i}) = -E[\Delta Q_{oa} R_{oa}] - E[\Delta P_{oa} X_{oa}] = 0. \tag{5.20}$$

In order to compute variance of real and imaginary components of the voltage change, covariance between two term of (5.16) and (5.17) needs to be computed as:

$$\begin{aligned} \text{Cov}(\Delta P_{oa} R_{oa}, \Delta Q_{oa} X_{oa}) &= E[\Delta P_{oa} \Delta Q_{oa} R_{oa} X_{oa}] \\ &= E[\Delta P_{oa} \Delta Q_{oa}] E[R_{oa} X_{oa}] \\ &= \rho_{pq} \sigma_p \sigma_q \rho_{RX} \sigma_{Ro} \sigma_{Xo}, \end{aligned} \tag{5.21}$$

$$\begin{aligned} \text{Cov}(\Delta Q_{oa} R_{oa}, \Delta P_{oa} X_{oa}) &= E[\Delta Q_{oa} \Delta P_{oa} R_{oa} X_{oa}] \\ &= E[\Delta P_{oa} \Delta Q_{oa}] E[R_{oa} X_{oa}] \\ &= \rho_{pq} \sigma_p \sigma_q \rho_{RX} \sigma_{Ro} \sigma_{Xo}, \end{aligned} \tag{5.22}$$

Now, variance of real and imaginary components of the voltage change can be written as:

$$\text{Var}(\Delta V_{oa}^{r}) = \sigma_p^2(\sigma_{Ro}^2 + \mu_{Ro}^2) + \sigma_q^2(\sigma_{Xo}^2 + \mu_{Xo}^2) - \rho_{pq} \sigma_p \sigma_q \rho_{RX} \sigma_{Ro} \sigma_{Xo} \tag{5.23}$$

$$\text{Var}(\Delta V_{oa}^{i}) = \sigma_q^2(\sigma_{Ro}^2 + \mu_{Ro}^2) + \sigma_p^2(\sigma_{Xo}^2 + \mu_{Xo}^2) + \rho_{pq} \sigma_p \sigma_q \rho_{RX} \sigma_{Ro} \sigma_{Xo} \tag{5.24}$$

2. Calculate covariance between ΔV_{oa}^r and ΔV_{oa}^i

As mean of real and imaginary part of complex voltage change is zero, covariance between ΔV_{oa}^r and ΔV_{oa}^i can be calculated as:

$$\begin{aligned}
\text{Cov}(\Delta V_{oa}^r, \Delta V_{oa}^i) &= E[\Delta V_{oa}^r \Delta V_{oa}^i] - E[\Delta V_{oa}^r]E[\Delta V_{oa}^i] \\
&= E\left[(-\Delta P_{oa} R_{oa} + \Delta Q_{oa} X_{oa})(-\Delta Q_{oa} R_{oa} - \Delta P_{oa} X_{oa})\right] \\
&= E[\Delta P_{oa}\Delta Q_{oa}]E[R_{oa}^2] - E[\Delta Q_{oa}^2]E[R_{oa}X_{oa}] \\
&\quad + E[\Delta P_{oa}^2]E[R_{oa}X_{oa}] - E[\Delta P_{oa}\Delta Q_{oa}]E[X_{oa}^2] \\
&= (\rho_{pq}\sigma_p\sigma_q)(\sigma_{Ro}^2 - \sigma_{Xo}^2 + \mu_{Ro}^2 - \mu_{Xo}^2) \\
&\quad + (\sigma_p^2 - \sigma_q^2)(\rho_{RX}\sigma_{Ro}\sigma_{Xo} + \mu_{Ro}\mu_{Xo}).
\end{aligned} \tag{5.25}$$

Consider a scenario where multiple active consumers are spatially distributed in the grid. From Lemma 1, effective change in voltage at the observation node can be written as:

$$\Delta V_o^r = \sum_{a=1}^{N} \Delta V_{oa}^r, \text{ and } \Delta V_o^i = \sum_{a=1}^{N} \Delta V_{oa}^i, \tag{5.26}$$

where N is the number of active consumers which is assumed to be known. Change in complex power of various active consumers can be modeled as correlated Gaussian random variables. For two different active consumers located at nodes $a1$ and $a2$, ρ_p indicates correlation coefficient between ΔP_{a1} and ΔP_{a2}. Similarly, ρ_q indicates correlation coefficient between ΔQ_{a1} and ΔQ_{a2}. Effect of geographical proximity of renewable generations is captured by ρ_p and ρ_q. Exact method to calculate covariance matrix is out of the scope of this research.

3. Calculate covariance between $\Delta V_{oa1}^{(r,i)}$ and $\Delta V_{oa2}^{r,i}$

Covariance between real and imaginary component of complex voltage change caused by two different active consumers located at actor node $a1$ and $a2$ can be calculated as:

$$\begin{aligned}
\mathrm{Cov}(\Delta V_{oa1}^{r}, \Delta V_{oa2}^{r}) &= E(\Delta V_{oa1}^{r} \Delta V_{oa2}^{r}) - E[\Delta V_{oa1}^{r}] E[\Delta V_{oa2}^{r}] \\
&= E((\Delta P_{a1} R_{oa1} - \Delta Q_{a1} X_{oa1})(\Delta P_{a2} R_{oa2} - \Delta Q_{a2} X_{oa2}) \\
&= E[\Delta P_{a1} \Delta P_{a2}] E[R_{oa1}] E[R_{oa2}] - E[\Delta P_{a1} \Delta Q_{a2}] \\
& E[R_{oa1}] E[X_{oa2}] - E[\Delta Q_{a1} \Delta P_{a2}] E[X_{oa1}] E[R_{oa2}] \\
& + E[\Delta Q_{a1} \Delta Q_{a2}] E[X_{oa1}] E[X_{oa2}] \\
&= \rho_p \sigma_p^2 \mu_{Ro}^2 - 2(\rho_{pq} \sigma_p \sigma_q) \mu_{Ro} \mu_{Xo} + \rho_q \sigma_q^2 \mu_{Xo}^2
\end{aligned} \tag{5.27}$$

$$\begin{aligned}
\mathrm{Cov}(\Delta V_{oa1}^{i}, \Delta V_{oa2}^{i}) &= E(\Delta V_{oa1}^{i} \Delta V_{oa2}^{i}) - E[\Delta V_{oa1}^{i}] E[\Delta V_{oa2}^{i}] \\
&= E((\Delta Q_{a1} R_{oa1} + \Delta P_{a1} X_{oa1})(\Delta Q_{a2} R_{oa2} + \Delta P_{a2} X_{oa2}) \\
&= E[\Delta Q_{a1} \Delta Q_{a2}] E[R_{oa1}] E[R_{oa2}] + E[\Delta Q_{a1} \Delta P_{a2}] \\
& E[R_{oa1}] E[X_{oa2}] + E[\Delta P_{a1} \Delta Q_{a2}] E[X_{oa1}] E[R_{oa2}] \\
& + E[\Delta P_{a1} \Delta P_{a2}] E[X_{oa1}] E[X_{oa2}] \\
&= \rho_q \sigma_q^2 \mu_{Ro}^2 + 2(\rho_{pq} \sigma_p \sigma_q) \mu_{Ro} \mu_{Xo} + \rho_p \sigma_p^2 \mu_{Xo}^2
\end{aligned} \tag{5.28}$$

4. Calculate mean and variance between ΔV_o^r and ΔV_o^i

Mean of sum of zero mean random variables is zero. Therefore, from (5.19) and (5.20) it can be shown that mean of ΔV_o^r and ΔV_o^i is zero. Variance of real and imaginary components of voltage change can be written as:

$$\mathrm{Var}(\sum_{a=1}^{N} \Delta V_{oa}^{r}) = N \ \mathrm{Var}(V_{oa}^{r}) + 2 \sum_{i<j} \mathrm{Cov}(\Delta V_{oi}^{r}, \Delta V_{oj}^{r})$$

$$\mathrm{Var}(\sum_{a=1}^{N} \Delta V_{oa}^{i}) = N \ \mathrm{Var}(V_{oa}^{i}) + 2 \sum_{i<j} \mathrm{Cov}(\Delta V_{oi}^{i}, \Delta V_{oj}^{i})$$

From central limit theorem, ΔV_o^r and ΔV_o^i converge to normal distribution as number of active consumers increases. This information about probability distributions of voltage change at all nodes can be used to identify most vulnerable node in the distribution system for a given penetration of active consumers. This result will help grid operators to plan the system better and find the most vulnerable node from voltage violation perspective. The proposed method of PVSA is verified using simulation in the next section.

5.3.1 Verification Using Simulation

In order to test the proposed probability distribution of real and imaginary part of the voltage change, the IEEE 69 bus balanced system is used as shown in Fig. 4.3. The nominal voltage of the test system is 12.66 kV. In this simulation, the actual distribution of real and imaginary part of the voltage change is obtained using Newton-Raphson based sensitivity analysis method, and the theoretical distribution is obtained using the proposed method of PVSA. A scenario is considered where 15 active consumers are located at random location in the distribution system. All active consumers change their power randomly. Changes in complex power of active consumers can be correlated. This correlation exist because change in power depends on change in price of electricity or change in solar generation in the area. Values of the correlation coefficients ρ_p, ρ_q and ρ_{pq} are user defined and are set to 0.2, 0.2, and -0.1, respectively. Values of change in real and reactive power variance may depend on the size of the home; and value of the correlation coefficient may depend on the geographical proximity of PVs. In this simulation, change in real and reactive power is modeled as Gaussian random variable. For nodes with active consumers, the variance of change in real power (ΔP) is set to 10 kW and the variance of change in reactive power ΔQ is set to 2 kvar. Fig. 5.3 shows actual probability distribution of real and imaginary components of the voltage change at node 27 and theoretical PDF of the Gaussian random variable with mean and variance approximated using the proposed method. Mean and variance of resistance between a random actor node and node 27 is 19.48 and 756.08 ^{2}; and mean and variance of reactance between a random actor node and node 27 is 7.82 and 93.17 ^{2}, which is calculated

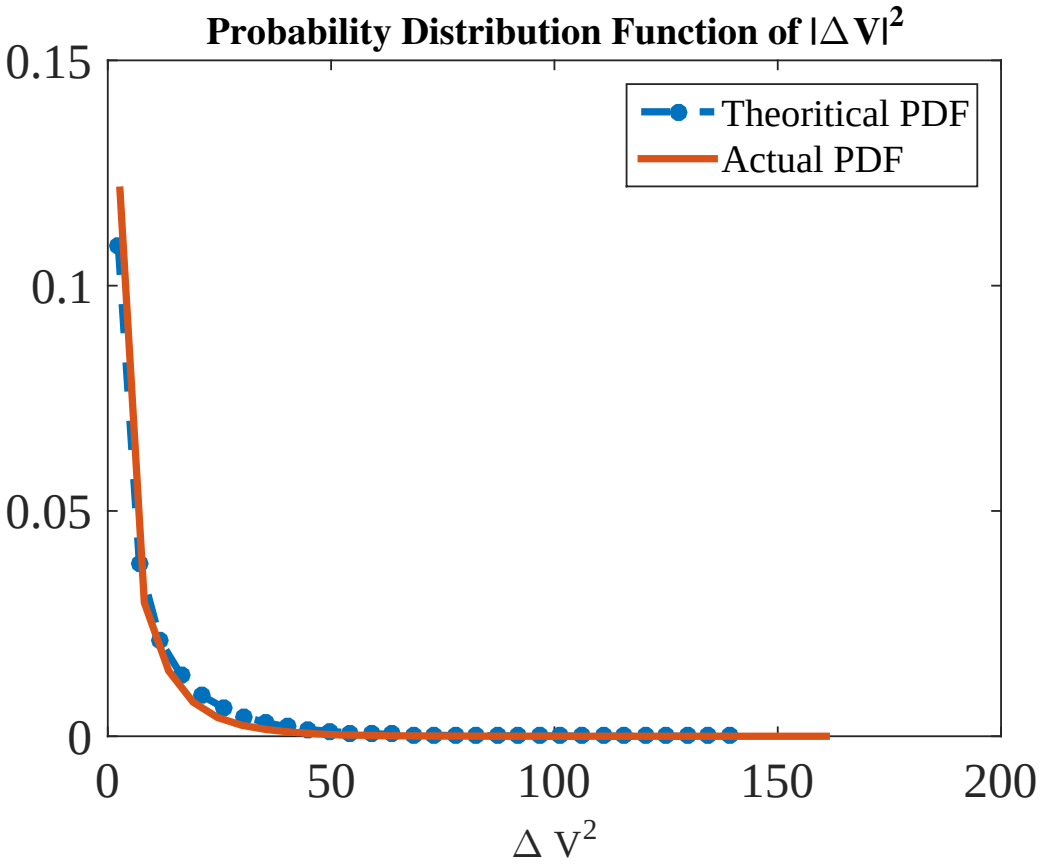

Figure 5.3: *PDF of* ΔV_{27}^r *and* ΔV_{27}^i

from data of the IEEE 69 bus test system. Value of correlation coefficient between resistance and reactance is 0.99. However, depending upon size and location of active consumers, these values can be different for different nodes.

To obtain actual distribution of ΔV_{27}^r and ΔV_{27}^i, powers of all nodes with active consumers are changed randomly and change in voltage at a particular node is calculated using Newton-Raphson based sensitivity analysis method. This is repeated 100, 000 times. Scaled histogram of ΔV_{27}^r and ΔV_{27}^i is plotted as solid line in Fig. 5.3. A theoretical distribution of real and imaginary value of the voltage change is presented by dashed line in Fig. 5.3. It can be seen that distribution calculated using the proposed method is very close to the actual distribution, which demonstrates the effectiveness of the proposed PVSA.

5.4 Summary

In this chapter, an analytical method to compute an upper bound on change in network voltage at a given node as function of change in complex powers of other nodes to study effect of multiple active consumers on voltage at an observation node is introduced. Real and imaginary part of voltage change due to random behavior of multiple active consumers with spatially random distribution can be approximated by the normal distribution. This method can be used for planing of distribution system to compute probability of voltage limit violation at a given node on the network.

Chapter 6

Dominant Influencer of Voltage Fluctuations

This chapter uses analytical method of voltage sensitivity analysis developed in chapter 4 to identify the dominant influencer of voltage fluctuations in a analytical and computationally efficient manner. Due increasing penetration of residential renewable generation in the power distribution system, power drawn/injected by active consumers is random and causes random fluctuations in distribution system voltage. These voltage fluctuations might cause voltage violations at multiple nodes in the power distribution system. Therefore, a control mechanism is needed to maintain the distribution system voltage within permissible limits. There are multiple ways of designing voltage control mechanism (i.e., (1) Using real-time electricity prices as an incentive to change consumer actions, or (2) installing voltage regulators or capacitor at optimal locations in the power distribution system). Implementation of these control mechanism requires identifying the dominant influencer source of voltage fluctuation.

6.1 Background

The dominant influencer source of voltage fluctuations at an observation node is the largest contributor of voltage fluctuations at the observation node. An actor node can be dominant influencer of voltage fluctuation at an observation node due to: 1) location of the actor node in the distribution system and 2) size of the renewable generation connected at the actor node which impacts the variance of random change in power drawn/injected by that node. Goal of this work is to identify the dominant influencer of voltage fluctuation in a computationally efficient manner. Currently, simulation based scenario analysis is the primary planning tool to identify the dominant influencer of voltage fluctuations. In order to identify the dominant influencer source of voltage fluctuations one must take following steps:

1. *Compute variance of voltage change at the observation node due to all actor nodes:* To compute variance of voltage change at the observation node using current simulation based scenario analysis, one must run hundreds of thousands of scenarios of Newton-Raphson based load flow algorithm to capture temporal variation in the renewable generations, which is computationally cumbersome.

2. *Calculate reduction in variance of voltage change at the observation node for each actor node by setting power drawn/injected by that actor node as constant:* This can be done by setting variance of change in power drawn/injected by the actor nodes as zero.

3. *Actor node that results in highest reduction in variance of voltage change at the observation node is the dominant influencer sources of the voltage fluctuations at the observation node.*

Computational complexity of such simulation based scenario analysis increases significantly with size of the network. This chapter investigates various information theoretic matrices to identify the dominant influencer sources of the voltage fluctuations in a computationally efficient manner, which can be used in real-time applications.

6.2 Differential Entropy Indicator

Differential entropy of a continuous random variable is a measure of the uncertainty of the random variable. Differential entropy of voltage change at the observation node due to change in power at an actor node is an excellent indicator of dominant influencer of voltage fluctuations. This section uses analytical method of voltage sensitivity analysis proposed in chapter 4 to compute differential entropy of voltage change at the observation node due to change in power at the actor nodes.

Proposition 1. *Actor node that maximizes the differential entropy of voltage change at the observation node ($H(\Delta V_{oa})$) is the dominant influencer source of voltage fluctuation (DI_H).*

$$\mathrm{DI}_H = \arg\max_a H(\Delta V_{oa}), \tag{6.1}$$

where ΔV_{oa} is change in complex voltage at an observation node (o) due to change in complex power at an actor node (a).

This section presents an analytical method of identifying the dominant influencer source of voltage fluctuation based on differential entropy. Let ΔS_a be change in complex power at the actor node (a). According to theorem 4, change in complex voltage at an observation node (o) due to change in power at an actor node (ΔV_{oa}) is given by:

$$\Delta V_{oa} \leq -\frac{\Delta S_a Z_{oa}}{V_a^*}, \tag{6.2}$$

where V_a^* is complex conjugate of voltage at the actor node; and Z_{oa} is impedance of shared line between observation node o and actor node a from the source node, as illustrated in Fig. (4.1) with the red line. Change in voltage at an observation node due to change in power at an actor nodes can be written in terms of real and imaginary components:

$$\Delta V_{oa} = \Delta V_{oa}^r + i\Delta V_{oa}^i, \tag{6.3}$$

where,

$$\Delta V_{oa}^{r} = -\frac{1}{|V_a|}\left(\Delta P_a(R_{oa}\cos\theta_a - X_{oa}\sin\theta_a) - \Delta Q_a(R_{oa}\sin\theta_a + X_{oa}\cos\theta_a)\right) \tag{6.4}$$

and

$$\Delta V_{oa}^{i} = -\frac{1}{|V_a|}\left(\Delta Q_a(R_{oa}\cos\theta_a - X_{oa}\sin\theta_a) + \Delta P_a(R_{oa}\sin\theta_a + X_{oa}\cos\theta_a)\right) \tag{6.5}$$

Here R_{oa} and X_{oa} are resistance and reactance of shared line between observation node o and actor node a from the source node. $|V_a|$ and ΔQ_a are magnitude and angle of complex voltage at the actor node. Real and imaginary part of voltage change at an observation node due to change in power at an actor node can be rewritten as:

$$\Delta V_{oa}^{r} = C_{oa}\Delta P_a - D_{oa}\Delta Q_a \tag{6.6}$$

$$\Delta V_{oa}^{i} = D_{oa}\Delta P_a + C_{oa}\Delta Q_a \tag{6.7}$$

where

$$C_{oa} = -\frac{R_{oa}\sin\theta_a + X_{oa}\cos\theta_a}{|V_a|} \tag{6.8}$$

$$D_{oa} = -\frac{R_{oa}\cos\theta_a - X_{oa}\sin\theta_a}{|V_a|} \tag{6.9}$$

Here, C_{oa} and D_{oa} are constants and depends on distribution system voltage and location of actor and observation node. Change in real and reactive power at an actor node can be modeled as zero mean Gaussian random vector as (6.10) with covariance matrix given by equation (6.11).

$$\mathbf{\Delta S_a} = \begin{bmatrix} \Delta P_a \\ \Delta Q_a \end{bmatrix} \sim \mathcal{N}\left(\mathbf{0}, \mathbf{\Sigma_{\Delta S_a}}\right), \tag{6.10}$$

where

$$\mathbf{\Sigma_{\Delta S_a}} = \begin{bmatrix} \sigma^2_{\Delta P_a} & \text{cov}(\Delta P_a, \Delta Q_a) \\ \text{cov}(\Delta P_a, \Delta Q_a) & \sigma^2_{\Delta Q_a} \end{bmatrix}. \tag{6.11}$$

Real and imaginary part of the voltage change at an observation node due to change in power at an actor node are weighted sum of correlated Gaussian random variables as shown in equation (6.6) and (6.7). Weighted sum of correlated Gaussian random variables is normally distributed. Therefore, real and imaginary part of voltage change at an observation node due to change in power at an actor node can be written as Gaussian random vector as shown in equation (6.12) with covariance matrix given by (6.13).

$$\mathbf{\Delta V_{oa}} = \begin{bmatrix} \Delta V^r_{oa} \\ \Delta V^i_{oa} \end{bmatrix} \sim \mathcal{N}\left(\mathbf{0}, \mathbf{\Sigma_{\Delta V_{oa}}}\right) \tag{6.12}$$

where,

$$\mathbf{\Sigma_{\Delta V_{oa}}} = \begin{bmatrix} \sigma^2_{\Delta V^r_{oa}} & \text{cov}(\Delta V^r_{oa}, \Delta V^i_{oa}) \\ \text{cov}(\Delta V^r_{oa}, \Delta V^i_{oa}) & \sigma^2_{\Delta V^r_{oa}} \end{bmatrix} \tag{6.13}$$

where,

$$\sigma^2_{\Delta V^r_{oa}} = \sigma^2_{\Delta P_a} C^2_{oa} - \sigma^2_{\Delta Q_a} D^2_{oa} - 2C_{oa}D_{oa}\text{cov}(\Delta P_a, \Delta Q_a), \tag{6.14}$$

$$\sigma^2_{\Delta V^i_{oa}} = \sigma^2_{\Delta Q_a} C^2_{oa} + \sigma^2_{\Delta P_a} D^2_{oa} + 2C_{oa}D_{oa}\text{cov}(\Delta P_a, \Delta Q_a), \tag{6.15}$$

and,

$$\begin{aligned} \text{cov}(\Delta V^r_{oa}, \Delta V^i_{oa}) &= E[\Delta V^r_{oa} \Delta V^i_{oa}] \\ &= E[(\Delta P_a C_{oa} - \Delta Q_a D_{oa})(\Delta Q_a C_{oa} + \Delta P_a D_{oa})] \\ &= \text{cov}(\Delta P_a, \Delta Q_a)(C^2_{oa} - D^2_{oa}) + (\sigma^2_{\Delta P_a} - \sigma^2_{\Delta Q_a})(C_{oa}D_{oa}) \end{aligned} \tag{6.16}$$

Differential entropy of voltage change at an observation node due to change in complex power

at an actor node (ΔV_{oa}) can be written as:

$$H(\mathbf{\Delta V_{oa}}) = \frac{1}{2}\ln((2\pi e)^2|\mathbf{\Sigma_{\Delta V_{oa}}}|). \tag{6.17}$$

Differential entropy of voltage change can be used to find the dominant influencer source of voltage fluctuations.

6.3 Joint Differential Entropy Indicator

Joint differential entropy ($H(\Delta V_o, \Delta V_{oa})$) between change in complex voltage at the observation node due change in power at an actor node a (ΔV_{oa}) and change in complex voltage at the observation node due to change in power at all actors nodes in the power distribution system (ΔV_o) is another potential indicator of dominant influencer of voltage fluctuations. Analytical method of voltage sensitivity analysis proposed in chapter 4 can be used to compute joint differential entropy of voltage change at the observation node due to change in power at the actor nodes.

Proposition 2. *Actor node that maximizes the joint differential entropy of voltage change at the observation node ($H(\Delta V_o, \Delta V_{oa})$) is the dominant influencer source of voltage fluctuation (DI_H).*

$$\mathrm{DI}_{JH} = \arg\max_a H(\Delta V_o, \Delta V_{oa}), \tag{6.18}$$

where ΔV_{oa} is change in complex voltage at an observation node (o) due to change in complex power at an actor node (a), and ΔV_o is change in voltage at the observation node due to cumulative actions of all active consumers.

This sections presents an analytical method of identifying the dominant influencer of voltage fluctuations based on joint differential entropy. Let $\mathbf{\Delta S}$ be a vector of change in real and reactive power changes at all nodes in the power distribution system defined by equation (6.19). $\mathbf{\Delta S}$ can be modeled as zero mean Gaussian random vector with covariance matrix

defined by equation (6.20).

$$\mathbf{\Delta S} = \begin{bmatrix} \Delta P_1 \\ \vdots \\ \Delta P_N \\ \Delta Q_1 \\ \vdots \\ \Delta Q_N \end{bmatrix} \sim \mathcal{N}\left(\mathbf{0}, \mathbf{\Sigma}\right) \tag{6.19}$$

where

$$\mathbf{\Sigma} = \begin{bmatrix} \sigma^2_{\Delta P_1} & \cdots & \text{cov}(\Delta P_1, \Delta P_N) & \text{cov}(\Delta P_1, \Delta Q_1) & \cdots & \text{cov}(\Delta P_1, \Delta Q_N) \\ \vdots & \ddots & \vdots & \vdots & \ddots & \vdots \\ \text{cov}(\Delta P_N, \Delta P_1) & \cdots & \sigma^2_{\Delta P_N} & \text{cov}(\Delta P_N, \Delta Q_1) & \cdots & \text{cov}(\Delta P_N, \Delta Q_N) \\ \text{cov}(\Delta Q_1, \Delta P_1) & \cdots & \text{cov}(\Delta Q_1, \Delta P_N) & \sigma^2_{\Delta Q_1} & \cdots & \text{cov}(\Delta Q_1, \Delta Q_N) \\ \vdots & \ddots & \vdots & \vdots & \ddots & \vdots \\ \text{cov}(\Delta Q_N, \Delta P_1) & \cdots & \text{cov}(\Delta Q_N, \Delta P_N) & \text{cov}(\Delta Q_N, \Delta Q_1) & \cdots & \sigma^2_{\Delta Q_N} \end{bmatrix} \tag{6.20}$$

According to lemma 1, change in voltage at an observation node (o) due to change in power at multiple actor nodes can be upper bounded by equation (6.21) and written in terms of real and imaginary components.

$$\Delta V_o = \Delta V_o^r + i\Delta V_o^i \leq \sum_{i=1}^{N} -\frac{\Delta S_i Z_{oi}}{V_i^*} \tag{6.21}$$

Real and imaginary part of voltage change at the observation node can be written as weighted sum of Gaussian random variables and are normally distributed as shown in equation (6.22-6.23).

$$\Delta V_o^r = \mathbf{C_o^r}^T \mathbf{\Delta S} \sim \mathcal{N}(0, \mathbf{C_o^{rT} \Sigma C_o^r}) \tag{6.22}$$

$$\Delta V_o^i = \mathbf{C_o^i}^T \mathbf{\Delta S} \sim \mathcal{N}(0, \mathbf{C_o^{iT} \Sigma C_o^i}) \tag{6.23}$$

where

$$\mathbf{C_o^r} = \begin{bmatrix} C_{o1} \\ \vdots \\ C_{oN} \\ -D_{o1} \\ \vdots \\ -D_{oN} \end{bmatrix} = \begin{bmatrix} -\frac{R_{o1}\cos\theta_1 - X_{o1}\sin\theta_1}{|V_1|} \\ \vdots \\ -\frac{R_{oN}\cos\theta_N - X_{oN}\sin\theta_N}{|V_N|} \\ \frac{R_{o1}\sin\theta_1 + X_{o1}\cos\theta_1}{|V_1|} \\ \vdots \\ \frac{R_{oN}\sin\theta_N + X_{oN}\cos\theta_N}{|V_N|} \end{bmatrix}, \tag{6.24}$$

and

$$\mathbf{C_o^i} = \begin{bmatrix} D_{o1} \\ \vdots \\ D_{oN} \\ C_{o1} \\ \vdots \\ C_{oN} \end{bmatrix} = \begin{bmatrix} -\frac{R_{o1}\sin\theta_1 + X_{o1}\cos\theta_1}{|V_1|} \\ \vdots \\ -\frac{R_{oN}\sin\theta_N + X_{oN}\cos\theta_N}{|V_N|} \\ -\frac{R_{o1}\cos\theta_1 - X_{o1}\sin\theta_1}{|V_1|} \\ \vdots \\ -\frac{R_{oN}\cos\theta_N - X_{oN}\sin\theta_N}{|V_N|} \end{bmatrix}. \tag{6.25}$$

Let $\mathbf{\Delta V_o}$ be vector of real and imaginary part of voltage change defined by equation (6.26). $\mathbf{\Delta V_o}$ can be written as bivariate Gaussian random vector with covariance matrix defined by equation (6.27)

$$\mathbf{\Delta V_o} = \begin{bmatrix} \Delta V_o^r \\ \Delta V_o^i \end{bmatrix} \sim \mathcal{N}\left(\mathbf{0}, \mathbf{\Sigma_{\Delta V_o}}\right). \tag{6.26}$$

$$\mathbf{\Sigma_{\Delta V_o}} = \begin{bmatrix} \mathbf{C_o^{rT}\Sigma C_o^r} & \mathbf{C_o^{rT}\Sigma C_i^r} \\ \mathbf{C_o^{rT}\Sigma C_i^r} & \mathbf{C_o^{rT}\Sigma C_o^r} \end{bmatrix} \tag{6.27}$$

where

$$\mathrm{cov}(V_o^r, V_o^i) = \mathbf{C_o^{rT}\Sigma C_i^r} \tag{6.28}$$

In order to calculate join differential entropy between ΔV_{oa} and ΔV_o, we can write a vector of real and imaginary components of ΔV_{oa} and ΔV_o as Gaussian random vector shown in

equations (6.29) and (6.30).

$$\begin{bmatrix} \Delta V_{oa}^{r} \\ \Delta V_{oa}^{i} \\ \Delta V_{o}^{r} \\ \Delta V_{o}^{i} \end{bmatrix} = \mathcal{N}(\mathbf{0}, \mathbf{\Sigma_{V_{oa}, V_o}}) \tag{6.29}$$

$$\mathbf{\Sigma_{V_{oa}, V_o}} = \begin{bmatrix} \sigma^2_{\Delta V_{oa}^{r}} & \text{cov}(\Delta V_{oa}^{r}, \Delta V_{oa}^{i}) & \text{cov}(\Delta V_{oa}^{r}, \Delta V_{o}^{r}) & \text{cov}(\Delta V_{oa}^{r}, \Delta V_{o}^{i}) \\ \text{cov}(\Delta V_{oa}^{r}, \Delta V_{oa}^{i}) & \sigma^2_{\Delta V_{oa}^{i}} & \text{cov}(\Delta V_{oa}^{i}, \Delta V_{o}^{r}) & \text{cov}(\Delta V_{oa}^{i}, \Delta V_{o}^{i}) \\ \text{cov}(\Delta V_{oa}^{r}, \Delta V_{o}^{r}) & \text{cov}(\Delta V_{oa}^{i}, \Delta V_{o}^{r}) & \mathbf{C_o^{rT} \Sigma C_o^{r}} & \mathbf{C_o^{rT} \Sigma C_i^{r}} \\ \text{cov}(\Delta V_{oa}^{r}, \Delta V_{o}^{i}) & \text{cov}(\Delta V_{oa}^{i}, \Delta V_{o}^{i}) & \mathbf{C_o^{rT} \Sigma C_i^{r}} & \mathbf{C_o^{rT} \Sigma C_o^{r}} \end{bmatrix} \tag{6.30}$$

Elements of covariance matrix (6.30) are derived in Appendix B. Joint differential entropy between ΔV_o, and ΔV_{oa} can be written as:

$$H(\mathbf{\Delta V_o}, \mathbf{\Delta V_{oa}}) = \frac{1}{2} \ln((2\pi e)^4 |\mathbf{\Sigma_{\Delta V_{oa} \Delta V_o}}| \tag{6.31}$$

Joint differential entropy of voltage change can be used to find the dominant influencer source of voltage fluctuations.

6.4 Kullback-Leibler Distance Indicator

Kullback-Leibler (KL) distance or relative entropy is a measure of distance between two distributions. KL divergence between two multivariate normal distributions ($\mathcal{N}_0$ and $\mathcal{N}_1$) of dimension k with means ($\mu_\mathbf{0}$ and $\mu_\mathbf{1}$) and covariance matrices ($\mathbf{\Sigma_0}$ and $\mathbf{\Sigma_1}$) is given by:

$$D_{KL}(\mathcal{N}_0 \| \mathcal{N}_1) = \frac{1}{2} \left[\text{tr} \left(\mathbf{\Sigma_1^{-1} \Sigma_0} \right) + (\mu_1 - \mu_0)^T \mathbf{\Sigma_1}^{-1} (\mu_\mathbf{1} - \mu_\mathbf{0}) - k + \ln \frac{|\mathbf{\Sigma_1}|}{|\mathbf{\Sigma_0}|} \right]. \tag{6.32}$$

KL distance between change in complex voltage at the observation node due change in power at an actor node a (ΔV_{oa}) and change in complex voltage at the observation node due to

change in power at all actor nodes (ΔV_o) is another potential indicator of the dominant influencer of voltage fluctuations.

Proposition 3. *Actor node that minimizes the Kullback-Leibler distance between ΔV_o and ΔV_{oa} is the dominant influencer source of voltage fluctuation (DI_{KL}).*

$$\mathrm{DI}_{KL} = \arg\min_{a} D_{KL}(\mathbf{V_{oa}} \| \mathbf{\Delta V_o}), \tag{6.33}$$

As ΔV_o and ΔV_{oa} are zero mean bi-variate Gaussian random vector, KL distance between ΔV_o and ΔV_{oa} can be computed using equation (6.34).

$$D_{KL}(\mathbf{V_{oa}} \| \mathbf{\Delta V_o}) = \frac{1}{2}\left[\mathrm{tr}\left(\mathbf{\Sigma^{-1}_{\Delta V_o}} \mathbf{\Sigma_{\Delta V_{oa}}}\right) - 2 + \ln \frac{|\mathbf{\Sigma_{\Delta V_o}}|}{|\mathbf{\Sigma_{\Delta V_{oa}}}|}\right] \tag{6.34}$$

where $\mathbf{\Sigma_{\Delta V_{oa}}}$ and $\mathbf{\Sigma_{\Delta V_o}}$ are covariances of $\mathbf{\Delta V_{oa}}$ and $\mathbf{\Delta V_o}$ given by equations (6.13) and (6.27) respectively. Here, $\mathrm{tr}(\cdot)$ indicates trace of the matrix.

6.5 Frechet Distance Indicator

Another potential indicator similarity between two distributions. Frechet distance between two multivariate normal distributions ($\mathcal{N}_0$ and $\mathcal{N}_1$) with means ($\mu_{\mathbf{0}}$ and $\mu_{\mathbf{1}}$) and covariance matrices ($\mathbf{\Sigma_0}$ and $\mathbf{\Sigma_1}$) is given by

$$d_F^2(\mathcal{N}_0, \mathcal{N}_1) = |\mu_{\mathbf{0}} - \mu_{\mathbf{1}}|^2 + \mathrm{tr}\left[\mathbf{\Sigma_0} + \mathbf{\Sigma_1} - 2(\mathbf{\Sigma_0}\mathbf{\Sigma_1})^{\frac{1}{2}}\right]. \tag{6.35}$$

Frechet distance between ΔV_{oa} and ΔV_o is another potential indicator of the dominant influencer of the voltage fluctuations.

Proposition 4. *Actor node that minimizes the Frechet distance between ΔV_o and ΔV_{oa} is the dominant influencer source of the voltage fluctuation (DI_{FD}).*

$$\mathrm{DI}_{FD} = \arg\min_{a} d_F^2(\mathbf{V_{oa}}, \mathbf{\Delta V_o}), \tag{6.36}$$

As ΔV_o and ΔV_{oa} are zero mean bi-variate Gaussian random vector, Frechet distance between ΔV_o and ΔV_{oa} can be computed using equation (6.37).

$$d_F^2(\mathbf{V_{oa}}, \mathbf{\Delta V_o}) = \text{tr}\left[\mathbf{\Sigma_{\Delta V_o}} + \mathbf{\Sigma_{\Delta V_{oa}}} - 2(\mathbf{\Sigma_{\Delta V_o}}\mathbf{\Sigma_{\Delta V_{oa}}})^{\frac{1}{2}}\right]. \tag{6.37}$$

where $\mathbf{\Sigma_{\Delta V_{oa}}}$ and $\mathbf{\Sigma_{\Delta V_o}}$ are covariances of $\mathbf{\Delta V_{oa}}$ and $\mathbf{\Delta V_o}$ given by equations (6.13) and (6.27) respectively. Here, tr$(\cdot)$ indicates trace of the matrix.

6.6 Mutual Information Indicator

Mutual information between two random variable is a measure of the amount of information that one random variable contains about the other random variable. Mutual information ($I(\Delta V_o; \Delta V_{oa})$) between ΔV_{oa} and ΔV_o is another potential indicator of dominant influencer of voltage fluctuations.

Proposition 5. *Actor node that maximizes the joint mutual information between ΔV_o and ΔV_{oa} is the dominant influencer source of the voltage fluctuation (DI_{MI}).*

$$\text{DI}_{MI} = \arg\max_a I(\mathbf{\Delta V_o}; \mathbf{\Delta V_{oa}}), \tag{6.38}$$

Mutual information between two bi-variate random vectors $\mathbf{\Delta V_o}$ and $\mathbf{\Delta V_{oa}}$ can be computed using equation (6.39).

$$I(\mathbf{\Delta V_o}; \mathbf{\Delta V_{oa}}) = H(\mathbf{\Delta V_o}) + H(\mathbf{\Delta V_{oa}}) - H(\mathbf{\Delta V_o}, \mathbf{\Delta V_{oa}}) \tag{6.39}$$

where

$$H(\mathbf{\Delta V_o}) = \frac{1}{2}\ln((2\pi e)^2|\mathbf{\Sigma}_{\Delta V_o}|), \tag{6.40}$$

$$H(\mathbf{\Delta V_{oa}}) = \frac{1}{2}\ln((2\pi e)^2|\mathbf{\Sigma}_{\Delta V_{oa}}|), \tag{6.41}$$

and $H(\mathbf{\Delta V_o}, \mathbf{\Delta V_{oa}})$ is given by equation (6.31). Validity of proposed metrics as an indicator of the dominant influencer of the voltage fluctuation is tested using simulation in the next section.

6.7 Simulation and Results

To order to test effectiveness of proposed metrics as an indicators of the dominant influencer of the voltage fluctuation, the IEEE 69 bus balanced system is used as shown in Fig. 4.3. The nominal voltage of the test system is 12.66 kV. A scenario is created where there are active consumers with renewable generation at every even numbered nodes of the IEEE 69 bus system. Active consumers with three different sizes of rooftop PVs are considered in this simulation. Change in real and reactive power at actor nodes is modeled as zero mean Gaussian random vector. Mean and variance of real and reactive power change of all three kind of active consumers and their locations are given by equations (6.42), (6.43) and (6.44).

$$\mathbf{\Delta S_i} = \begin{bmatrix} \Delta P_i \\ \Delta Q_i \end{bmatrix} \sim \mathcal{N}\left(\begin{bmatrix} 0 \\ 0 \end{bmatrix}, \begin{bmatrix} 1 & -0.0447 \\ -0.0447 & 0.2 \end{bmatrix} \right), \forall i \in \{2, 8, 14, 20, \cdots\} \tag{6.42}$$

$$\mathbf{\Delta S_i} = \begin{bmatrix} \Delta P_i \\ \Delta Q_i \end{bmatrix} \sim \mathcal{N}\left(\begin{bmatrix} 0 \\ 0 \end{bmatrix} \begin{bmatrix} 2 & -0.0894 \\ -0.0894 & 0.4 \end{bmatrix} \right), \forall i \in \{4, 10, 16, 22, \cdots\} \tag{6.43}$$

$$\mathbf{\Delta S_i} = \begin{bmatrix} \Delta P_i \\ \Delta Q_i \end{bmatrix} \sim \mathcal{N}\left(\begin{bmatrix} 0 \\ 0 \end{bmatrix}, \begin{bmatrix} 3 & -0.1342 \\ -0.1342 & 0.6 \end{bmatrix} \right), \forall i \in \{6, 12, 18, 24, \cdots\} \tag{6.44}$$

Changes in complex power of active consumers are correlated. Values of correlation coefficients ρ_p, ρ_q, ρ_{pq} are set to 0.2, 0.2 and -0.1. This correlation exist because change in power

is effected by environmental factors like changes in the price of electricity and changes in the solar generation in the area.

In order to identify true dominant influencer of voltage fluctuations a Monte-Carlo simulation is conducted as explained in section 6.1. First, variance of change in voltage magnitude at node 27 due to actions of all active consumers of the IEEE 69 bus distribution system is computed using simulation of $100,000$ scenarios. The reduction in variance of change in voltage magnitude is computed by setting $\mathbf{\Sigma_{\Delta S_a}}$ to zero for each active consumers sequentially. The dominant influencer of the voltage fluctuations is the node that results in highest reduction in variance of voltage change at node 27 when variance of real and reactive power change at that node is set to zero.

$$\text{DI} = \arg\max_{a} \left[\text{var}(\Delta|V_o|) - \text{var}(\Delta|V_o^{-a}|)\right], \tag{6.45}$$

where $\text{var}(\Delta|V_o|)$ is variance of change in voltage magnitude due to all actor nodes and $\text{var}(\Delta|V_o^{-a}|)$ is variance change in voltage magnitude due to all actor nodes except for the actor node a. List of nodes and caused reduction in variance of voltage change at node 27 is presented in Table 6.2. From Table 6.2 it can be seen that node 24 is the dominant influencer source of voltage fluctuation at node 27. This is because of high variance of power change and proximity of node 24 to node 27 in IEEE 69 bus test system. Computation time for this scenario analysis is $22,389.63$ seconds. Here negative values of reduction in variance is because of small sample size of number of Monte-Carlo simulations performed for this case. To obtain more accurate results more number of scenarios must be simulated which will increase computational time significantly.

To test proposition 1 and effectiveness of differential entropy as an indicator of the dominant influencer of voltage fluctuations, differential entropy of complex voltage change at node 27 due to each actor nodes $H(\Delta V_{27a})$ is computed using equation (6.17). Table 6.3 lists differential entropy of ΔV_{27a} for all actor nodes in order of maximum to minimum differential entropy. From table 6.3 it can be seen that we can estimate top 11 dominant influencer nodes of voltage fluctuations with reasonable accuracy using differential entropy as

Table 6.1: *Dominant Influencer of Voltage Fluctuation*

Indicator Metric	Dominant Influencer Node	Computation Time (s)
Monte-Carlo based simulation	24	22389.63
Differential entropy	24	0.66
Joint differential entropy	18	0.71
KL distance	24	0.68
Frechet distance	24	0.70

a measure. Computation time of calculating the dominant influencer of voltage fluctuation using differential entropy is 0.62 second, which is a significant improvement over Monte-Carlo simulation based scenario analysis.

To test proposition 2 and test effectiveness of joint differential entropy as an indicator of the dominant influencer of voltage fluctuations, joint differential entropy between ΔV_{27} and ΔV_{27a} due to all active consumers is computed using equation (6.31). Table 6.4 lists joint differential entropy for all actor nodes in order of maximum to minimum differential entropy. From table 6.4, it can be seen that joint differential entropy can be used to estimate the dominant influencer of the voltage fluctuations with fair accuracy. Computation time to calculate the dominant influencer of the voltage fluctuation using joint differential entropy is 0.71 second. Performance of the joint differential entropy as an indicator of the dominant influencer of voltage fluctuation is inferior to differential entropy both in term of accuracy and computation time.

Similar simulation is done to investigate effectiveness of Kullback-Leibler distance, Frechet distance and mutual information as an indicator of the dominant influencer of voltage fluctuations. Table 6.3 lists Kullback-Leibler Distance for all actor nodes in order of minimum to maximum KL Distance. Similarly, Table 6.5 lists Frechet distance for all actor nodes in order of minimum to maximum distance. From Tables 6.3 and 6.5, it can be seen that KL distance and Frechet distance estimate the dominant influencer of the voltage fluctuations with fair accuracy. However, mutual information fails to identify the dominant influencer of voltage fluctuations. Computation time of calculating the dominant influencer of voltage fluctuation using all theses metrics is less then one second. Table 6.1 shows the dominant

influencer of voltage fluctuation using all the proposed metrics and their computation time.

6.8 Summary

This chapter introduces concept of the dominant influencer of voltage fluctuations and investigates various information theoretic metrics to analytically identify the dominant influencer of voltage fluctuations at the observation node in the power distribution system. First, all the candidate metrics are analytically derived. Then, accuracy and computational efficiency these metrics are verified using IEEE 69 bus test system. It is shown that differential entropy of voltage change at the observation node due to change in power at an actor node is an excellent indicator of the dominant influencer of voltage fluctuation. Proposed analytical method of identifying the dominant influencer of voltage fluctuation is shown to be computationally efficient.

Table 6.2: *Numerical Dominant Influencer of the Voltage Fluctuation*

Rank	Node	Reduction in Variance ($\times 10^{-3} p.u.^2$)
1	24	0.2992
2	18	0.2199
3	22	0.2027
4	16	0.1680
5	26	0.1659
6	20	0.1284
7	12	0.1135
8	14	0.0966
9	66	0.0495
10	68	0.0483
11	10	0.0334
12	52	0.0217
13	6	0.0183
14	62	0.0156
15	54	0.0152
16	64	0.0127
17	60	0.0116
18	8	0.0094
19	50	0.0077
20	56	0.0077
21	58	0.0066
22	40	-0.0037
23	48	-0.0038
24	4	-0.0042
25	42	-0.0047
26	2	-0.0051
27	32	-0.0063
28	34	-0.0132
29	36	-0.0136
30	30	-0.0137
31	28	-0.0156
32	46	-0.0158
33	44	-0.0159
34	38	-0.0185

Table 6.3: *Differential Entropy and Kullback-Leibler Divergence Indicator*

Rank	Node	$H(\Delta V_{oa})$ nats	$D_{KL}(\mathbf{V_o} \| \mathbf{\Delta V_{oa}})$
1	24	6.8934	1.1064
2	18	6.4968	1.4478
3	22	6.3536	1.5761
4	26	6.0498	1.8543
5	16	5.9688	1.9295
6	20	5.5602	2.3158
7	14	4.8065	3.0452
8	12	4.7565	3.0941
9	66	4.1377	3.7012
10	68	3.6579	4.1711
11	10	3.5318	4.2937
12	60	2.7004	5.0730
13	54	2.7004	5.0730
14	64	2.2957	5.4096
15	58	2.2957	5.4096
16	52	2.1860	5.4921
17	62	1.6070	5.8406
18	56	1.6070	5.8406
19	8	1.4984	5.8879
20	6	1.0408	6.0284
21	2	-0.6160	6.1454
22	44	-0.6160	6.1454
23	38	-0.6160	6.1454
24	32	-0.6160	6.1454
25	46	-0.6160	6.1454
26	40	-0.6160	6.1454
27	34	-0.6160	6.1454
28	28	-0.6160	6.1454
29	42	-0.6160	6.1454
30	36	-0.6160	6.1454
31	30	-0.6160	6.1454
32	50	-0.6160	6.1454
33	4	-0.6160	6.1454
34	48	-0.6160	6.1454

Table 6.4: *Joint Differential Entropy Indicator*

Rank	Node	$H(\mathbf{\Delta V_o}, \mathbf{\Delta V_{oa}})$ nats
1	18	14.8608
2	22	14.8148
3	24	14.6642
4	26	14.6394
5	16	14.5745
6	20	14.2546
7	14	13.5760
8	12	13.5239
9	66	12.9335
10	68	12.4691
11	10	12.3437
12	60	11.5207
13	54	11.5207
14	64	11.1189
15	58	11.1189
16	52	11.0096
17	62	10.4295
18	56	10.4295
19	8	10.3198
20	6	9.8521
21	2	5.7673
22	44	5.7673
23	38	5.7673
24	32	5.7673
25	46	5.7673
26	40	5.7673
27	34	5.7673
28	28	5.7673
29	42	5.7673
30	36	5.7673
31	30	5.7673
32	50	5.7673
33	4	5.7673
34	48	5.7673

Table 6.5: *Frechet Distance Indicator*

Rank	Node	$d_F^2(\mathbf{V_{oa}}, \mathbf{\Delta V_o})$
1	24	819.1
2	18	948.0
3	22	990.8
4	26	1074.8
5	16	1095.4
6	20	1191.2
7	14	1330.4
8	12	1337.9
9	66	1420.7
10	68	1470.9
11	10	1482.1
12	54	1542.3
13	60	1542.3
14	58	1564.1
15	64	1564.1
16	52	1569.3
17	56	1592.8
18	62	1592.8
19	8	1596.5
20	6	1610.3
21	48	1662.8
22	4	1662.9
23	50	1663.0
24	30	1663.1
25	36	1663.1
26	42	1663.1
27	28	1663.1
28	34	1663.1
29	40	1663.1
30	46	1663.1
31	32	1663.1
32	38	1663.1
33	44	1663.1
34	2	1663.2

Chapter 7

Security and Stability of Transactive Energy Market-based Smart Power Distribution System

After developing model of the active consumers and analyzing impact of their actions on distribution grid voltage, this chapter investigates impact of the false data injection attack on operation of the transactive energy market based power distribution system. Since future power systems with active consumers will be more complex, there will be a continuing need to consider cyber-physical system (CPS) perspective in the operation, control, and design of these systems. Therefore, understanding, modeling and quantifying the security and stability of smart power distribution system driven by transactive energy market forces is critical.

Allowing consumers to actively participate in energy transactions poses risks to the grid itself. A number of possible factors are: 1) consumers gaming the system to gain unfair financial advantages, 2) consumer activities that destabilize the grid and cause potential hazardous conditions, and 3) tampering with smart metering devices and commit some type of fraud [73]. All these threats need to be analyzed taking into account the roles of the players and their incentives. Analyzing stability and security of transactive energy market based power distribution system is a crucial aspect of this work. In recent years, cyber

security has been become a significant concern to modern power system due to the prevalent application of information technologies. In a successful false data injection (FDI) attack, an attacker compromises measurements from grid sensors in such a way that undetected errors are introduced into estimates of system parameters such as electricity price, total energy demand, and bus voltages. Evading detection by commonly employed residue-based bad data detection tests, FDI attacks are capable of severely threatening power system security [74]. Moreover, weaknesses in cyber security can also threaten the stability of the distribution system voltage due to the deep integration of the physical and cyber system [75, 76].

7.1 Dynamics of Electricity Prices and Demand

Consider a model of future power distribution system with multiple active consumers with possible renewable generation and multiple third party aggregators.Here, each aggregator is expected to be in a contractual agreement with a subset of consumers. In this contractual agreement, the aggregator decides real-time price of electricity and communicates it to active consumers over a communication infrastructure. For example, AMI serves as a conduit for bidirectional information exchange between an active consumer and their aggregator. Active consumers receive real-time electricity prices and decide their electricity consumption based on price of electricity at a given time. Information about electricity consumptions of consumers is communicated back to the aggregator. This work focuses only on the interaction between a single aggregator and active consumers that are in contractual agreement with the aggregator of interest. That is ,the aggregator can only interact and communicate with their contracted consumers and do not have information about energy consumption of other active consumers.

Let $\mathcal{N} = \{1, 2, \cdots, n\}$ denote the set of active consumers that are served by the aggregator of interest; and $E_n(t)$ be the energy consumed by n^{th} active consumer at time t. The aggregator receives this information though AMI resulting in a vector of energy consumptions denoted as: $\mathbf{E}(t) = [E_1(t), E_2(t), \cdots, E_n(t)]$. The total energy demand $\mathcal{D}(t)$ for the aggregator at time t can be computed as: $\mathcal{D}(t) = \mathbf{E}(t)^T\mathbf{1}$. Based on total demand at time t,

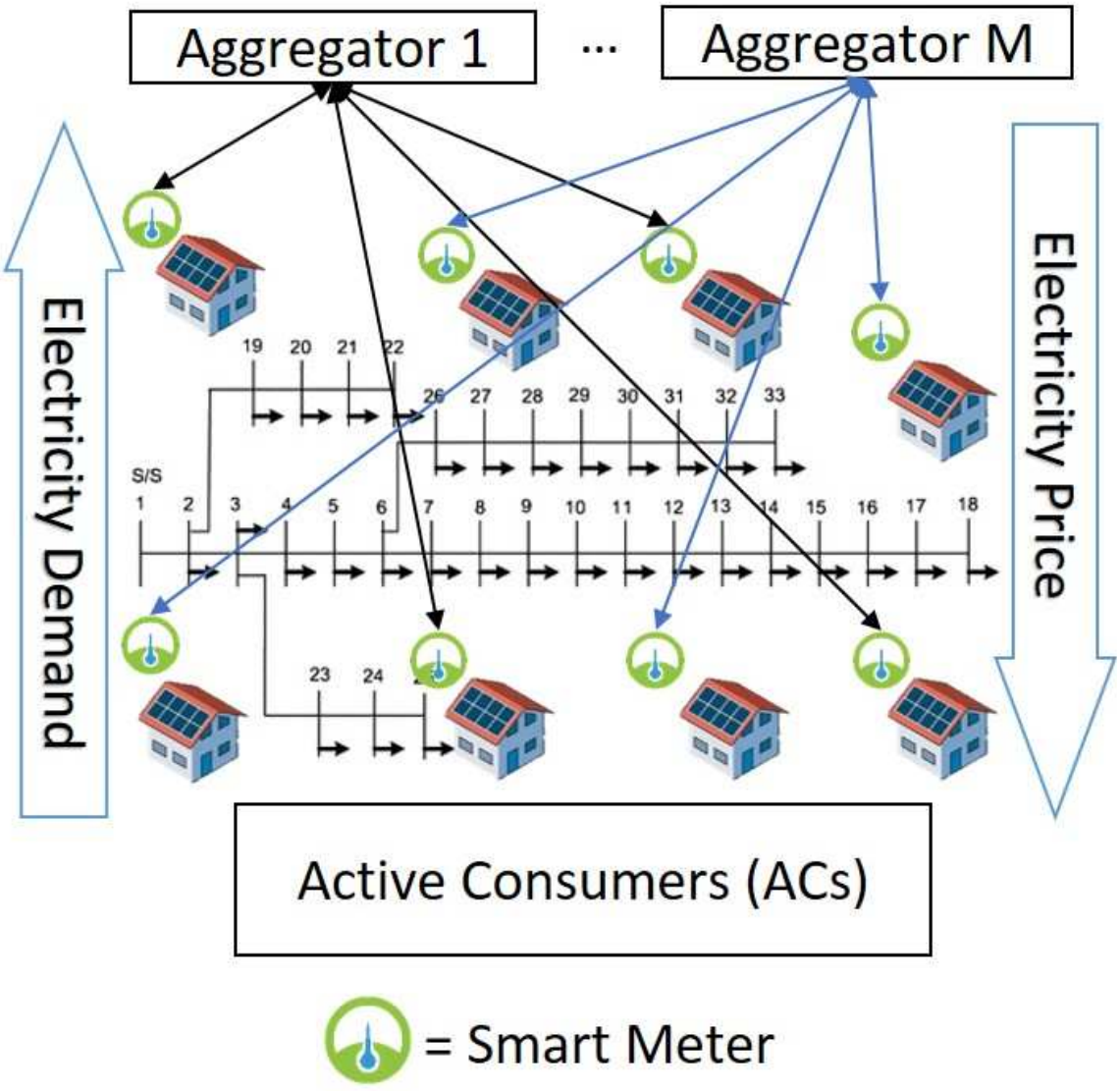

Figure 7.1: *System Model*

the aggregator decides the price of electricity for time $t+1$ as [77]

$$\mathcal{P}(t+1) = \alpha_0 + \alpha_1 \mathcal{D}(t). \tag{7.1}$$

Here $\mathcal{P}(t)$ is the real-time price of electricity at time t, $\alpha_0 > 0$ is the base electricity price in dollars and $\alpha_1 \geq 0$ is the incremental price of electricity in $\$/kWh$. Value of α_0 and α_1 are decided by the aggregator. It is expected that the aggregator will increase/decrease price of electricity as demand increases/decreases. Criteria for selecting a favorable value of α_0 and

α_1 is discussed in section 7.2.2.

Real-time electricity prices decided by the aggregator are communicated to all the active consumers that are in contract with the aggregator. Active consumers may alter their electricity consumption behavior in response to changes in electricity prices. Consumers are expected to increase their electricity consumption as electricity prices decrease and decrease their electricity consumption as price of electricity increases. Different class of consumers may behave differently in response to changes in electricity prices. There have been various efforts to model electricity consumption behavior of active consumers within a transactive energy market [15, 35]. Irrespective of exact model of consumer behavior, the total demand of electricity ($\mathcal{D}(t)$) for the aggregator at time t can be estimated as a function of electricity prices as

$$\mathcal{D}(t) = \beta_0 + \frac{\beta_1}{\mathcal{P}(t)} + \frac{\beta_2}{\mathcal{P}^2(t)}, \tag{7.2}$$

where β_0, β_1 and β_2 are coefficients of demand elasticity that can be estimated based on historical data related to change in total demand in response to changes in electricity prices as discussed next (in section 7.1.1).

7.1.1 Estimation of β_0, β_1, and β_2

Let $\mathcal{D}_m$ denote the total demand when price of electricity is $\mathcal{P}_m$. With availability of m data points, the value of demand coefficients can be estimated using a simple least square approach, i.e.,

$$\begin{bmatrix} \hat{\beta}_0 \\ \hat{\beta}_1 \\ \hat{\beta}_2 \end{bmatrix} = (\mathbf{A^T A})^{-1} \mathbf{A^T} \begin{bmatrix} \mathcal{D}_1 \\ \mathcal{D}_2 \\ \vdots \\ \mathcal{D}_m \end{bmatrix}, \tag{7.3}$$

where,

$$\mathbf{A} = \begin{bmatrix} 1 & \mathcal{P}_1^{-1} & \mathcal{P}_1^{-2} \\ 1 & \mathcal{P}_2^{-1} & \mathcal{P}_2^{-2} \\ \vdots & \vdots & \vdots \\ 1 & \mathcal{P}_m^{-1} & \mathcal{P}_m^{-2} \end{bmatrix}, \tag{7.4}$$

Here $\hat{\beta}_0$, $\hat{\beta}_1$, and $\hat{\beta}_2$ are estimated values of coefficients of demand elasticity. Although availability of such data may seem a bit presumptuous at present, with broader implementation of smart-grid/transactive energy market, more data is expected to be available in the future. This will enable a more accurate estimation of coefficients of demand elasticity. Proposed model of total demand vs electricity price is general enough and can be used to estimate wide range of load models by selecting different values of β parameters.

7.2 Equilibrium and Stability Analysis

As seen in equation (7.1) and (7.2), demand dynamics impacts electricity pricing dynamics and vice versa. Therefore, obvious question to ask in this interactive transactive energy market is the following: What are the stable equilibrium electricity price and demand? The interaction between aggregator and multiple active consumers and dynamics of the electricity price and the demand can be modeled as discrete time non-linear autonomous (no forcing input) control system with the electricity price or the total demand as state variables of the system.

$$f\mathcal{P}(t+1) = \alpha_0 + \alpha_1\beta_0 + \frac{\alpha_1\beta_1}{\mathcal{P}(t)} + \frac{\alpha_1\beta_2}{\mathcal{P}^2(t)}. \tag{7.5}$$

$$\mathcal{D}(t+1) = \beta_0 + \frac{\beta_1}{\alpha_0 + \alpha_1\mathcal{D}(t)} + \frac{\beta_2}{(\alpha_0 + \alpha_1\mathcal{D}(t))^2}. \tag{7.6}$$

This non-linear autonomous system have equilibrium price of electricity and equilibrium demand. This section compute equilibrium price and demand of the proposed system model

and establishes conditions for stability of the equilibrium point.

7.2.1 Equilibrium and Stability of Electricity Prices:

Theorem 5. *The equilibrium price of electricity* ($\mathcal{P}^*$) *for the discrete time non-linear autonomous dynamical system in (7.5) and (7.6) is given by:*

$$\mathcal{P}^* = -\frac{1}{3}\left(b_{\mathcal{P}} + C_{\mathcal{P}} + \frac{\Delta_{\mathcal{P}0}}{C_{\mathcal{P}}}\right), \tag{7.7}$$

where

$$\begin{aligned} C_{\mathcal{P}} &= \sqrt[3]{\frac{\Delta_{\mathcal{P}1} \pm \sqrt{\Delta_{\mathcal{P}1}^2 - 4\Delta_{\mathcal{P}0}^3}}{2}}, \\ \Delta_{\mathcal{P}0} &= b_{\mathcal{P}}^2 - 3c_{\mathcal{P}}, \\ \Delta_{\mathcal{P}1} &= 2b_{\mathcal{P}}^3 - 9b_{\mathcal{P}}c_{\mathcal{P}} + 27d_{\mathcal{P}}, \end{aligned} \tag{7.8}$$

and

$$\begin{aligned} b_{\mathcal{P}} &= -\alpha_0 + \alpha_1\beta_0, \\ c_{\mathcal{P}} &= -\alpha_1\beta_1, \\ d_{\mathcal{P}} &= -\alpha_1\beta_2. \end{aligned} \tag{7.9}$$

Proof. From equation (7.1) and (7.2), state dynamics of the discrete time autonomous control system can be written in terms of electricity prices as

$$\mathcal{P}(t+1) = \alpha_0 + \alpha_1\beta_0 + \frac{\alpha_1\beta_1}{\mathcal{P}(t)} + \frac{\alpha_1\beta_2}{\mathcal{P}^2(t)}. \tag{7.10}$$

Let $f(\mathcal{P}(t))$ denote the price state dynamic function defined as:

$$\begin{aligned} f(\mathcal{P}(t)) &:= \mathcal{P}(t+1) - \mathcal{P}(t) \\ &= \alpha_0 + \alpha_1\beta_0 + \frac{\alpha_1\beta_1}{\mathcal{P}(t)} + \frac{\alpha_1\beta_2}{\mathcal{P}^2(t)} - \mathcal{P}(t) \end{aligned} \tag{7.11}$$

Let $\mathcal{P}^*$ be the equilibrium electricity price of the system. At the state of equilibrium $\mathcal{P}(t+1) = \mathcal{P}(t) = \mathcal{P}^* \Rightarrow f(\mathcal{P}^*) = 0$.

$$\alpha_0 + \alpha_1\beta_0 + \frac{\alpha_1\beta_1}{\mathcal{P}^*} + \frac{\alpha_1\beta_2}{\mathcal{P}^{*2}} - \mathcal{P}^* = 0 \tag{7.12}$$

$$\mathcal{P}^{*3} - (\alpha_0 + \alpha_1\beta_0)\mathcal{P}^{*2} - \alpha_1\beta_1\mathcal{P}^* - \alpha_1\beta_2 = 0 \tag{7.13}$$

Solutions of the cubic equation (7.13) can be calculated analytically via equations (7.7) - (7.9) □

The cubic equation given in (7.13) has three solutions resulting in three equilibrium points. Therefore its important to establish conditions for stability of the equilibrium point. Here, the notion of BIBO (bounded input bounded output) stability is considered.

Lemma 2. *The set of BIBO stable equilibrium price of electricity* ($\mathcal{B}_\mathcal{P}$) *for the discrete time non-linear autonomous dynamical system in (7.5) and (7.6) is given by:*

$$\mathcal{B}_\mathcal{P} = \{\, \mathcal{P} \mid -2 < \frac{f(\mathcal{P}) - f(\mathcal{P}^*)}{\mathcal{P} - \mathcal{P}^*} < 0 \,\}. \tag{7.14}$$

Proof. Let $f'(\mathcal{P}^*)$ be the slope of $f(\mathcal{P})$ at the equilibrium point. The trajectory of electricity price diverges away from equilibrium when $f'(\mathcal{P}^*)$ is greater than zero at equilibrium. The trajectory converges towards the equilibrium point without oscillations when $f'(\mathcal{P}^*)$ is less than zero and greater than -1 at equilibrium. The trajectory converges towards the equilibrium point with oscillation when $f'(\mathcal{P}^*)$ is less than -1 and greater than -2 at equilibrium. The trajectory diverges away from the equilibrium point with oscillation when $f'(\mathcal{P}^*)$ is less than -2 at equilibrium. Therefore, the equilibrium point is stable if:

$$-2 < f'(\mathcal{P}^*) = \left.\frac{df(\mathcal{P})}{d\mathcal{P}}\right|_{\mathcal{P}^*} < 0. \tag{7.15}$$

Differentiating equation (7.11):

$$-2 < -\frac{\alpha_1\beta_1}{\mathcal{P}^{*2}(t)} - \frac{2\alpha_1\beta_2}{\mathcal{P}^{*3}(t)} - 1 < 0 \tag{7.16}$$

The stable equilibrium point is BIBO stable for set of $\mathcal{P}$ that satisfy following conditions:

$$f(\mathcal{P}) - f(\mathcal{P}^*) > -2(\mathcal{P} - \mathcal{P}^*), \forall \mathcal{P} > \mathcal{P}^* \tag{7.17}$$

$$f(\mathcal{P}) - f(\mathcal{P}^*) < -2(\mathcal{P} - \mathcal{P}^*), \forall \mathcal{P} < \mathcal{P}^* \tag{7.18}$$

$$-2 < \frac{f(\mathcal{P}) - f(\mathcal{P}^*)}{\mathcal{P} - \mathcal{P}^*} < 0, \forall \mathcal{P} \tag{7.19}$$

Therefore, the BIBO stable set of electricity prices ($\mathcal{B}_{\mathcal{P}}$) is the set of electricity prices that satisfy equation (7.19). □

The equilibrium and stability of electricity prices depends on values of coefficients of demand elasticity, no-load and incremental electricity prices. Although values of coefficients of demand elasticity can be estimated based on consumer behavior, aggregator can choose favorable values of no-load and incremental electricity prices in order to achieve desired equilibrium price of electricity and ensuring a higher level of stability.

7.2.2 Selection of α_0, and α_1

In proposed system model, values of no load electricity price (α_0) and incremental electricity price α_1 are decided by the aggregator based on economic factors, stability criteria and engineering judgment. Steps for deciding good values of α_0, α_1 are given by algorithm 3 and criteria to consider are described.

Algorithm 3 Selection of α_0, and α_1

1: Select the desired equilibrium price of electricity ($\mathcal{P}^*$)
2: Select favorable value of $f'(\mathcal{P}^*)$
3: Calculate value of incremental electricity price α_1
4: Calculate value of no-load electricity price α_0

1. Select the desired equilibrium price of electricity ($\mathcal{P}^*$):

Value of equilibrium price of electricity is selected based on the total demand at a given electricity price. Value of total demand at for given price of electricity can be evaluated using a curve of total demand vs price of electricity obtained using historical data. Fig. 7.2 shows an example curve of total demand vs price of electricity obtained from active consumer behavior model introduced in [15]

2. Select the slope of price dynamics at equilibrium $f'(\mathcal{P}^*)$

Once value of equilibrium electricity price and total demand is established, value of no load electricity price (α_0) and incremental electricity price (α_1) can be calculated based on the selected value of f' using equation (7.20). Equilibrium price of electricity is positive ($\mathcal{P}^* > 0$, and value of $\beta_1 > 0$ and $\beta_2 > 0$) as total demand decreases as price of electricity increases. Slope of price dynamics ($f'(\mathcal{P}^*)$) at equilibrium must be less than or equal to -1 as incremental price of electricity must be non negative ($\alpha_1 \geq 0$). From equation (7.9) it can be concluded that $-2 < f'(\mathcal{P}^*) < -1$. Value of incremental electricity price is zero ($\alpha_1 = 0$) when $f' = -1$. This results in the largest set of BIBO stable electricity price and lower oscillations in demand and pricing. From an economic perspective higher value of α_1 is desirable, which results in lower value of f' resulting in smaller set of BIBO stable electricity prices and greater price/demand oscillations. Therefore, selecting a favorable value of $f'(\mathcal{P}^*)$ is a tradeoff between one that results in a more stable system and one with higher value of incremental electricity price.

3. Calculate value of incremental electricity price α_1

Based on value of $f'(\mathcal{P}^*)$, incremental price of electricity can be computed as,

$$\alpha_1 = -\frac{(f'(\mathcal{P}^*) + 1)\mathcal{P}^{*3}}{\beta_1 \mathcal{P}^* + 2\beta_2} \tag{7.20}$$

4. Calculate value of no-load electricity price α_0

Based on value of α_0, α_1 and $\mathcal{P}^*$, value of no load electricity price α_0 can be calculated as follows:

$$\alpha_0 = -\alpha_1\beta_0 - \frac{\alpha_1\beta_1}{\mathcal{P}^*} - \frac{\alpha_1\beta_2}{\mathcal{P}^{*2}} - \mathcal{P}^* \tag{7.21}$$

7.2.3 Equilibrium and Stability of Total Demand

Theorem 6. *The equilibrium demand of electricity ($\mathcal{D}^*$) for the discrete time non-linear autonomous dynamical system in (7.5) and (7.6) is given by:*

$$\mathcal{D}^* = -\frac{1}{3}\left(b_{\mathcal{D}} + C_{\mathcal{D}} + \frac{\Delta_{\mathcal{D}0}}{C_{\mathcal{D}}}\right), \tag{7.22}$$

where,

$$\begin{aligned} C_{\mathcal{D}} &= \sqrt[3]{\frac{\Delta_{\mathcal{D}1} \pm \sqrt{\Delta_{\mathcal{D}1}^2 - 4\Delta_{\mathcal{D}0}^3}}{2}}, \\ \Delta_{\mathcal{D}0} &= b_{\mathcal{D}}^2 - 3a_{\mathcal{D}}c_{\mathcal{D}}, \\ \Delta_{\mathcal{D}1} &= 2b_{\mathcal{D}}^3 - 9a_{\mathcal{D}}b_{\mathcal{D}}c_{\mathcal{D}} + 27a_{\mathcal{D}}^2 d_{\mathcal{D}}, \end{aligned} \tag{7.23}$$

and

$$\begin{aligned} a_{\mathcal{D}} &= \alpha_1^2, \\ b_{\mathcal{D}} &= -(\alpha_1^2\beta_0 - 2\alpha_0\alpha_1), \\ c_{\mathcal{D}} &= -(2\alpha_0\alpha_1\beta_0 + \alpha_1\beta_1 - \alpha_0^2), \\ d_{\mathcal{D}} &= -(\alpha_0^2\beta_0 + \alpha_0\beta_1 + \beta_2). \end{aligned} \tag{7.24}$$

Proof. From equations (7.1) and (7.2), state dynamics of the discrete time autonomous control system can be written in terms of electricity demand as

$$\mathcal{D}(t+1) = \beta_0 + \frac{\beta_1}{\alpha_0 + \alpha_1 \mathcal{D}(t)} + \frac{\beta_2}{(\alpha_0 + \alpha_1 \mathcal{D}(t))^2}. \tag{7.25}$$

Let $g(\mathcal{D}(t))$ be demand dynamic function defined as:

$$g(\mathcal{D}(t)) = \beta_0 + \frac{\beta_1}{\alpha_0 + \alpha_1 \mathcal{D}(t)} + \frac{\beta_2}{(\alpha_0 + \alpha_1 \mathcal{D}(t))^2} - \mathcal{D}(t) \tag{7.26}$$

Let $\mathcal{D}(t)^*$ be the equilibrium demand of the system. At the equilibrium demand $\mathcal{D}(t+1) = \mathcal{D}(t) = \mathcal{D}(t)^* \Rightarrow g(\mathcal{D}^*) = 0$.

$$\beta_0 + \frac{\beta_1}{\alpha_0 + \alpha_1 \mathcal{D}^*} + \frac{\beta_2}{(\alpha_0 + \alpha_1 \mathcal{D}^*)^2} - \mathcal{D}^* = 0 \tag{7.27}$$

$$\beta_0(\alpha_0 + \alpha_1 \mathcal{D}^*)^2 + \beta_1(\alpha_0 + \alpha_1 \mathcal{D}^*) + \beta_2 - \mathcal{D}^*(\alpha_0 + \alpha_1 \mathcal{D}^*)^2 = 0 \tag{7.28}$$

$$\begin{aligned} &\alpha_1^2 \mathcal{D}^{*3} - (\alpha_1^2 \beta_0 - 2\alpha_0 \alpha_1) \mathcal{D}^{*2} - (2\alpha_0 \alpha_1 \beta_0 + \alpha_1 \beta_1 - \alpha_0^2) \mathcal{D}^* \\ &- (\alpha_0^2 \beta_0 + \alpha_0 \beta_1 + \beta_2) = 0 \end{aligned} \tag{7.29}$$

Solutions of the cubic equation (7.29) can be calculated analytically using equations (7.22) - (7.24) □

The cubic equation in (7.29) has three solutions resulting in three equilibrium points. Therefore its important to establish conditions for stability of the equilibrium point. Once again, the notion of BIBO stability is invoked.

Lemma 3. *The set of BIBO stable equilibrium demand of electricity* ($\mathcal{B}_\mathcal{D}$) *for the discrete time non-linear autonomous dynamical system in (7.5) and (7.6) is given by:*

$$\mathcal{B}_\mathcal{D} = \{\, \mathcal{D} \mid -2 < \frac{g(\mathcal{D}) - g(\mathcal{D}^*)}{\mathcal{D} - \mathcal{D}^*} < 0 \,\} \tag{7.30}$$

Proof. Let $g'(\mathcal{D}^*)$ be the slope of $g(\mathcal{D})$ at the equilibrium point. The trajectory of electricity demand diverges away from equilibrium when $g'(\mathcal{D}^*)$ is greater than zero at equilibrium.

The trajectory converges towards the equilibrium point without oscillation when $g'(\mathcal{D}^*)$ is less than zero and greater than -1 at equilibrium. The trajectory converges towards the equilibrium point with oscillation when $g'(\mathcal{D}^*)$ is less than -1 and greater than -2 at equilibrium. The trajectory diverges away from the equilibrium point with oscillation when $g'(\mathcal{D}^*)$ is less than -2 at equilibrium. Therefore, the equilibrium point is stable if:

$$-2 < g'(\mathcal{D}^*) = \left.\frac{dg(\mathcal{D})}{d\mathcal{D}}\right|_{\mathcal{D}^*} < 0 \tag{7.31}$$

Differentiating equation (7.26):

$$-2 < \frac{-\alpha_1\beta_1}{(\alpha_0+\alpha_1\mathcal{D}^*)^2} + \frac{-2\alpha_1\beta_2}{(\alpha_0+\alpha_1\mathcal{D}^*)^3} - 1 < -1 \tag{7.32}$$

The stable equilibrium point is BIBO stable for set of $\mathcal{D}$ that satisfy following condition:

$$g(\mathcal{D}) - g(\mathcal{D}^*) > -2(\mathcal{D}-\mathcal{D}^*), \forall \mathcal{D} > \mathcal{D}^* \tag{7.33}$$

$$g(\mathcal{D}) - g(\mathcal{D}^*) < -2(\mathcal{D}-\mathcal{D}^*), \forall \mathcal{D} < \mathcal{D}^* \tag{7.34}$$

$$-2 < \frac{g(\mathcal{D}) - g(\mathcal{D}^*)}{\mathcal{D}-\mathcal{D}^*} < 0, \forall \mathcal{D} \tag{7.35}$$

Therefore, BIBO stable set of total demand is the set $\mathcal{D}$ that satisfies equation (7.35). □

After analyzing the equilibrium and stability conditions for given discrete time non-linear autonomous control system, impact of FDI attacks on distribution system can be analyzed.

7.3 Impact of Cyber Attack

Any smart power distribution system with smart meters and communication infrastructure is prone to cyber attacks. An attacker can manipulate electricity prices communicated over the cyber infrastructure or compromise a subset of smart meters altering their measurements. Such cyber attacks may have impacts on electricity prices, energy consumption of active consumers and distribution system voltage. Additionally, impact of such attack can last

for multiple time periods even when the system is attacked during only one time period. In case of an attack on electricity demand information, the attacker can manipulate energy consumption measurements of multiple active consumers that results in incorrect calculation of total demand resulting in change in electricity prices in future time periods. In case of an attack on electricity pricing, the attacker can manipulate price of electricity at any given time. In response to the change in price of electricity active consumers may adjust their energy consumption resulting in a change in electricity demand, which eventually may result in changed price of electricity in future time periods. Due to mutual coupling between electricity price and demand, a cyber attack on electricity price information impacts the total demand and vice versa. Let $\hat{\mathcal{D}}(t)$ denote the manipulated demand of electricity at time t, and $\epsilon_{\mathcal{D}}(t) = \hat{\mathcal{D}}(t) - \mathcal{D}(t)$ be the error in total demand at time t. Similarly, let $\hat{\mathcal{P}}(t)$ denote the manipulated electricity price at time t, and $\epsilon_{\mathcal{P}}(t) = \hat{\mathcal{P}}(t) - \mathcal{P}(t)$ be the error in electricity price at time t. Change in demand at time t ($\hat{\mathcal{D}}(t)$) results in change in price of electricity at time $t+1$ as illustrated by the relationship,

$$\hat{\mathcal{P}}(t+1) = \alpha_0 + \alpha_1 \hat{\mathcal{D}}(t). \tag{7.36}$$

Similarly, change in the electricity price at time t ($\hat{\mathcal{P}}(t)$) results in change in the demand at time t as

$$\hat{\mathcal{D}}(t) = \beta_0 + \frac{\beta_1}{\hat{\mathcal{P}}(t)} + \frac{\beta_2}{\hat{\mathcal{P}}^2(t)}. \tag{7.37}$$

Error in electricity price at time $t+1$ can be written in terms of error in total demand at time t as:

$$\epsilon_{\mathcal{P}}(t+1) = \alpha_0 + \alpha_1(\mathcal{D}(t) + \epsilon_{\mathcal{D}}(t)) - \alpha_0 + \alpha_1 \mathcal{D}(t) \tag{7.38}$$

$$\epsilon_{\mathcal{P}}(t+1) = \alpha_1 \epsilon_{\mathcal{D}}(t) \tag{7.39}$$

Similarly error in total demand at time t can be written in terms of error in electricity price at time t as:

$$\epsilon_{\mathcal{D}}(t) = \frac{-\beta_1 \epsilon_{\mathcal{P}}(t)}{\mathcal{P}(t)(\mathcal{P}(t) + \epsilon_{\mathcal{P}}(t))} + \frac{\beta_2(2\mathcal{P}(t)\epsilon_{\mathcal{P}}(t) + \epsilon_{\mathcal{P}}^2(t))}{\mathcal{P}^2(t)(\mathcal{P}(t) + \epsilon_{\mathcal{P}}(t))^2} \tag{7.40}$$

Equation (7.39) and (7.40) are error propagation dynamics of the system. Equation (7.39) indicates that lower value of α_1 results in lower propagation of the error to future time periods. When there is error introduced in price or demand, system will asymptotically come back to the stable equilibrium point. However, before coming to stable state system will oscillate around the the stable state, the which causes oscillations in price of electricity, demand and network voltage. The higher the magnitude of the error, higher the impact. However, when introduced error is large enough to push the state out of BIBO stable region the the system will suffer higher degree of damage.

7.4 Simulation and Results

The dynamics, stability and impact of cyber attacks on proposed transactive energy market based power distribution system is analyzed using simulations on the modified IEEE 69 bus balanced test system as shown in Fig. 4.3. The nominal voltage of the test system is 12.66 kV. In this simulation setup one active consumer is assumed to be located at each node of the IEEE 69 bus test system. Model of active consumers proposed in [15] is used to mimic energy consumption behavior of active consumers. For simplicity of demonstration, a scenario is considered where all the active consumers in the distribution system are in contractual agreement with a single aggregator. Additionally, all active consumers are assumed to be identical with coefficient of comfort 0.65 and 10 kWh of renewable generation [15]. Active consumers do not consider distribution grid voltage while making their energy consumption decision. However, the proposed system model is valid for more general case where multiple aggregators operate within a single distribution system with active consumers that have varying preferences for electricity consumption.

Values of coefficients of demand elasticity (β_0, β_1, β_2) are estimated using curve of total demand vs normalized electricity pricing obtained using model of active consumer behavior proposed in [15] and shown in Fig. 7.2. In order to obtain the curve of total demand vs normalized electricity pricing, price of electricity is varied from 0.1 to 1.0 normalized cost unit (ncu) and energy consumption of all active consumers is observed. Total demand for given

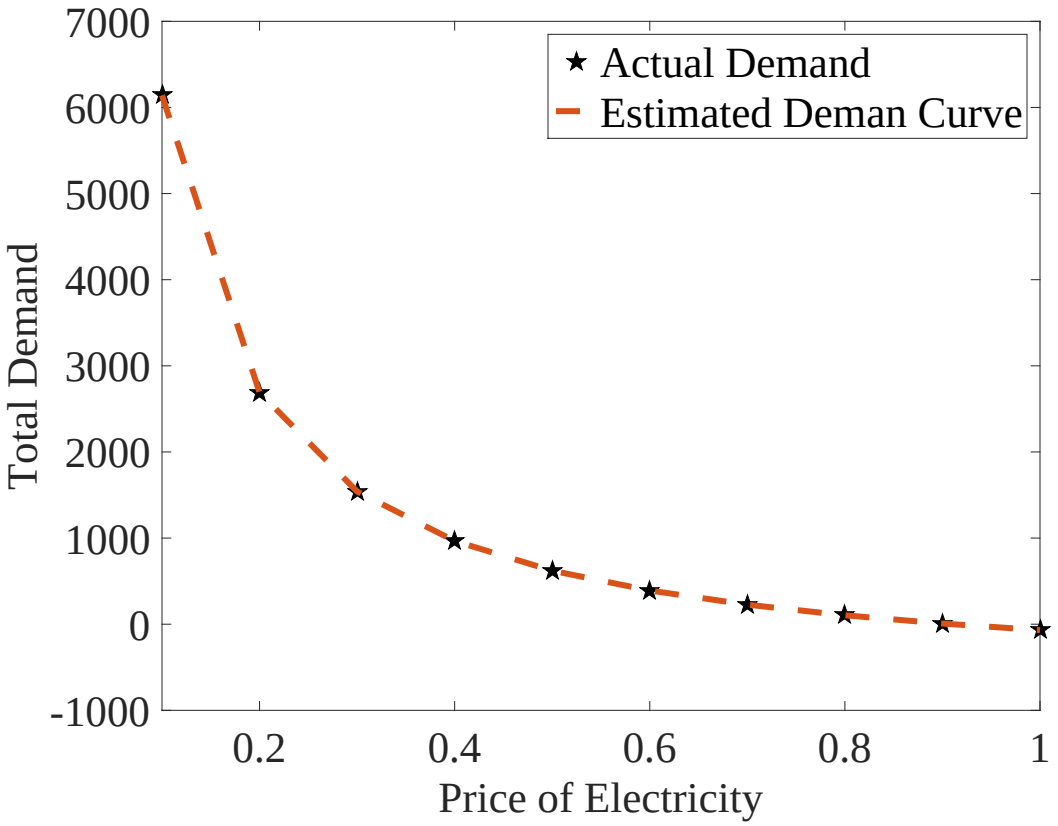

Figure 7.2: *Change in total demand with respect to price of electricity*

price of electricity is sum of individual energy consumption of all active consumers. From Fig. 7.2, it can be seen that as price of electricity increases, total demand decreases. For extremely high values of electricity price, the total demand becomes negative as consumers start selling their renewable generation back to the grid. To estimate the coefficients of demand elasticity, 10 sample data points of demand curve are used as shown by black stars in Fig. 7.2. Values of demand elasticity β_0, β_1, and β_2 are obtained using least square method illustrated in section 7.1.1. Computed values are: $\beta_0 = -759$kWh, $\beta_1 = 690$ncu kWh and $\beta_2 = 3.37 \times 10^{-14}$ncu^{2}kWh. Estimated curve of the total demand vs normalized price of electricity is shown by red dashed line in Fig. 7.2. Although, this work uses model of active consumer behavior proposed in [15] to obtain curve of total demand vs price of electricity as more data become available values of coefficients of demand elasticity can be estimated using actual historical data. Regardless of the data source, proposed system model is general

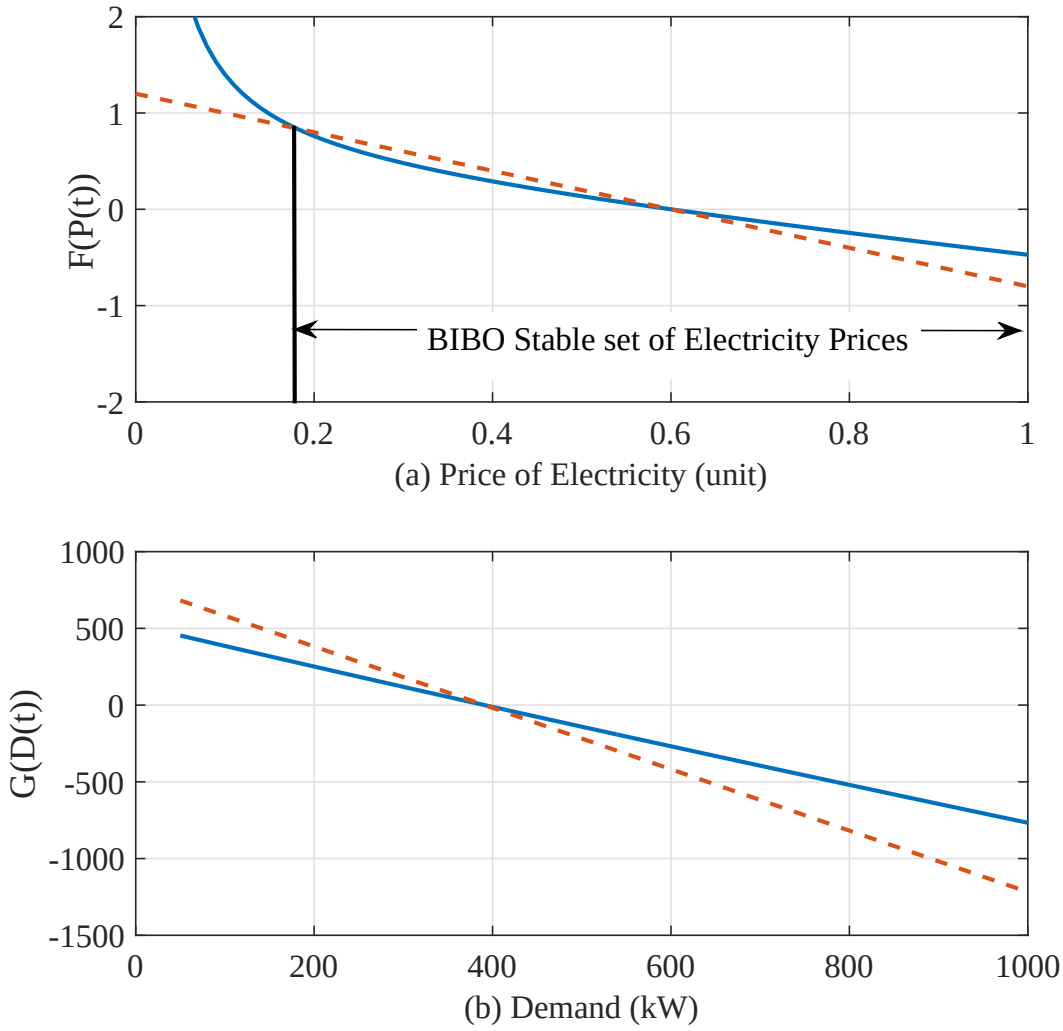

Figure 7.3: *Price and Demand Dynamic function*

enough to accommodate various types of active consumer models.

After obtaining values of coefficients of demand elasticity, no-load and incremental price of electricity is calculated using algorithm 3. The equilibrium price of electricity is chosen as 0.6 ncu, which results in equilibrium demand of 391 kWh. Slope of price dynamic function at point of equilibrium ($f'(\mathcal{P}^*)$) is chosen as -1.3. Based on $\mathcal{P}^* = 0.6$ and $f'(\mathcal{P}^*) = -1.3$, calculated values of no-load and incremental price of electricity using algorithm 3 are $\alpha_0 = 0.54$ ncu and $\alpha_1 = 1.56 \times 10^{-4}$ ncu/kWh. Based on these values of coefficients of demand elasticity and coefficients of electricity prices, Fig. 7.3(a) shows the plot of price dynamics

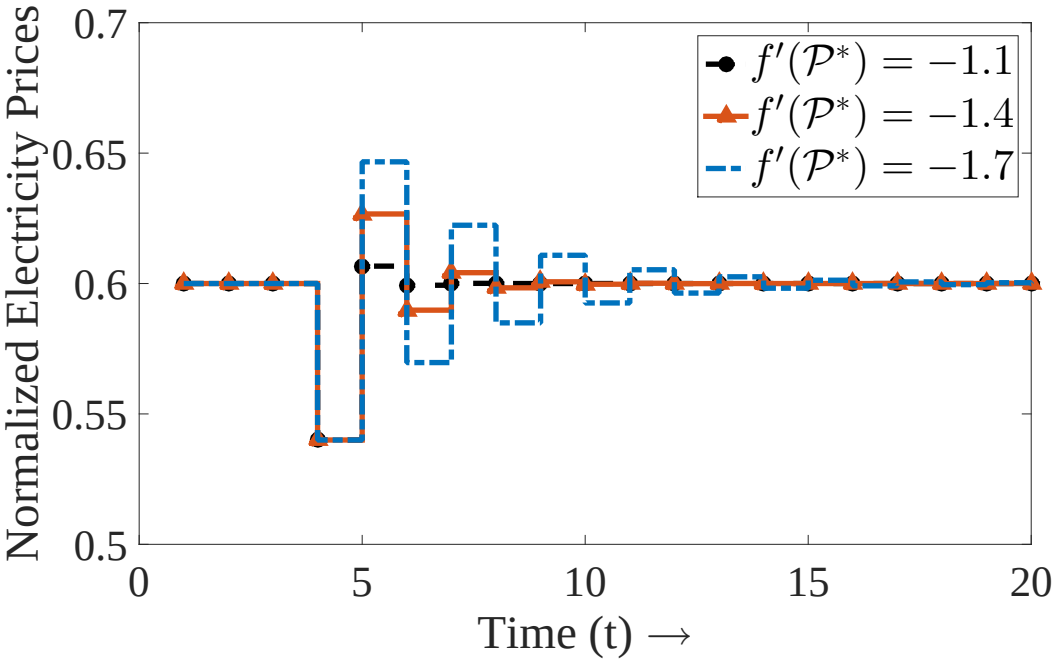

Figure 7.4: *Impact of cyber attack on electricity price for different values of* $f'(\mathcal{P}^*)$

and Fig. 7.3(b) shows the plot of demand dynamics using a solid blue line. Red dashed line in both figures are lines of slope -2 passing through point of equilibrium. From Fig. 7.3(a) it can be seen that the set of BIBO stable electricity prices ($\mathcal{B}_{\mathcal{P}}$) is $[0.18, 1.0]$. In case of a cyber attack, when error introduced in price of electricity at time t ($\epsilon_{\mathcal{P}}(t)$) is large enough to create a scenario where $\mathcal{P} \notin \mathcal{B}_{\mathcal{P}}$, error in price of electricity at time $t+1$ will be higher than error in price of electricity at time t ($\epsilon_{\mathcal{P}}(t+1) > \epsilon_{\mathcal{P}}(t)$).

Lower $f'(\mathcal{P}^*)$ results in higher value of α_1, which makes price of electricity more responsive to changes in total load. However, higher $f'(\mathcal{P}^*)$ also results in higher fluctuations in electricity prices, demand and voltage in case of cyber attack. Fig. 7.4 shows fluctuations in normalized price of electricity when price of electricity is reduced by 10% at time period $t = 4$ for three different values of $f'(\mathcal{P}^*)$. It shows that when the value of $f'(\mathcal{P}^*)$ is low, oscillations in price of electricity have higher magnitude and they last longer compared to the case when $f'(\mathcal{P}^*)$ is higher. These oscillations in price of electricity results in oscillations in energy consumption of active consumers, which results in oscillations in distribution system voltage. Fig. 7.5 shows voltage at node 20 of the IEEE 69 bus test system. It can

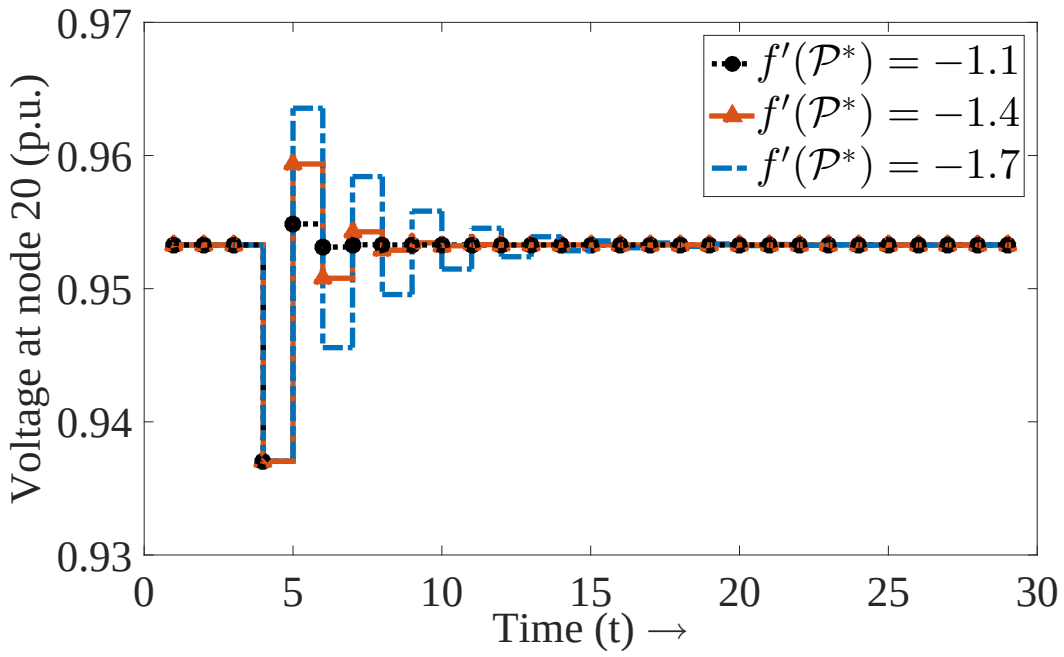

Figure 7.5: *Impact of cyber attack on voltage at node* 20 *for different values of* $f'(\mathcal{P}^*)$

be seen that magnitude of voltage fluctuation is highest for the lowest value of $f'(\mathcal{P}^*)$, and magnitude of voltage fluctuation is low for higher $f'(\mathcal{P}^*)$ (i.e. -1.1).

Choice of $f'(\mathcal{P}^*)$ also impacts number of violations in the distribution system voltage. Fig. 7.6 shows number of voltage violation over time for different values of $f'(\mathcal{P}^*)$ when electricity price is externally reduced by 10%. From Fig. 7.6 it can be seen that number of voltage violations increase as $f'(\mathcal{P}^*)$ decreases. Number of voltage violations are minimum when $f'(\mathcal{P}^*) = 1$. When $f'(\mathcal{P}^*) = 1$ value of $\alpha_1 = 0$; therefore, error introduced in electricity price does not result in oscillations of electricity prices, demand and voltage in future time periods. All voltage violations observed in this case occurs in the same time period as error in the electricity price is introduced. Lower values of $f'(\mathcal{P}^*)$ creates oscillations in electricity price, demand and voltage in case of cyber attack. For lower values of $f'(\mathcal{P}^*)$, number of violations are higher due to sustained oscillations in electricity prices that results in sustained oscillations in total demand causing higher number of voltage violation. All additional voltage violations in these cases occur in future time periods.

To analyze impact of cyber attacks on distribution system voltage, a scenario is considered where errors of different values is introduced in electricity pricing signal and total number of

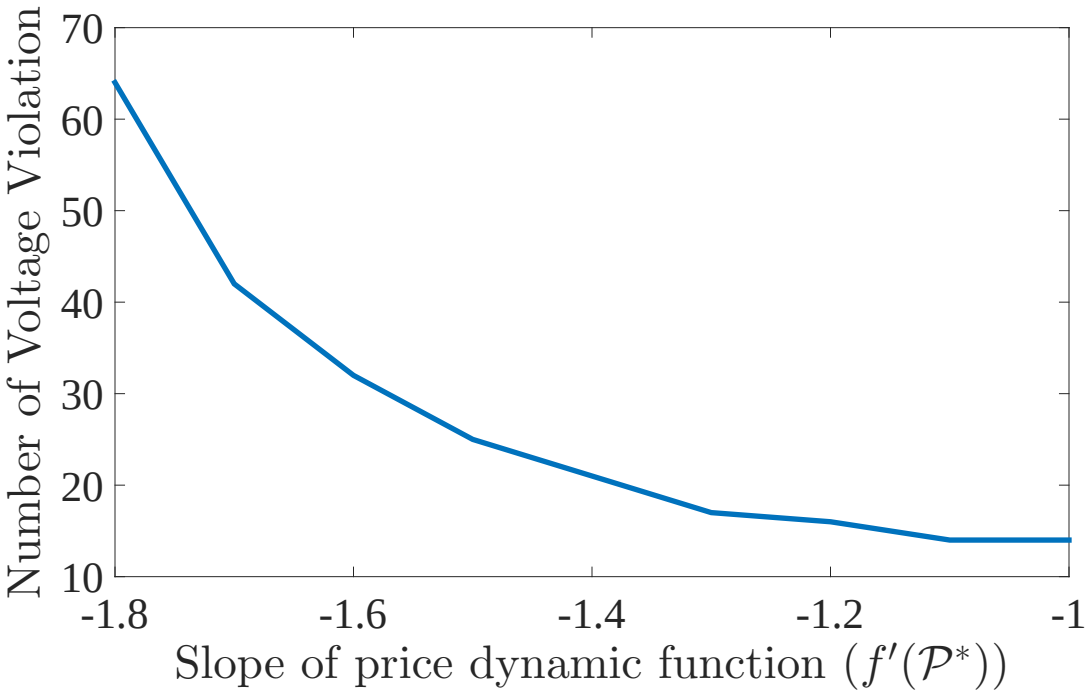

Figure 7.6: *Number of voltage violation vs slope of price dynamic function*

voltage violations in the network are observed. Fig. 7.7 shows number of voltage violations over time due vs error introduced in electricity pricing ($\epsilon_{\mathcal{P}}(t)$). Here, negative values of error indicates that price of electricity is artificially reduced resulting in increased power drawn by active consumers that eventually results in higher number of voltage violations. Positive values of error indicates that the electricity price is artificially increased resulting in reduced energy consumption. Positive values of $\epsilon_{\mathcal{P}}(t)$ do not result in large number of voltage violations as power injection capacity of active consumers is limited by the amount of available renewable generation. However, positive error results in oscillations in electricity prices resulting in reduced price of electricity in the next time period which leads to higher power drawn by active consumers and higher number of voltage violations.

A false data injection (FDI) attack on a transactive energy market (TEM) based smart power distribution system can be engineered by manipulating electricity price or hacking a subset of smart meters and manipulating energy consumption information of active consumers. Fig. 7.8(a) shows impact of cyber attack on electricity prices, and Fig. 7.8(b) shows impact of cyber attack on total demand. In Fig. 7.8, red dotted curve with triangle marker

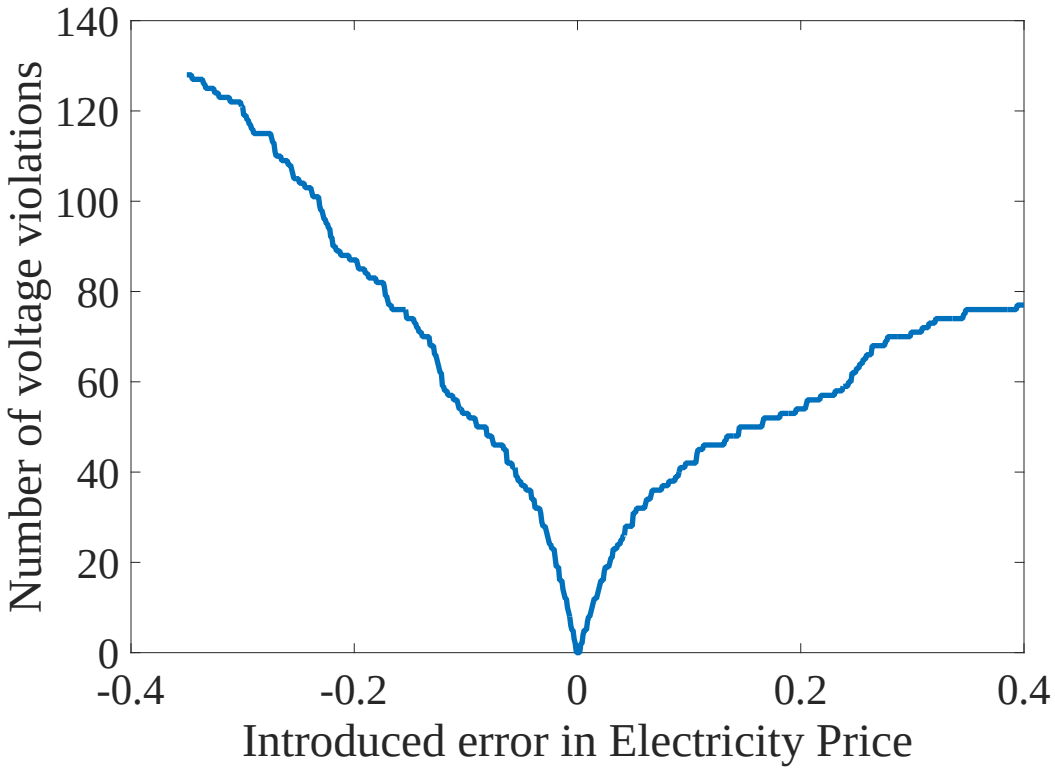

Figure 7.7: *Number of voltage violation over time with error in electricity pricing*

represents a case where demand of electricity is reduced by 20% at time $t = 3$, and blue solid curve represents a case where price of electricity is decreased by 20% at time $t = 4$. From Fig. 7.8, it can be seen that attack on price of electricity can cause more fluctuation in demand and prices that can result in higher voltage violations. In order to engineer FDI attack on total demand with significant impact on the grid, one may have to hack a large number of smart meters and introduce error in smart meter data in a coordinated manner, which could be challenging. Such carefully design FDI attack on demand will have lower impact on the system compare to an attack on electricity prices which requires manipulation of only one parameter. This indicates that security and integrity of electricity pricing signal is much more critical.

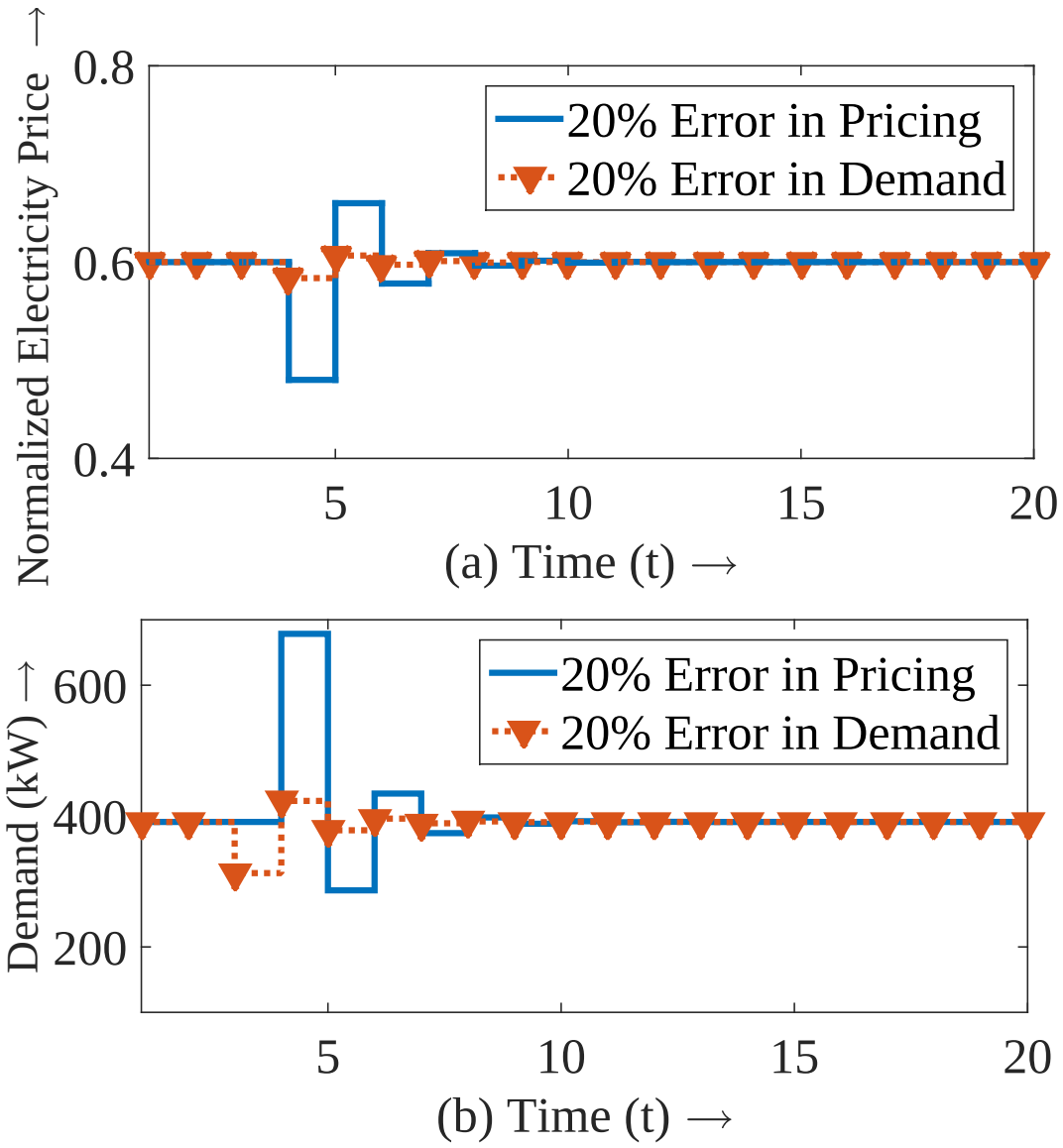

Figure 7.8: *Dynamics of price and demand due to error in electricity price and demand*

7.5 Summary

This paper builds on a discrete time non-linear autonomous control system model to capture the iteration and dynamics of electricity prices and total demand in a transactive energy market based power distribution system. The conditions for equilibrium and stability of electricity price and demand are derived and used to develop an algorithm to design a stable real-time electricity pricing scheme. Impact of false data injection attack on this transactive energy based power distribution system is studied, and dynamics of electricity price, demand

and distribution system voltage is analyzed using simulations on the IEEE 69 bus test system. This work shows that an FDI attack on electricity price can have a much more severe impact on the power distribution system compared to an FDI attack on demand. Therefore, more resources should be spend for developing new security mechanisms to protect electricity pricing signal from a cyber-attack.

Chapter 8

Conclusions and Future Work

This concluding chapter summarizes the contributions of this dissertation and discusses future research directions.

8.1 Conclusions

This dissertation addresses the fundamental questions in areas of (1) active consumer modeling, (2) analyzing impact of renewable generation on distribution system, and (3) impact of cyber attack on the power distribution system in order to enable transactive energy market.

Firstly, this dissertation develops a Prospect Theory based model of the active consumer behavior in response to changes in the real-time price of electricity with varied preferences for electricity consumption and different levels of rationality. The interaction between the aggregator and the active consumers is modeled as a Stackelberg leader-follower game. Unlike previous efforts this dissertation considers this interaction from a techno-economic perspective by including physical grid constraints in terms of voltage violation within the analysis. This work analyzes the impact of consumer actions and irrationality on distribution system voltage and the aggregator profit using simulation of IEEE 69 bus test system.

After developing model of consumer behavior, this dissertation develops analytical tools for grid analysis. First, an analytical method of voltage sensitivity analysis is developed

that provides an upper bound on change in the distribution system voltage at a given bus as a function of change in complex power at another bus due to actions of multiple active consumers. This method can be used to compute an upper bound on the voltage sensitivity matrix elements in a computationally efficient manner. Then, this analytical method of voltage sensitivity analysis is used to develop the probabilistic voltage sensitivity analysis (PVSA) for known and random spatial distribution of active consumers. Change in voltage magnitude due to multiple active consumers located at known places in the network changing their power randomly can be approximated by Gamma distribution. Additionally, real and imaginary part of voltage change due to random behavior of multiple active consumers with spatially random distribution can be approximated by the normal distribution. This method can be extremely valuable for distribution system operators and planning as it helps to compute the probability of voltage limit violation at a given node on the network with random penetration of active consumers. Next, proposed analytical method of voltage sensitivity analysis is used to investigate various infromation theoretic metrics to identify the dominant influencer of voltage fluctuations. This work shows that differential entropy, Kullback-Leibler Distance and Frechet Distance are excellent indicators of the dominant influencer of the voltage fluctuations. Validity and effectiveness of proposed metrics to identify the dominant influencer of the voltage fluctuations is shown to be computationally efficient. All the theoretical results have been validated via simulation on IEEE 69 bus test systems.

Finally, this dissertation models this transactive energy market based power distribution system as a discrete time non-linear autonomous dynamical system and capture the iteration and dynamics of electricity prices and total demand. The equilibrium and stability conditions of electricity price and demand for this system are derived and used to develop an algorithm to design a stable real-time electricity pricing scheme. Impact of the false data injection attack on the transactive energy market based power distribution system is studied, and dynamics of electricity price, demand and distribution system voltage is analyzed using simulations on the IEEE 69 bus test system. Results show that the false data injection attack on electricity price can have a much more severe impact on the power distribution

system compared to the false data injection attack attack on demand. Therefore, more resources should be spend for developing new security mechanisms to protect electricity pricing signal from a cyber-attack.

8.2 Future Work

This section present possible future directions in areas of consumer modeling, analyzing impact of renewable generation and cyber attacks on the power distribution system. Extensions to the work presented in this dissertation are following:

- The prospect theory based model of active consumer behavior developed in chapter 3 assumes that changes in the real-time price of electricity at a given time does not affect future actions of the active consumers. However, this model does not capture impact of flexible and delayed loads (i.e., washer/dryer, electric vehicles). Developing a time dependent model of the active consumer behavior along with correlated load scheduling can be pursued in the future.

- Chapter 4 of this dissertation develops an analytical method of voltage sensitivity analysis for the balanced three phase power distribution system assuming constant power model of loads. This analysis can be extended for an unbalanced three phase power distribution system with various types of load models (i.e., constant current and constant impedance loads).

- Chapter 5 develops the probabilistic voltage sensitivity analysis (PVSA) for known and random spatial distribution of multiple active consumers in balanced three phase power distribution system. This analysis can be extended to a general three phase unbalanced distribution network with a variety of load models including hybrid loads.

- Change in the power drawn/injected by the active consumers located at a specific node of the distribution system causes change in the line losses in the power distribution system. Future work in this area involves development of the probabilistic loss sensitivity

analysis (PLSA) by developing an analytical method of loss sensitivity analysis for the unbalanced three phase power distribution system with a variety of load models.

- Proposed probabilistic sensitivity analysis of voltage and losses can be used in association with traditional load flow algorithms to enable more practical and computationally efficient hybrid control. Such hybrid control can be helpful in understanding the stress points in a transactive energy market based power distribution system and developing optimal corrective control strategies.

- The dominant influencer model of Chapter 6 can also be extended to a general three phase unbalanced distribution system with a variety of load models. Proposed dominant influencer model can be used to identify the most vulnerable nodes in the network and create vulnerability rank database for all nodes of the power distribution system.

- Chapter 7 of this dissertation assumes that the price of electricity can take any value. This work can be extended to analysis of security and stability of multi-tiered pricing structure with a stochastic model of consumer.

Bibliography

[1] "The smart grid: An introduction," *US DOE Publication*, 2008.

[2] A. Faruqui and S. George, "Quantifying customer response to dynamic pricing," *The Electricity Journal*, vol. 18, no. 4, pp. 53–63, 2005. [Online]. Available: https://EconPapers.repec.org/RePEc:eee:jelect:v:18:y:2005:i:4:p:53-63

[3] A. Faruqui, "Breaking out of the bubble," *Public Utilities Fortnightly*, pp. 46–51, march 2007.

[4] A. Faruqui and R. Hledik, "The impact of dynamic pricing on westar energy," *Smart Grid and Energy Storage Roundtable, Topeka-Kansas*, 2009.

[5] A. Faruqui and S. Sergici, "Household response to dynamic pricing of electricity: a survey of 15 experiments," *Journal of Regulatory Economics*, vol. 38, no. 2, pp. 193–225, Oct 2010. [Online]. Available: https://doi.org/10.1007/s11149-010-9127-y

[6] S. E. Widergren, A. Somani, K. Subbarao, C. Marinovici, J. Fuller, J. Hammerstrom, and D. Chassin, "Aep ohio gridsmart demonstration project real-time pricing demonstration analysis," *PNNL-23192, Department of Energy*, February 2014.

[7] S. Widergren, C. Marinovici, J. Fuller, K. Subbarao, D. Chassin, and A. Somani, "Customer engagement in aep gridsmart residential transactive system," *Transactive Energy Conference*, December 2014.

[8] "The future of the grid: Evolving to meet americas needs," *GridWise Alliance*, December 2014.

[9] "Gridwise transactive energy framework version 1.0," *The GridWise Architecture Council*, January 2015.

[10] R. B. Jr, J. Romanowiz, and C. Staples, "Energy management and home automation system," *US Patent 5,544,036*, 1996.

[11] M. Inoue, T. Higuma, Y. Ito, N. Kushiro, and H. Kubota, "Network architecture for home energy management system," *IEEE Transactions on Consumer Electronics*, vol. 49, no. 3, pp. 606–613, Aug 2003.

[12] M. Kuzlu, M. Pipattanasomporn, and S. Rahman, "Hardware demonstration of a home energy management system for demand response applications," *IEEE Transactions on Smart Grid*, vol. 3, no. 4, pp. 1704–1711, Dec 2012.

[13] M. Pipattanasomporn, M. Kuzlu, and S. Rahman, "An algorithm for intelligent home energy management and demand response analysis," *IEEE Transactions on Smart Grid*, vol. 3, no. 4, pp. 2166–2173, Dec 2012.

[14] M. A. A. Pedrasa, T. D. Spooner, and I. F. MacGill, "Coordinated scheduling of residential distributed energy resources to optimize smart home energy services," *IEEE Transactions on Smart Grid*, vol. 1, no. 2, pp. 134–143, Sept 2010.

[15] K. Jhala, B. Natarajan, and A. Pahwa, "Prospect theory based active consumer behavior under variable electricity pricing," *IEEE Transactions on Smart Grid*, pp. 1–1, 2018.

[16] ——, "Probabilistic voltage sensitivity analysis (pvsa) - a novel approach to quantify impact of active consumers," *IEEE Transactions on Power Systems*, vol. PP, no. 99, pp. 1–1, 2017.

[17] ——, "Probabilistic voltage sensitivity analysis (pvsa) for random spatial distribution of active consumers," in *2018 IEEE Power Energy Society Innovative Smart Grid Technologies Conference (ISGT)*, Feb 2018, pp. 1–5.

[18] K. Jhala, B. Natarajan, A. Pahwa, and H. Wu, "Identifying the dominant influencer of voltage fluctuations," *IEEE Transactions on Power Systems (Under review)*, 2018.

[19] ——, "Security and stability of transactive energy market-based power distribution system," *IEEE Transactions on Smart Grid (Under review)*, 2018.

[20] S. Salinas, M. Li, and P. Li, "Multi-objective optimal energy consumption scheduling in smart grids," *IEEE Transactions on Smart Grid*, vol. 4, no. 1, pp. 341–348, March 2013.

[21] S. Althaher, P. Mancarella, and J. Mutale, "Automated demand response from home energy management system under dynamic pricing and power and comfort constraints," *IEEE Transactions on Smart Grid*, vol. 6, no. 4, pp. 1874–1883, July 2015.

[22] C. Chen, J. Wang, and S. Kishore, "A distributed direct load control approach for large-scale residential demand response," *IEEE Transactions on Power Systems*, vol. 29, no. 5, pp. 2219–2228, Sept 2014.

[23] A. H. Mohsenian-Rad and A. Leon-Garcia, "Optimal residential load control with price prediction in real-time electricity pricing environments," *IEEE Transactions on Smart Grid*, vol. 1, no. 2, pp. 120–133, Sept 2010.

[24] E. Vrettos, K. Lai, F. Oldewurtel, and G. Andersson, "Predictive control of buildings for demand response with dynamic day-ahead and real-time prices," in *2013 European Control Conference (ECC)*, July 2013, pp. 2527–2534.

[25] Z. Wen, D. ONeill, and H. Maei, "Optimal demand response using device-based reinforcement learning," *IEEE Transactions on Smart Grid*, vol. 6, no. 5, pp. 2312–2324, Sept 2015.

[26] A. H. Mohsenian-Rad, V. W. S. Wong, J. Jatskevich, R. Schober, and A. Leon-Garcia, "Autonomous demand-side management based on game-theoretic energy consumption scheduling for the future smart grid," *IEEE Transactions on Smart Grid*, vol. 1, no. 3, pp. 320–331, Dec 2010.

[27] Z. Chen, L. Wu, and Y. Fu, "Real-time price-based demand response management

for residential appliances via stochastic optimization and robust optimization," *IEEE Transactions on Smart Grid*, vol. 3, no. 4, pp. 1822–1831, Dec 2012.

[28] D. Eryilmaz, T. Smith, S. Dhople, E. Wilson, and J. Schmitt, "Demand response for industrial-scale energy users in midwest iso: A dynamic programming approach for curtailing energy use," in *2014 IEEE PES T D Conference and Exposition*, April 2014, pp. 1–4.

[29] D. Arnone, V. Croce, G. Patern, A. Rossi, S. Emma, R. Miceli, and A. O. D. Tommaso, "Energy management of multi-carrier smart buildings for integrating local renewable energy systems," in *2016 IEEE International Conference on Renewable Energy Research and Applications (ICRERA)*, Nov 2016, pp. 845–850.

[30] D. Minoli, K. Sohraby, and B. Occhiogrosso, "Iot considerations, requirements, and architectures for smart buildings x2014;energy optimization and next-generation building management systems," *IEEE Internet of Things Journal*, vol. 4, no. 1, pp. 269–283, Feb 2017.

[31] Y. Wang, Y. Xu, Z. Dong, and W. Zhang, "Multi-stage planning and economic analysis of intelligent energy management system in a smart building," in *10th International Conference on Advances in Power System Control, Operation Management (APSCOM 2015)*, Nov 2015, pp. 1–6.

[32] S. L. Arun and M. P. Selvan, "Intelligent residential energy management system for dynamic demand response in smart buildings," *IEEE Systems Journal*, vol. PP, no. 99, pp. 1–12, 2017.

[33] K. Jhala, B. Natarajan, A. Pahwa, and L. Erickson, "Coordinated electric vehicle charging solutions using renewable energy sources," in *2014 IEEE Symposium on Computational Intelligence Applications in Smart Grid (CIASG)*, Dec 2014, pp. 1–6.

[34] ——, "Coordinated electric vehicle charging for commercial parking lot with renewable energy sources," *Electric Power Components and Systems*, vol. 45, no. 03, pp.

344–353, 2017. [Online]. Available: http://www.tandfonline.com/doi/abs/10.1080/15325008.2016.1248253

[35] ——, "Real-time differential pricing scheme for active consumers with electric vehicles," *Electric Power Components and Systems*, vol. 45, no. 14, pp. 1487–1497, 2017. [Online]. Available: https://doi.org/10.1080/15325008.2017.1362074

[36] K. Jhala, "Coordinated electric vehicle charging with renewable energy sources," *Master's Thesis, Department of Electrical and Computer Engineering, Kansas State University*, Aug 2015. [Online]. Available: http://krex.k-state.edu/dspace/handle/2097/19767

[37] I. O. Volkova, M. V. Gubko, and E. A. Salnikova, "Active consumer: Optimization problems of power consumption and self-generation," *Automation and Remote Control*, vol. 75, no. 3, pp. 551–562, 2014. [Online]. Available: http://dx.doi.org/10.1134/S0005117914030114

[38] S. Ghosh, X. A. Sun, and X. Zhang, "Consumer profiling for demand response programs in smart grids," in *IEEE PES Innovative Smart Grid Technologies*, May 2012, pp. 1–6.

[39] N. Zhang, Y. Yan, S. Xu, and W. Su, "Game-theory-based electricity market clearing mechanisms for an open and transactive distribution grid," in *2015 IEEE Power Energy Society General Meeting*, July 2015, pp. 1–5.

[40] N. Zhang, Y. Yan, and W. Su, "A game-theoretic economic operation of residential distribution system with high participation of distributed electricity prosumers," *Applied Energy*, vol. 154, pp. 471 – 479, 2015. [Online]. Available: http://www.sciencedirect.com/science/article/pii/S0306261915006212

[41] L. Xiao, N. B. Mandayam, and H. V. Poor, "Prospect theoretic analysis of energy exchange among microgrids," *IEEE Transactions on Smart Grid*, vol. 6, no. 1, pp. 63–72, Jan 2015.

[42] Y. Wang, W. Saad, N. B. Mandayam, and H. V. Poor, "Integrating energy storage into the smart grid: A prospect theoretic approach," in *2014 IEEE International Conference on Acoustics, Speech and Signal Processing (ICASSP)*, May 2014, pp. 7779–7783.

[43] R. Aghatehrani and R. Kavasseri, "Sensitivity-analysis-based sliding mode control for voltage regulation in microgrids," *IEEE Transactions on Sustainable Energy*, vol. 4, no. 1, pp. 50–57, Jan 2013.

[44] R. Aghatehrani and A. Golnas, "Reactive power control of photovoltaic systems based on the voltage sensitivity analysis," in *2012 IEEE Power and Energy Society General Meeting*, July 2012, pp. 1–5.

[45] S. Weckx, R. DHulst, and J. Driesen, "Voltage sensitivity analysis of a laboratory distribution grid with incomplete data," *IEEE Transactions on Smart Grid*, vol. 6, no. 3, pp. 1271–1280, May 2015.

[46] Q. Zhou and J. W. Bialek, "Generation curtailment to manage voltage constraints in distribution networks," *IET Generation, Transmission Distribution*, vol. 1, no. 3, pp. 492–498, May 2007.

[47] G. Valverde and T. V. Cutsem, "Model predictive control of voltages in active distribution networks," *IEEE Transactions on Smart Grid*, vol. 4, no. 4, pp. 2152–2161, Dec 2013.

[48] M. Brenna, E. Berardinis, F. Foiadelli, G. Sapienza, and D. Zaninelli, "Voltage control in smart grids: An approach based on sensitivity theory," in *Journal of Electromagnetic Analysis and Applications*, vol. 2, no. 80, August 2010, pp. 467–447.

[49] B. B. Zad, J. Lobry, and F. Valle, "A centralized approach for voltage control of mv distribution systems using dgs power control and a direct sensitivity analysis method," in *2016 IEEE International Energy Conference (ENERGYCON)*, April 2016, pp. 1–6.

[50] B. B. Zad, H. Hasanvand, J. Lobry, and F. Valle, "Optimal reactive power control of {DGs} for voltage regulation of {MV} distribution systems using

sensitivity analysis method and {PSO} algorithm," *International Journal of Electrical Power and Energy Systems*, vol. 68, pp. 52 – 60, 2015. [Online]. Available: http://www.sciencedirect.com/science/article/pii/S014206151400773X

[51] B. B. Zad, J. Lobry, F. Vallee, and H. Hasanvand, "Optimal reactive power control of dgs for voltage regulation of mv distribution systems considering thermal limit of the system branches," in *Power System Technology (POWERCON), 2014 International Conference on*, Oct 2014, pp. 2951–2958.

[52] V. Klonari, B. B. Zad, J. Lobry, and F. Valle, "Application of voltage sensitivity analysis in a probabilistic context for characterizing low voltage network operation," in *2016 International Conference on Probabilistic Methods Applied to Power Systems (PMAPS)*, Oct 2016, pp. 1–7.

[53] A. A. Cardenas, S. Amin, and S. Sastry, "Secure control: Towards survivable cyber-physical systems," in *2008 The 28th International Conference on Distributed Computing Systems Workshops*, June 2008, pp. 495–500.

[54] Y. Liu, P. Ning, and M. K. Reiter, "False data injection attacks against state estimation in electric power grids," in *Proceedings of the 16th ACM Conference on Computer and Communications Security*, ser. CCS '09. New York, NY, USA: ACM, 2009, pp. 21–32. [Online]. Available: http://doi.acm.org/10.1145/1653662.1653666

[55] Y. Yuan, Z. Li, and K. Ren, "Quantitative analysis of load redistribution attacks in power systems," *IEEE Transactions on Parallel and Distributed Systems*, vol. 23, no. 9, pp. 1731–1738, Sept 2012.

[56] S. Bhattarai, L. Ge, and W. Yu, "A novel architecture against false data injection attacks in smart grid," in *2012 IEEE International Conference on Communications (ICC)*, June 2012, pp. 907–911.

[57] M. Talebi, C. Li, and Z. Qu, "Enhanced protection against false data injection by

dynamically changing information structure of microgrids," in *2012 IEEE 7th Sensor Array and Multichannel Signal Processing Workshop (SAM)*, June 2012, pp. 393–396.

[58] H. Zhang, W. Meng, J. Qi, X. Wang, and W. X. Zheng, "Distributed load sharing under false data injection attack in inverter-based microgrid," *IEEE Transactions on Industrial Electronics*, vol. PP, no. 99, pp. 1–1, 2018.

[59] H. S. Karimi, K. Jhala, and B. Natarajan, "Stochastic hybrid modeling and analysis of real-time pricing response attack in distribution system," in *2018 IEEE North American Power Symposium (NAPS)*, Sep 2018, pp. 1–6.

[60] S. K. Singh, K. Khanna, R. Bose, B. K. Panigrahi, and A. Joshi, "Joint-transformation-based detection of false data injection attacks in smart grid," *IEEE Transactions on Industrial Informatics*, vol. 14, no. 1, pp. 89–97, Jan 2018.

[61] D. Cardwell, "Solar power battle puts hawaii at forefront of worldwide changes," *New York Times*, April 2015.

[62] D. Kahneman and A. Tversky, "Prospect theory: An analysis of decision under risk," *Econometrica*, vol. 47, no. 2, pp. 263–291, 1979. [Online]. Available: http://www.jstor.org/stable/1914185

[63] A. Tversky and D. Kahneman, "Advances in prospect theory: Cumulative representation of uncertainty," *Journal of Risk and Uncertainty*, vol. 5, no. 4, pp. 297–323, 1992. [Online]. Available: http://dx.doi.org/10.1007/BF00122574

[64] D. Prelec, "The probability weighting function," *Econometrica*, vol. 66, no. 3, pp. 497–528, 1998. [Online]. Available: http://EconPapers.repec.org/RePEc:ecm:emetrp:v:66:y:1998:i:3:p:497-528

[65] M. N. Faqiry and S. Das, "A budget balanced energy distribution mechanism among consumers and prosumers in microgrid," in *2016 IEEE International Conference on Internet of Things (iThings)*, Dec 2016, pp. 516–520.

[66] L. Akter and B. Natarajan, "Modeling fairness in resource allocation for secondary users in a competitive cognitive radio network," in *2010 Wireless Telecommunications Symposium (WTS)*, April 2010, pp. 1–6.

[67] F. Tamp and P. Ciufo, "A sensitivity analysis toolkit for the simplification of mv distribution network voltage management," *Smart Grid, IEEE Transactions on*, vol. 5, no. 2, pp. 559–568, March 2014.

[68] R. Broderick, J. Quiroz, M. Reno, A. Ellis, J. Smith, and R. Durgan, "Time series power flow analysis for distribution connected pv generation," in *Sandia National Laboratories*, Jan 2013, pp. 1–62.

[69] D. Parmar and L. Yao, "Impact of unbalanced penetration of single phase grid connected photovoltaic generators on distribution network," in *Universities' Power Engineering Conference (UPEC), Proceedings of 2011 46th International*, Sept 2011, pp. 1–8.

[70] R. Tonkoski, D. Turcotte, and T. H. M. EL-Fouly, "Impact of high pv penetration on voltage profiles in residential neighborhoods," *IEEE Transactions on Sustainable Energy*, vol. 3, no. 3, pp. 518–527, July 2012.

[71] R. Aghatehrani and A. Golnas, "Reactive power control of photovoltaic systems based on the voltage sensitivity analysis," in *Power and Energy Society General Meeting, 2012 IEEE*, July 2012, pp. 1–5.

[72] L.-L. Chuang and Y.-S. Shih, "Approximated distributions of the weighted sum of correlated chi-squared random variables," *Journal of Statistical Planning and Inference*, vol. 142, no. 2, pp. 457 – 472, 2012. [Online]. Available: http://www.sciencedirect.com/science/article/pii/S0378375811003156

[73] Y. Liu, P. Ning, and M. K. Reiter, "False data injection attacks against state estimation in electric power grids," *ACM Trans. Inf. Syst. Secur.*, vol. 14, no. 1, pp. 13:1–13:33, Jun. 2011. [Online]. Available: http://doi.acm.org/10.1145/1952982.1952995

[74] G. Liang, J. Zhao, F. Luo, S. R. Weller, and Z. Y. Dong, "A review of false data injection attacks against modern power systems," *IEEE Transactions on Smart Grid*, vol. 8, no. 4, pp. 1630–1638, July 2017.

[75] O. Kosut, L. Jia, R. J. Thomas, and L. Tong, "Malicious data attacks on the smart grid," *IEEE Transactions on Smart Grid*, vol. 2, no. 4, pp. 645–658, Dec 2011.

[76] A. Teixeira, S. Amin, H. Sandberg, K. H. Johansson, and S. S. Sastry, "Cyber security analysis of state estimators in electric power systems," in *49th IEEE Conference on Decision and Control (CDC)*, Dec 2010, pp. 5991–5998.

[77] P. H. Divshali, B. J. Choi, and H. Liang, "Multi-agent transactive energy management system considering high levels of renewable energy source and electric vehicles," *IET Generation, Transmission Distribution*, vol. 11, no. 15, pp. 3713–3721, 2017.

Appendix A

Concavity Analysis

Lemma 4. *Optimal action of an active consumer a_i^*, given by equation (3.6), is convex decreasing function of $\mathbb{P}$.*

Proof. Numerator of equation (3.6) is linear and decreasing function of $\hat{P}$. Denominator of (3.6) is $y - \sqrt{y^2 - 4xz}$, where x, y, and z are given by equation (A.1), (A.2), and (A.3). Here y is linear and decreasing function of $\hat{P}$; and $\sqrt{y^2 - 4xz}$ is convex and decreasing function of $\hat{P}$, which is proved in lemma 8. As reciprocal of a positive convex function is convex (see Lemma 5), it can be shown that $\frac{-1}{y-\sqrt{y^2-4xz}}$ is convex and increasing function of $\hat{P}$ and product of such two functions is concave (Lemma 6).

$$x = -2\gamma_i \mathbf{S}(i,i)^2, \tag{A.1}$$

$$y = 2\gamma_i \mathbf{S}(i,i)(\mathbf{v}(i) + \mathbf{S}(i,i)\hat{a}_i - 1) - \hat{P} - 2\gamma_i \mathbf{S}(i,i)^2(R_i + 1) \tag{A.2}$$

$$z = \beta_i - \hat{P}(R_i + 1) + 2\gamma_i \mathbf{S}(i,i)(\mathbf{v}(i) + \mathbf{S}(i,i)\hat{a}_i - 1)(R_i + 1) \tag{A.3}$$

□

Lemma 5. *Reciprocal of a positive convex function is convex.*

Proof. Consider function $f : \mathbb{D} \to \mathbb{R}$ where domain of the function is convex. Let $f(x) > 0$ be a positive convex function. In order to prove that reciprocal of $f(x)$, $F(x) = \frac{1}{f(x)}$ is convex, let us investigate conditions under which $F(x)$ is convex. For $F(x)$ to be convex, by definition of convexity:

$$F(\lambda x + (1-\lambda)y) \leq \lambda F(x) + (1-\lambda)F(y), \tag{A.4}$$

for all $x, y \in \mathbb{D}$ and $\lambda \in [0, 1]$. Replacing F by $\frac{1}{f}$:

$$\frac{1}{f(\lambda x + (1-\lambda)y)} \leq \frac{\lambda}{f(x)} + \frac{(1-\lambda)}{f(y)}. \tag{A.5}$$

Multiplying on right hand side,

$$\frac{1}{f(\lambda x + (1-\lambda)y)} \leq \frac{\lambda f(y) + (1-\lambda)f(x)}{f(x)f(y)}. \tag{A.6}$$

If $f(x)$ is convex than $f(\lambda x + (1-\lambda)y) \leq \lambda f(x) + (1-\lambda)f(y)$.

$$\frac{[\lambda f(y) + (1-\lambda)f(x)][\lambda f(x) + (1-\lambda)f(y)]}{f(x)f(y)} \geq 1, \tag{A.7}$$

which can be simplified as following.

$$\frac{\lambda(1-\lambda)[f^2(x) + f^2(y)]}{f(x)f(y)} + \lambda^2 + (1-\lambda)^2 \geq 1 \tag{A.8}$$

$$\lambda(1-\lambda)[f^2(x) + f^2(y)] + [\lambda^2 + (1-\lambda)^2 - 1]f(x)f(y) \geq 0 \tag{A.9}$$

Here, $[\lambda^2 + (1-\lambda)^2 - 1] = -2\lambda(1-\lambda)$; therefore, equation above can be rewritten as following.

$$[f^2(x) + f^2(y)] - 2f(x)f(y) \geq 0, \tag{A.10}$$

$$[f^2(x) - f^2(y)]^2 \geq 0. \tag{A.11}$$

This condition is always true. Therefore, sufficient condition for a reciprocal of a convex function to be convex is that $f(x) > 0$ □

Lemma 6. *Product of two convex functions $F(x) = g(x)h(x)$ is concave if $g(x)$ is non-decreasing and $h(x)$ is non-increasing function.*

From the definition of concavity, function $F(x)$ is concave if

$$\lambda F(x) + (1-\lambda)F(y) \leq F(\lambda x + (1-\lambda)y). \tag{A.12}$$

Replacing $F(x) = g(x)h(x)$ into equation (A.12), it can be rewritten as:

$$\begin{aligned} \lambda g(x)h(x) + (1-\lambda)g(y)h(y) \leq & g(\lambda x + (1-\lambda)y) \\ & h(\lambda x + (1-\lambda)y). \end{aligned} \tag{A.13}$$

Now $h(x)$ and $g(x)$ are convex; therefore,

$$g(\lambda x + (1-\lambda)y) \leq \lambda g(x) + (1-\lambda)g(y), \tag{A.14}$$

and

$$h(\lambda x + (1-\lambda)y) \leq \lambda h(x) + (1-\lambda)h(y). \tag{A.15}$$

Substituting equation (A.14) and (A.15) into equation (A.13),

$$\begin{aligned} \lambda g(x)h(x) + (1-\lambda)g(y)h(y) \leq & [\lambda g(x) + (1-\lambda)g(y)] \\ & [\lambda h(x) + (1-\lambda)h(y)]. \end{aligned} \tag{A.16}$$

Equation (A.16) can be simplied further as following:

$$\lambda(1-\lambda)[g(x)h(x) + g(y)h(y) - g(x)h(y) - g(y)h(x)] \leq 0 \tag{A.17}$$

$$[g(x) - g(y)][h(x) - h(y)] \leq 0 \tag{A.18}$$

Equation (A.18) shows that product of two convex functions is concave if one function is convex and non-increasing and other is convex non-decreasing.

Lemma 7. *Square of a concave function $F(x) = f(x)^2$ is convex.*

Proof. From the definition of convexity, function $F(x)$ is convex if

$$\lambda F(x) + (1-\lambda)F(y) \geq F(\lambda x + (1-\lambda)y) \tag{A.19}$$

Substituting $F(x) = f^2(x)$,

$$\lambda f(x)f(x) + (1-\lambda)f(y)f(y) \geq f^2(\lambda x + (1-\lambda)y) \tag{A.20}$$

$$\lambda f(x)f(x) + (1-\lambda)f(y)f(y) - [\lambda f(x) + (1-\lambda)f(y)]^2 \geq 0 \tag{A.21}$$

$$\lambda(1-\lambda)f^2(x) + \lambda(1-\lambda)f^2(y) - 2\lambda(1-\lambda)f(x)f(y) \geq 0 \tag{A.22}$$

$$f^2(x) + f^2(y) - 2f(x)f(y) \geq 0 \tag{A.23}$$

$$[f(x) - f(y)] \geq 0 \tag{A.24}$$

Equation (A.24) is always true; therefore, square of a concave function is always convex. □

Lemma 8. *Action of an active consumer that maximizes its perceived payoff given by equation (3.6).*

$$\sqrt{y^2 - 4xz}, \tag{A.25}$$

where, x, y, and z is given by equation (A.1), (A.2), and (A.3) is convex and increasing function of $\mathbb{P}$.

Proof. Let $b = y^2 - 4xz$. Therefore,

$$\sqrt{b} = \Big([2\gamma_i \mathbf{S}(i,i)(\mathbf{v}(i) + \mathbf{S}(i,i)\hat{a}_i - 1 - \mathbf{S}(i,i)(R_i+1))]^2 + \hat{P}^2 \\ - 4\hat{P}\gamma_i \mathbf{S}(i,i)(\mathbf{v}(i) + \mathbf{S}(i,i)\hat{a}_i - 1 - \mathbf{S}(i,i)(R_i+1)) + 8\gamma_i \mathbf{S}(i,i)^2 \\ [\beta_i - \hat{P}(R_i+1) + 2\gamma_i \mathbf{S}(i,i)(\mathbf{v}(i) + \mathbf{S}(i,i)\hat{a}_i - 1)(R_i+1)] \Big)^{0.5}. \tag{A.26}$$

Taking first and second order derivative:

$$\frac{\partial}{\partial \hat{P}} \sqrt{b} = \frac{1}{2} b^{\frac{-1}{2}} \frac{\partial b}{\partial \hat{P}} \tag{A.27}$$

$$\frac{\partial^2}{\partial \hat{P}^2} \sqrt{b} = \frac{1}{2} b^{\frac{-1}{2}} \frac{\partial^2 b}{\partial \hat{P}^2} - \frac{1}{4} b^{\frac{-3}{2}} \left(\frac{\partial b}{\partial \hat{P}} \right)^2 \tag{A.28}$$

$$\frac{\partial b}{\partial \hat{P}} = \hat{P}[2 - 4\gamma_i \mathbf{S}(i,i)(\mathbf{v}(i) + \mathbf{S}(i,i)\hat{a}_i - 1 + \mathbf{S}(i,i)(R_i+1))] \geq 0 \tag{A.29}$$

$$\frac{\partial^2 b}{\partial \hat{P}^2} = [2 - 4\gamma_i \mathbf{S}(i,i)(\mathbf{v}(i) + \mathbf{S}(i,i)\hat{a}_i - 1 + \mathbf{S}(i,i)(R_i+1))] \geq 0 \tag{A.30}$$

Therefore, $\frac{\partial^2}{\partial \hat{P}^2}\sqrt{b} \geq 0$. From this it can be proved that $\sqrt{y^2 - 4xz}$ is convex non-decreasing function function. □

Lemma 9. $\theta \|\mathbf{v} + \mathbf{S}(\hat{\mathbf{a}} - \mathbf{a}) - 1\|$ *is convex function of* $\mathbb{P}$

Proof. According to lemma 4, a is convex function of $\mathbb{P}$. As convex function of convex function is convex, $\theta \|\mathbf{v} + \mathbf{S}(\hat{\mathbf{a}} - \mathbf{a}) - 1\|$ is convex function of $\mathbb{P}$ □

Appendix B

Covariance Matrix $\Sigma_{\Delta V_{oa},\Delta V_o}$

$$\begin{bmatrix} \Delta V_{oa}^r \\ \Delta V_{oa}^i \\ \Delta V_o^r \\ \Delta V_o^i \end{bmatrix} = \mathcal{N}(\mathbf{0}, \mathbf{\Sigma_{V_{oa},V_o}}) \tag{B.1}$$

$$\mathbf{\Sigma_{V_{oa},V_o}} = \begin{bmatrix} \sigma^2_{\Delta V_{oa}^r} & \text{cov}(\Delta V_{oa}^r, \Delta V_{oa}^i) & \text{cov}(\Delta V_{oa}^r, \Delta V_o^r) & \text{cov}(\Delta V_{oa}^r, \Delta V_o^i) \\ \text{cov}(\Delta V_{oa}^r, \Delta V_{oa}^i) & \sigma^2_{\Delta V_{oa}^i} & \text{cov}(\Delta V_{oa}^i, \Delta V_o^r) & \text{cov}(\Delta V_{oa}^i, \Delta V_o^i) \\ \text{cov}(\Delta V_{oa}^r, \Delta V_o^r) & \text{cov}(\Delta V_{oa}^i, \Delta V_o^r) & \mathbf{C_o^{rT} \Sigma C_o^r} & \mathbf{C_o^{rT} \Sigma C_i^r} \\ \text{cov}(\Delta V_{oa}^r, \Delta V_o^i) & \text{cov}(\Delta V_{oa}^i, \Delta V_o^i) & \mathbf{C_o^{rT} \Sigma C_i^r} & \mathbf{C_o^{rT} \Sigma C_o^r} \end{bmatrix} \tag{B.2}$$

where $\sigma^2_{\Delta V^r_{oa}}$, $\sigma^2_{\Delta V^i_{oa}}$, and $\mathrm{cov}(\Delta V^r_{oa}, \Delta V^i_{oa})$ is given by equations (6.14-6.16) and

$$\begin{aligned}
\mathrm{cov}(\Delta V^r_o, \Delta V^r_{oa}) &= E[\Delta V^r_o \Delta V^r_{oa}] - E[\Delta V^r_o]E[\Delta V^r_{oa}] \\
&= E[\Delta V^r_o \Delta V^r_{oa}] \\
&= E\left[\Delta V^r_{oa}\left(\sum_{i=1}^{N} \Delta V^r_{oi}\right)\right] \\
&= E\left[\sum_{i=1}^{N} \Delta V^r_{oi}\Delta V^r_{oa}\right] \\
&= E[\Delta V^r_{oa}\Delta V^r_{oa}] + E\left[\sum_{\substack{i=1 \\ i\neq a}}^{N} \Delta V^r_{oi}\Delta V^r_{oa}\right] \\
&= \mathrm{var}(\Delta V^r_{oa}) + \sum_{\substack{i=1 \\ i\neq a}}^{N} \mathrm{cov}(\Delta V^r_{oi}, \Delta V^r_{oa}),
\end{aligned} \tag{B.3}$$

$$\begin{aligned}
\mathrm{cov}(\Delta V^i_o, \Delta V^i_{oa}) &= E[\Delta V^i_o \Delta V^i_{oa}] - E[\Delta V^i_o]E[\Delta V^i_{oa}] \\
&= E[\Delta V^i_o \Delta V^i_{oa}] \\
&= E\left[\Delta V^i_{oa}\left(\sum_{i=1}^{N} \Delta V^i_{oi}\right)\right] \\
&= E\left[\sum_{i=1}^{N} \Delta V^i_{oi}\Delta V^i_{oa}\right] \\
&= E[\Delta V^i_{oa}\Delta V^i_{oa}] + E\left[\sum_{\substack{i=1 \\ i\neq a}}^{N} \Delta V^i_{oi}\Delta V^i_{oa}\right] \\
&= \mathrm{var}(\Delta V^i_{oa}) + \sum_{\substack{i=1 \\ i\neq a}}^{N} \mathrm{cov}(\Delta V^i_{oi}, \Delta V^i_{oa}),
\end{aligned} \tag{B.4}$$

$$
\begin{aligned}
\operatorname{cov}(\Delta V_o^r, \Delta V_{oa}^i) &= E[\Delta V_o^r \Delta V_{oa}^i] - E[\Delta V_o^r] E[\Delta V_{oa}^i] \\
&= E[\Delta V_o^r \Delta V_{oa}^i] \\
&= E\left[\Delta V_{oa}^i \left(\sum_{i=1}^{N} \Delta V_{oi}^r\right)\right] \\
&= E\left[\sum_{i=1}^{N} \Delta V_{oi}^r \Delta V_{oa}^i\right] \\
&= E[\Delta V_{oa}^i \Delta V_{oa}^r] + E\left[\sum_{\substack{i=1 \\ i \neq a}}^{N} \Delta V_{oi}^r \Delta V_{oa}^i\right] \\
&= \operatorname{cov}(\Delta V_{oa}^r, \Delta V_{oa}^i) + \sum_{\substack{i=1 \\ i \neq a}}^{N} \operatorname{cov}(\Delta V_{oi}^r, \Delta V_{oa}^i),
\end{aligned}
\tag{B.5}
$$

$$
\begin{aligned}
\operatorname{cov}(\Delta V_o^i, \Delta V_{oa}^r) &= E[\Delta V_o^i \Delta V_{oa}^r] - E[\Delta V_o^i] E[\Delta V_{oa}^r] \\
&= E[\Delta V_o^i \Delta V_{oa}^r] \\
&= E\left[\Delta V_{oa}^r \left(\sum_{i=1}^{N} \Delta V_{oi}^i\right)\right] \\
&= E\left[\sum_{i=1}^{N} \Delta V_{oi}^i \Delta V_{oa}^r\right] \\
&= E[\Delta V_{oa}^t \Delta V_{oa}^r] + E\left[\sum_{\substack{i=1 \\ i \neq a}}^{N} \Delta V_{oi}^i \Delta V_{oa}^r\right] \\
&= \operatorname{cov}(\Delta V_{oa}^i, \Delta V_{oa}^r) + \sum_{\substack{i=1 \\ i \neq a}}^{N} \operatorname{cov}(\Delta V_{oi}^i, \Delta V_{oa}^r).
\end{aligned}
\tag{B.6}
$$

Where

$$\begin{aligned}
\mathrm{cov}(\Delta V_{o1}^r, \Delta V_{o2}^r) &= E[\Delta V_{o1}^r \Delta V_{o2}^r] - E[\Delta V_{o1}^r] E[\Delta V_{o2}^r] \\
&= E[(\Delta P_1 C_{o1} - \Delta Q_1 D_{o1})(\Delta P_2 C_{o2} - \Delta Q_2 D_{o2})] \\
&= C_{o1} C_{o2} E[\Delta P_1 \Delta P_2] + D_{o1} D_{o2} E[\Delta Q_1 \Delta Q_2] \\
&- C_{o1} D_{o2} E[\Delta P_1 \Delta Q_2] - C_{o2} D_{o1} E[\Delta P_2 \Delta Q_1] \\
&= C_{o1} C_{o2} \mathrm{cov}(\Delta P_1, \Delta P_2) + D_{o1} D_{o2} \mathrm{cov}(\Delta Q_1, \Delta Q_2) \\
&- C_{o1} D_{o2} \mathrm{cov}(\Delta P_1, \Delta Q_2) - C_{o2} D_{o1} \mathrm{cov}(\Delta P_2, \Delta Q_1),
\end{aligned} \tag{B.7}$$

$$\begin{aligned}
\mathrm{cov}(\Delta V_{o1}^i, \Delta V_{o2}^i) &= E[\Delta V_{o1}^i \Delta V_{o2}^i] - E[\Delta V_{o1}^i] E[\Delta V_{o2}^i] \\
&= E[(\Delta P_1 D_{o1} + \Delta Q_1 C_{o1})(\Delta P_2 D_{o2} + \Delta Q_2 C_{o2})] \\
&= D_{o1} D_{o2} E[\Delta P_1 \Delta P_2] + C_{o1} C_{o2} E[\Delta Q_1 \Delta Q_2] \\
&+ D_{o1} C_{o2} E[\Delta P_1 \Delta Q_2] + D_{o2} C_{o1} E[\Delta P_2 \Delta Q_1] \\
&= D_{o1} D_{o2} \mathrm{cov}(\Delta P_1, \Delta P_2) + C_{o1} C_{o2} \mathrm{cov}(\Delta Q_1, \Delta Q_2) \\
&+ D_{o1} C_{o2} \mathrm{cov}(\Delta P_1, \Delta Q_2) + D_{o2} C_{o1} \mathrm{cov}(\Delta P_2, \Delta Q_1),
\end{aligned} \tag{B.8}$$

and

$$\begin{aligned}
\mathrm{cov}(\Delta V_{o1}^r, \Delta V_{o2}^i) &= E[\Delta V_{o1}^r \Delta V_{o2}^i] - E[\Delta V_{o1}^r] E[\Delta V_{o2}^i] \\
&= E[(\Delta P_1 C_{o1} - \Delta Q_1 D_{o1})(\Delta P_2 D_{o2} + \Delta Q_2 C_{o2})] \\
&= C_{o1} D_{o2} E[\Delta P_1 \Delta P_2] - D_{o1} C_{o2} E[\Delta Q_1 \Delta Q_2] \\
&+ C_{o1} C_{o2} E[\Delta P_1 \Delta Q_2] - D_{o2} D_{o1} E[\Delta P_2 \Delta Q_1] \\
&= C_{o1} D_{o2} \mathrm{cov}(\Delta P_1, \Delta P_2) - D_{o1} C_{o2} \mathrm{cov}(\Delta Q_1, \Delta Q_2) \\
&+ C_{o1} C_{o2} \mathrm{cov}(\Delta P_1, \Delta Q_2) - D_{o2} D_{o1} \mathrm{cov}(\Delta P_2, \Delta Q_1).
\end{aligned} \tag{B.9}$$